The Strange Lake Peralkaline Complex, Québec-Labrador: The Hypersolvus-Subsolvus Granite Transition and Feldspar Mineralogy

Gary J. Nassif

Department of Earth and Planetary Sciences
McGill University, Montréal
July 1993

A Thesis submitted to the Faculty of Graduate Studies and Research in partial fulfilment of the requirements of the degree of Master of Science

Name GARY J NASH

Dissertation Abstracts International is arranged by broad general subject categories. Please select the one subject which most nearly describes the content of your dissertation. Enter the corresponding four digit code in the spaces provided.

[illegible]
SUBJECT TERM

0412
SUBJECT CODE

U·M·I

Subject Categories

THE HUMANITIES AND SOCIAL SCIENCES

COMMUNICATIONS AND THE ARTS

Architecture 0729
Art History 0377
Cinema 0900
Dance 0378
Fine Arts 0357
Information Science 0723
Journalism 0391
Library Science 0399
Mass Communications 0708
Music 0413
Speech Communication 0459
Theater 0465

EDUCATION

General 0515
Administration 0514
Adult and Continuing 0516
Agricultural 0517
Art 0273
Bilingual and Multicultural 0282
Business 0688
Community College 0275
Curriculum and Instruction 0727
Early Childhood 0518
Elementary 0524
Finance 0277
Guidance and Counseling 0519
Health 0680
Higher 0745
History of 0520
Home Economics 0278
Industrial 0521
Language and Literature 0279
Mathematics 0280
Music 0522
Philosophy of 0998
Physical 0523
Psychology 0525
Reading 0535
Religious 0527
Sciences 0714
Secondary 0533
Social Sciences 0534
Sociology of 0340
Special 0529
Teacher Training 0530
Technology 0710
Tests and Measurements 0288
Vocational 0747

LANGUAGE, LITERATURE AND LINGUISTICS

Language
- General 0679
- Ancient 0289
- Linguistics 0290
- Modern 0291

Literature
- General 0401
- Classical 0294
- Comparative 0295
- Medieval 0297
- Modern 0298
- African 0316
- American 0591
- Asian 0305
- Canadian (English) 0352
- Canadian (French) 0355
- English 0593
- Germanic 0311
- Latin American 0312
- Middle Eastern 0315
- Romance 0313
- Slavic and East European 0314

PHILOSOPHY, RELIGION AND THEOLOGY

Philosophy 0422
Religion
- General 0318
- Biblical Studies 0321
- Clergy 0319
- History of 0320
- Philosophy of 0322

Theology 0469

SOCIAL SCIENCES

American Studies 0323
Anthropology
- Archaeology 0324
- Cultural 0326
- Physical 0327

Business Administration
- General 0310
- Accounting 0272
- Banking 0770
- Management 0454
- Marketing 0338

Canadian Studies 0385
Economics
- General 0501
- Agricultural 0503
- Commerce-Business 0505
- Finance 0508
- History 0509
- Labor 0510
- Theory 0511

Folklore 0358
Geography 0366
Gerontology 0351
History
- General 0578
- Ancient 0579
- Medieval 0581
- Modern 0582
- Black 0328
- African 0331
- Asia, Australia and Oceania 0332
- Canadian 0334
- European 0335
- Latin American 0336
- Middle Eastern 0333
- United States 0337

History of Science 0585
Law 0398
Political Science
- General 0615
- International Law and Relations 0616
- Public Administration 0617

Recreation 0814
Social Work 0452
Sociology
- General 0626
- Criminology and Penology 0627
- Demography 0938
- Ethnic and Racial Studies 0631
- Individual and Family Studies 0628
- Industrial and Labor Relations 0629
- Public and Social Welfare 0630
- Social Structure and Development 0700
- Theory and Methods 0344

Transportation 0709
Urban and Regional Planning 0999
Women's Studies 0453

THE SCIENCES AND ENGINEERING

BIOLOGICAL SCIENCES

Agriculture
- General 0473
- Agronomy 0285
- Animal Culture and Nutrition 0475
- Animal Pathology 0476
- Food Science and Technology 0359
- Forestry and Wildlife 0478
- Plant Culture 0479
- Plant Pathology 0480
- Plant Physiology 0817
- Range Management 0777
- Wood Technology 0746

Biology
- General 0306
- Anatomy 0287
- Biostatistics 0308
- Botany 0309
- Cell 0379
- Ecology 0329
- Entomology 0353
- Genetics 0369
- Limnology 0793
- Microbiology 0410
- Molecular 0307
- Neuroscience 0317
- Oceanography 0416
- Physiology 0433
- Radiation 0821
- Veterinary Science 0778
- Zoology 0472

Biophysics
- General 0786
- Medical 0760

EARTH SCIENCES

Biogeochemistry 0425
Geochemistry 0996
Geodesy 0370
Geology 0372
Geophysics 0373
Hydrology 0388
Mineralogy 0411
Paleobotany 0345
Paleoecology 0426
Paleontology 0418
Paleozoology 0985
Palynology 0427
Physical Geography 0368
Physical Oceanography 0415

HEALTH AND ENVIRONMENTAL SCIENCES

Environmental Sciences 0768
Health Sciences
- General 0566
- Audiology 0300
- Chemotherapy 0992
- Dentistry 0567
- Education 0350
- Hospital Management 0769
- Human Development 0758
- Immunology 0982
- Medicine and Surgery 0564
- Mental Health 0347
- Nursing 0569
- Nutrition 0570
- Obstetrics and Gynecology 0380
- Occupational Health and Therapy 0354
- Ophthalmology 0381
- Pathology 0571
- Pharmacology 0419
- Pharmacy 0572
- Physical Therapy 0382
- Public Health 0573
- Radiology 0574
- Recreation 0575
- Speech Pathology 0460
- Toxicology 0383

Home Economics 0386

PHYSICAL SCIENCES

Pure Sciences

Chemistry
- General 0485
- Agricultural 0749
- Analytical 0486
- Biochemistry 0487
- Inorganic 0488
- Nuclear 0738
- Organic 0490
- Pharmaceutical 0491
- Physical 0494
- Polymer 0495
- Radiation 0754

Mathematics 0405
Physics
- General 0605
- Acoustics 0986
- Astronomy and Astrophysics 0606
- Atmospheric Science 0608
- Atomic 0748
- Electronics and Electricity 0607
- Elementary Particles and High Energy 0798
- Fluid and Plasma 0759
- Molecular 0609
- Nuclear 0610
- Optics 0752
- Radiation 0756
- Solid State 0611

Statistics 0463

Applied Sciences

Applied Mechanics 0346
Computer Science 0984
Engineering
- General 0537
- Aerospace 0538
- Agricultural 0539
- Automotive 0540
- Biomedical 0541
- Chemical 0542
- Civil 0543
- Electronics and Electrical 0544
- Heat and Thermodynamics 0348
- Hydraulic 0545
- Industrial 0546
- Marine 0547
- Materials Science 0794
- Mechanical 0548
- Metallurgy 0743
- Mining 0551
- Nuclear 0552
- Packaging 0549
- Petroleum 0765
- Sanitary and Municipal 0554
- System Science 0790

Geotechnology 0428
Operations Research 0796
Plastics Technology 0795
Textile Technology 0994

PSYCHOLOGY

General 0621
Behavioral 0384
Clinical 0622
Developmental 0620
Experimental 0623
Industrial 0624
Personality 0625
Physiological 0989
Psychobiology 0349
Psychometrics 0632
Social 0451

Feldspar mineralogy of the Strange Lake complex, Québec-Labrador

ABSTRACT

The four main units of the epizonal Strange Lake peralkaline complex (Quebec Labrador) document a transition from early hypersolvus granite, to transsolvus granite, to geochemically more evolved subsolvus granite and, finally, to highly K-enriched pegmatites. The felsic and mafic minerals constrain the temperatures of crystallization of the different units. The hypersolvus granite has a solidus above 650°C, and the pegmatite has a solidus below ~590°C at 0.7 kbar. The textural transition and reduced solidi of the units are explained by an increase in (Na+K)/Al and fluorine in the evolved granitic melt, which allows crystallization to lower temperatures, and thus the nucleation of two separate primary feldspars. The composition and structural state of the feldspars of the pluton indicate temperatures of equilibration of ~300° to 100°C. The increasing K/Na value of the bulk feldspar is explained by: 1) the shift of the haplogranite minimum toward the Qtz-Or sideline due to the addition of excess alkalis, and 2) the loss of Na by degassing. The high degree of order in the K-feldspar is attributed to the presence of an alkaline fluid phase. The geochemical evolution of the alkali feldspars is consistent with the fractionation of a single batch of evolved granitic magma. Degassing of the magma led to an important increase in $f(O_2)$, and to the escape of the peralkaline fluid into the wallrocks. Mineralization in the complex is attributed to the late re-distribution of ore constituents *via* a contaminated peralkaline fluid, which gained Ca, Sr and Mg by interaction with the country rock.

RESUME

Les quatres unités du complexe hyperalcalin de Strange Lake (Québec-Labrador) démontrent une transition de granite hypersolvus à granite transsolvus, à un granite subsolvus plus évolue et, finalement, a des pegmatites extrêmement enrichies en K. Les minéraux felsiques et mafiques exercent des contraintes sur les températures de cristallisation des différentes unités. Le granite hypersolvus a un solidus supérieur à 650°C, et les pegmatites ont un solidus inférieur à ~590°C à une pression de 0,7 kbar. La transition texturale et l'abaissement du solidus résulteraient d'une augmentation du rapport (Na+K)/Al et de la teneur élevée en fluor dans le magma granitique le plus évolué, ce qui prolonge le cours de cristallisation à des températures plus basses. Ceci a permis la cristallisation de deux feldspaths primaires distincts dans le granite subsolvus et les pegmatites. La composition et l'état structural des feldspaths alcalins du pluton indiquent des températures d'équilibrage entre ~300° et 100°C. La hausse en K/Na des concentrés de feldspath serait due: 1) au déplacement du minimum haplogranitique vers le côté Qtz-Or par l'excédant en alcalis et 2) la perte de Na par dégazage. Le degré d'ordre élevé du feldspath potassique est attribué à la présence d'une phase aqueuse alcaline. L'évolution géochimique des feldspaths est compatible avec le fractionnement d'une seule venue de magma granitique évolué. Le dégazage a mene à une hausse importante en $f(O_2)$ et à la fuite du fluide hyperalcalin dans les roches encaissantes. La minéralisation du complexe est attribuée à la répartition des constituants du minerai dans la phase fluide hyperalcaline contaminée en Ca, Sr et Mg par interaction avec l'encaissant.

ACKNOWLEDGEMENTS

I thank Robert (Bob) Martin for his supervision, constructive criticism, and patience during the course of this study. Bob provided a wealth of information on granites and feldspars via discussions and the literature that he suggested I read.

Sincere thanks are extended to S. Salvi, J. Mungall, B. Linnen and F. Sakoma for many stimulating discussions. Special thanks go to the founder of the Willy-"beer" seminar which provided a relaxed forum where these discussions could be addressed. I appreciate the technical assistance of G. Keating and I. Ahmedali for atomic-absorption and X-ray fluorescence analyses, M. Mackinnon and G. Poirier for electron microprobe; M. Boily for instrumental neutron activation; S. Jackson for induced coupled plasma - mass spectroscopy and R. F. Martin for X-ray diffraction analyses. Computer assistance was kindly provided by S. (Uncley) McCauley.

Thanks are expressed to a support group of friends which include Kim Bellefontaine, Jackie Hestrin, Anne Kosowski, Mark Mallamo, Bruce Mountain, Christine Petch, Andrea Rourke and Barbara Stefanini.

Special thanks go to Stefano Salvi for his friendship, his culinary expertise and his Italia.

I thank my parents for their constant support during the writing of this thesis.

TABLE OF CONTENTS

PREFACE

This thesis consists of a brief introduction (Chapter 1), two manuscripts (Chapters 2 and 3), and conclusions (Chapter 4). Dr. R.F. Martin is second author on the manuscripts. His contribution to the manuscripts consisted of help in evaluating and interpreting the data and advice in the organization and writing of the text. The two manuscripts are to be submitted for publication in a refereed scientific journal.

Geological mapping and sample collecting were carried out by the author in the summer of 1989 with the assistance of A.E. Williams-Jones, S. Salvi, S. Wood, M. Boily and R. Marr. Petrographic and electron-microprobe analyses were undertaken by the author. Major- and minor- element X-ray fluorescence analyses of whole rocks and atomic absorption analyses of feldspar separates were performed in the Geochemical Laboratory at McGill University. Instrumental neutron-activation analysis of the rare earths and selected elements were conducted at Ecole Polytechnique. X-ray-diffraction data of the feldspar separates were performed by R.F. Martin. Trace element ICP-Mass Spectrometer determinations on the feldspar separates were done by S. Jackson of Memorial University of Newfoundland, St. John's.

The research presented forms part of an ongoing project on high-tech metal deposits at McGill University involving the candidate (G. Nassif), co-author (R.F. Martin), A.E. Williams-Jones, S. Wood, M. Boily, S. Aja, S. Salvi, R. Marr, and J. Roelofsen. Financial support was provided by a NSERC strategic grant, a FCAR team grant and a Reinhardt summer bursary.

CHAPTER 1

Introductory Statement

Tuttle & Bowen (1958), in reference to the complexity of the phase relations of the alkali feldspars stated that "...it is not difficult to envisage the tremendous storage capacity of the feldspars for information concerning their thermal history and the thermal and chemical history of the rocks in which they are found." This view was confirmed by Parsons (1978), who described the evolution of exsolution textures and structural state of alkali feldspars in cooling plutons, by Martin (1982), who presented an overview of feldspar mineralogy of pegmatitic granites; and by Brown & Parsons (1989), who discussed rates of ordering, and kinetic aspects of the phase transformations.

This thesis consists of two manuscripts that focus on the alkali feldspars of the Strange Lake peralkaline granites. The first manuscript deals with the feldspar textures of the different intrusive units, coupled with whole-rock major- and trace-element geochemistry, the data record a transition from hypersolvus granite to a subsolvus granite within the complex. Plots of the normative mineralogy of the different units in terms of the pseudoternary haplogranite system lead to a comparison of the Strange Lake granites with results from experimental work on granitic compositions with excess alkalis, and the addition of F. The second manuscript considers the geochemistry and structural state of the alkali feldspars. Major-element chemistry provides information on the parental magma from which the feldspars crystallized, as well as temperatures of re-equilibration. The concentration of minor and trace elements in the feldspars indicate degree of fractionation in addition to subsolidus re-equilibration with late-stage residual fluids. XRD studies yield information on the subsolidus thermal conditions and the distribution of fluids during the cooling of this enigmatic complex.

References

Brown, W.L & Parsons, I. (1989): Alkali feldspars: ordering rates, phase transformations and behaviour diagrams for igneous rocks. *Mineral Mag* **53,** 25-42.

Martin, R.F. (1982): Quartz and the feldspars. *In* Granitic Pegmatites in science and industry (P. Černý, ed.). *Mineral. Assoc Can, Short-Course Handbook* **8,** 63-98.

Parsons, I. (1978): Feldspars and fluids in cooling plutons. *Mineral Mag* **42,** 1-17.

Tuttle, O. F. & Bowen, N. L. (1958): Origin of granite in light of experimental studies in the system $NaAlSi_3O_8$-$KAlSi_3O_8$-SiO_2-H_2O. *Geol Soc Amer Mem* **74.**

CHAPTER 2

The Hypersolvus Granite-Subsolvus Granite Transition at Strange Lake, Québec-Labrador

Abstract

The Strange Lake anorogenic peralkaline complex is a high-level Zr-Y-Be-*REE*-enriched granite subdivided into four distinct map-units based on texture, mineralogy and bulk composition. The main units document a transition from early hypersolvus granite, to transsolvus granite, to geochemically more evolved subsolvus granite and, finally, to highly K-enriched pegmatites. The evolution is marked geochemically by an increase in Fe^{3+}, Mg, Ca, Ti, Sr, HFS, Y, Zr, *REE*, and a decrease in Na, K, Al, Na/K, and $(La/Yb)_N$. The units are enriched in F. The felsic and mafic minerals constrain the temperatures of crystallization of the different units of this shallow pluton. The hypersolvus granite has a solidus above 650°C and the pegmatite has a solidus just below ~590°C at 0.7 kbar. The textural transition of the units is explained by the presence of excess alkalis and fluorine in the granitic melt. Excess alkalis, which are manifested by the presence of alkali amphibole and alkali zirconosilicates as well as normative acmite and sodium disilicate, depolymerizes melts, enhances water and silicate solubility, and extends the course of crystallization to reduced temperatures. Fluorine (inferred to have been up to 3.7 wt.%) lowered the solidus and liquidus temperatures of the more evolved subsolvus granites and pegmatites allowing the crystallization of two separate primary feldspars. The origin of very potassic pegmatites reflects the disequilibrium crystallization of K-feldspar, brought upon by an escaping sodic vapour phase. Degassing led to an important increase in $f(O_2)$, and to escape of the peralkaline fluid into the wallrocks. Infiltration of Ca- and Mg-bearing fluid back into the evacuated complex probably accounts for the geochemical anomalies in this unusual A-type granite.

Introduction

The Strange Lake anorogenic complex consists of unusually highly evolved peralkaline granite that is locally much enriched in high-field-strength elements. it sits astride the Québec-Labrador border near Lac Brisson, 230 km northeast of Schefferville, Québec and 150 km west of Nain, on the Labrador coast (Fig. 1), and is poorly exposed The long axis of this small (36 km^2) elliptical pluton trends northeasterly. It was emplaced in the eastern arm of the Rae Province (Hoffman 1988) at the contact between a quartz monzonite of Elsonian age to the southwest and a suite of Aphebian metagabbros, metadiorites, quartzofeldspathic and calc-silicate gneisses to the north. The pluton is middle Proterozoic in age. A Rb/Sr whole-rock isochron gave an age of 1189 ± 32 Ma and an initial $^{87}Sr/^{86}Sr$ ratio of 0.705 ± 0.028 (Pillet *et al* 1989).

The Strange Lake complex is of particular interest because of its enrichment in the incompatible elements Zr, Y, Nb, Be, as well as the rare-earth elements (*REE*). Parts of the pluton contain assemblages of exotic minerals such as gittinsite, elpidite, pyrochlore, armstrongite, gadolinite, and kainosite; allanite, fluorite, zircon, and thorite also are present (Birkett *et al* 1992). With reserves on the order of 30 million tonnes grading 3.25% ZrO_2, 0.66% Y_2O_3, 0.12% BeO, 0.56% Nb_2O_5 and 1.3% RE_2O_3 (Zajac *et al* 1984), the pluton hosts what is potentially the largest deposit of Y in the world. This extreme enrichment surpasses that encountered in other examples of peralkaline granite magmatism, e g., the Evisa complex in Corsica (Bonin 1986), the Kaffo Valley granite at Ririwai, in the Niger-Nigeria anorogenic province (Bowden *et al* 1987), and complexes of the Arabian Shield (Drysdall *et al* 1984, Jackson *et al.* 1985).

Figure 1. Map of the Strange Lake complex, Québec-Labrador. Units are named on the basis of petrographic observations from this study. The map has been modified from Miller (1986) and Salvi & Williams-Jones (1990). The bodies of granitic pegmatite were mostly emplaced in the altered subsolvus granite, and are not sufficiently large to appear on this map.

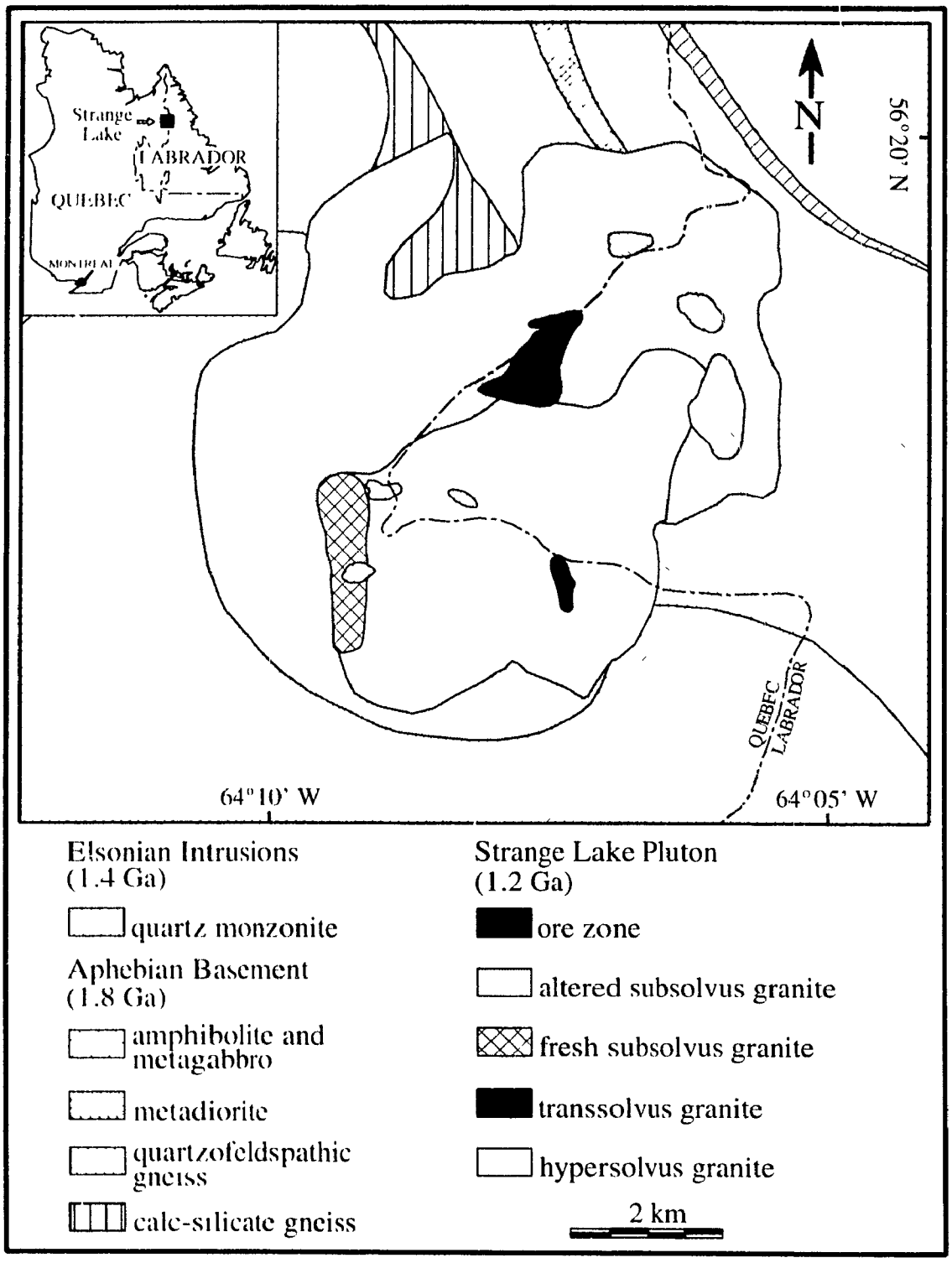
Strange Lake
LABRADOR
QUEBEC
MONTREAL
N
56°20' N
64°10' W
64°05' W
QUEBEC
LABRADOR
Elsonian Intrusions (1.4 Ga)
quartz monzonite
Aphebian Basement (1.8 Ga)
amphibolite and metagabbro
metadiorite
quartzofeldspathic gneiss
calc-silicate gneiss
Strange Lake Pluton (1.2 Ga)
ore zone
altered subsolvus granite
fresh subsolvus granite
transsolvus granite
hypersolvus granite
2 km

Previous investigators have distinguished several distinct facies of granite. Miller (1986) and Zajac *et al* (1984) subdivided the complex on the basis of modal proportion of the exotic minerals. Pillet *et al* (1992) and Currie (1985) referred to a quartz-rich and a feldspathic facies. Salvi & Williams-Jones (1990) referred to an altered and a fresh granite on the basis of extent of a postmagmatic overprint of hydrothermal activity. These terms do not contribute much insight into the petrogenesis of this unusual pluton.

The object of this study is to characterize the texture, mineralogy, and bulk composition of samples of the main units, exclusive of the ore zone. these descriptions document a transition from an early hypersolvus granite, firstly to transsolvus granite, then to the geochemically more evolved subsolvus granite. The juxtaposition of these three texturally different types of anorogenic granite in a single body places constraints on the pressure and temperature of crystallization of the granitic magma.

Field Relations

Field work on the Strange Lake complex in the summer of 1989 had, as its main objectives, 1) the documentation of the intrusive units and their relative age, and 2) the establishment of the nature of the contacts with the host rock. Exposures of the intrusive contact with the country rock unfortunately are scarce. To the north, a large tongue of quartzofeldspathic and metadioritic gneiss forms a re-entrant into the pluton (Fig. 1). In the northeastern portion of the pluton, the Aphebian gneisses are exposed as irregular masses interpreted to be roof pendants. The attitude of the foliation in these outcrops

is consistent with that in the host gneisses to the north. To the south and west, xenoliths of Elsonian quartz monzonite also occur as roof pendants. The granite shows no evidence of a chilled margin in contact with the roof pendants. The contact between granite and host rocks is sharp, and there is no evidence of brecciation and incipient metasomatism of the wallrock. A primary foliation generally is present within one meter of the contact. These features are consistent with the epizonal nature of the pluton.

Drill-core data and results of a very-low-frequency electromagnetic survey reveal the presence of a ring fault dipping 20° to 35° outward; this ring fault delineates the outer edge of the Strange Lake complex (Miller 1986, Zajac *et al* 1984). The fault is exposed in the northwestern portion of the complex, and marked by a fluorite-hematite breccia that contains entrained fragments of the Aphebian gneisses.

The Map Units

The Strange Lake granite is composed of alkali feldspar, quartz, arfvedsonite ± aegirine, and the several accessory phases that make it unusual. The modal proportion of the rock-forming minerals remains fairly constant (Pillet *et al* 1992, Table 2), yet textural variations abound within the complex, as is expected in a shallow intrusive body. Based on textural and mineralogical differences, the pluton is subdivided into two major units (*hypersolvus granite* and *subsolvus granite*) and two subsidiary units (*transsolvus granite*, intermediate between hypersolvus and subsolvus variants, and *pegmatite*, in bodies that cut the subsolvus granite, mostly). These are described below in an order consistent with their emplacement.

Hypersolvus granite

This unit is exposed in the southeastern and central portion of the complex (Fig. 1). It consists of leucocratic alkali feldspar granite (nomenclature of Streckeisen 1976). Outcrops are typically of "pavement" type. Macroscopically, this medium-grained rock is tan to pale green, and is characterized by 1) an even distribution of arfvedsonite grains from <1 to 10 mm across, and 2) the prominence of mesoperthite. Mineralogically, this rock seems invariant, on the other hand, textural variations are common. It is hypidiomorphic, equigranular to slightly porphyritic, with phenocrysts of perthite, quartz and, less commonly, arfvedsonite.

A mesoperthitic alkali feldspar (50 to 70%) dominates this granite (Fig. 2a). These grains are euhedral to subhedral, and up to 12 mm across. They are turbid owing to myriads of microscopic inclusions of arfvedsonite needles, aenigmatite, astrophyllite and minor albite laths. The acicular crystals may well be the result of "reworking" of iron formerly in the structure of the primary (magmatic) feldspar, released during its exsolution. In fact, the iron content of the K- and Na-rich feldspars is found to decrease as they approach end-member compositions (Chapter 3). The exsolution texture seems to have developed prior to the appearance of these acicular inclusions, which cut across the lamellae.

The mesoperthite grains display Manebach, Baveno and Carlsbad growth twins. Some grains display a "herring-bone" texture of albite lamellae owing to the combination of Manebach and Carlsbad twins. Regular lenticular lamellae of albite attributed to exsolution attain 50 μm across. Patch-type perthite also is common, the

Figure 2. Photomicrographs of representative samples from the different units of the Strange Lake complex. a. Hypersolvus granite, with mesoperthitic alkali feldspar, quartz and poikilitic amphibole. Note the swapped margins of alkali feldspar and arfvedsonite b Close-up of the swapped margins of perthite and arfvedsonite in the hypersolvus granite. The arfvedsonite invariably is intergrown with the albite lamellae. c. Transsolvus granite, with microperthitic phenocryst in a subsolvus two-feldspar matrix. The edges of the phenocrysts are almost devoid of albite, marking the transition from a hypersolvus to subsolvus crystallization. d. Subsolvus granite, with early-formed grains of quartz, arfvedsonite and isolated laths of albite and K-feldspar. e Magmatic quartz with grains of K- and Na-feldspar delineating a pseudohexagonal core. f Pegmatite with early-formed crystals of α-quartz and sprays of hematite-stained aegirine. Scale bars indicated at the lower right of each photomicrograph.

a.

2mm

b.

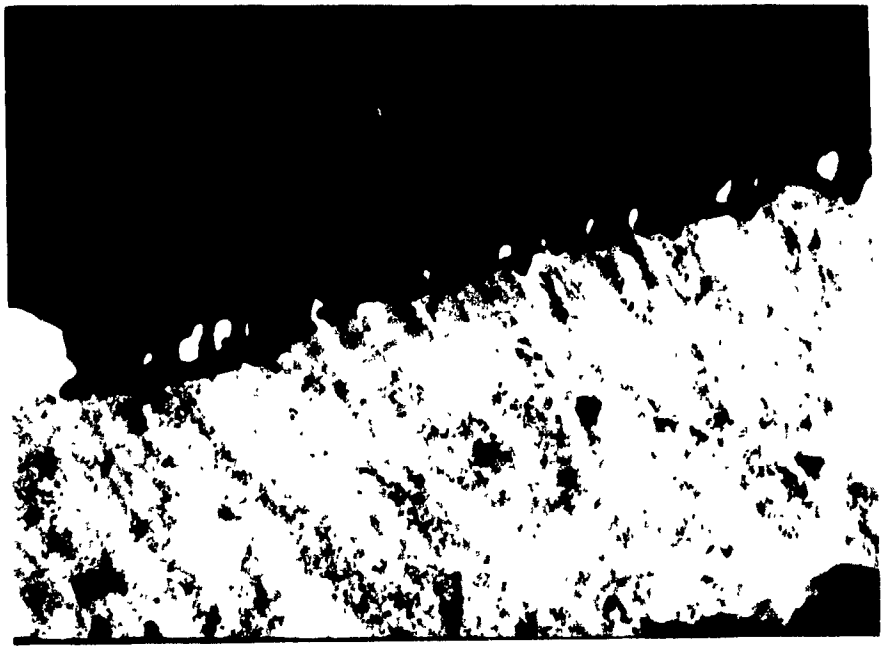

0.5 mm

c.

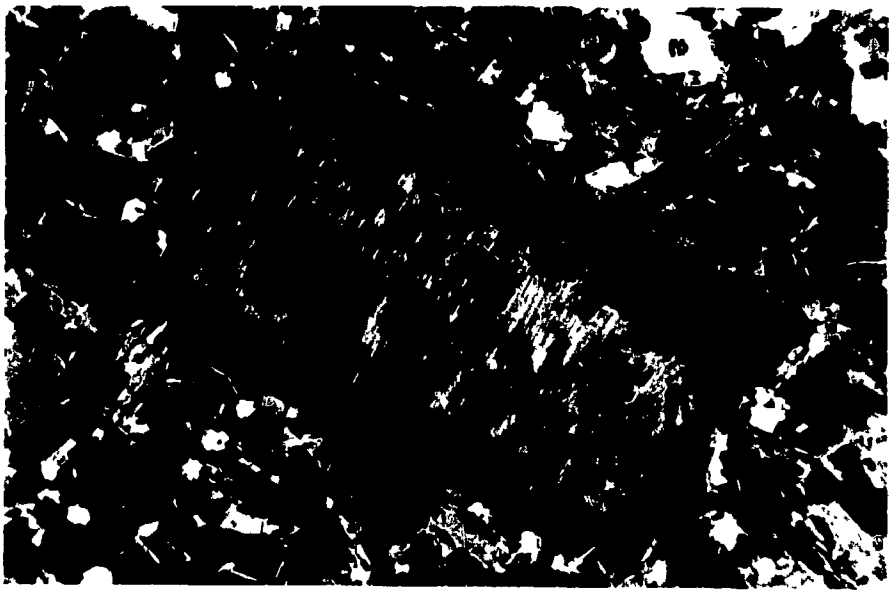

2mm

d.

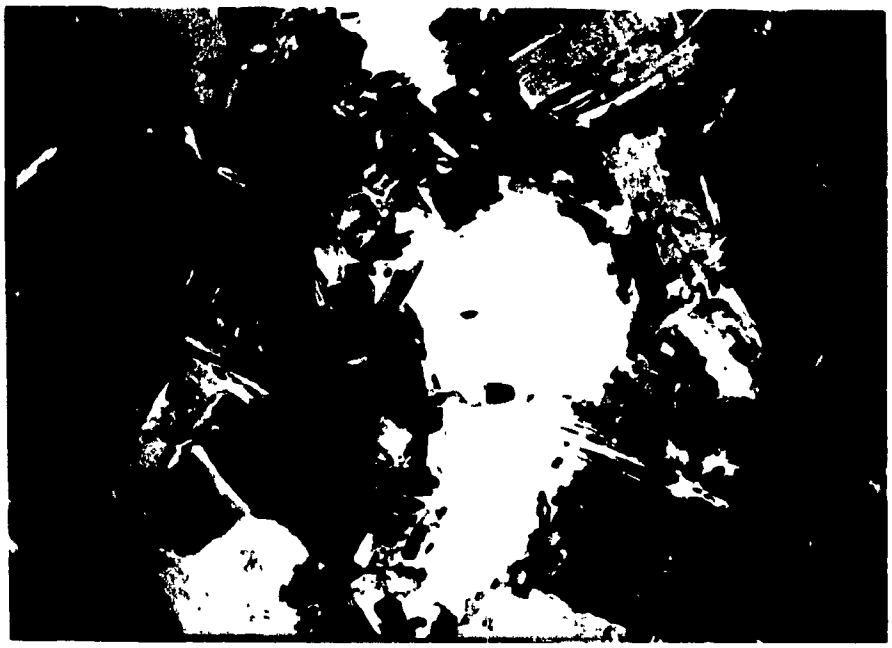

2mm

e.

2mm

f.

2mm

albite occurring as films, veins, patches, and blebs that seem randomly oriented throughout the K-feldspar host.

Quartz, the second most abundant mineral, constitutes 15 to 25% of the rock. It crystallizes following the alkali feldspar as interstitial, anhedral grains that mold earlier phases (Fig. 2a). Where formed early, its habit is typical of β-quartz. The quartz displays uniform extinction, attesting to a strain-free regime during and following crystallization of the pluton.

Sodic amphibole (10-15%) is the dominant mafic mineral. In some samples, the subhedral crystals display a colour zonation in plane light from core to margin, this optical variation reflects the gradation from a ferrorichteritic core to an arfvedsonitic margin (Pillet 1989). These grains are devoid of perthite inclusions, but do contain blebs of clear fluorite up to 200 μm across in the Ca-rich core. The fluorite contains what is interpreted to be devitrified melt inclusions (S. Salvi, pers. comm. 1992). These two observations are consistent with a magmatic origin for the fluorite. In other samples, the unzoned arfvedsonite occurs interstitially, and molds the earlier felsic minerals. Such grains may be poikilitic, enclosing quartz and alkali feldspar, as well as primary zircon, thorite, aenigmatite, and astrophyllite.

Subsolidus features are common but subtle in the hypersolvus granite. Albite commonly forms a syntactic overgrowth on the perthite grains. The coarse twin-lamellae (Albite Law) in the overgrowth parallel the finer (010) twin-lamellae in albite formed by exsolution in the host. Also, late-forming interstitial elpidite, narsarsukite, as well as aenigmatite and astrophyllite, are contemporaneous with the late arfvedsonitic

amphibole. Perthite grains in contact with such arfvedsonite are coated with albite, presumably deposited from a late pore fluid. Arfvedsonite "islands" result from the highly dentate interfaces (swapped margins) with perthite (Fig. 2b). The crystallization of much of the arfvedsonite in such samples seems to postdate the exsolution in the feldspar.

On the basis of the prominence of perthite and the lack of discrete grains of primary albite, crystallization occurred under hypersolvus conditions (Tuttle & Bowen 1958), *i.e.*, above the crest of the solvus in the system Ab-Or. Zircon, pyrochlore, and thorite seem to have preceded or cocrystallized with a homogeneous primary feldspar (sanidine solid-solution) near the liquidus. Fluorite crystallized near the liquidus. Quartz crystallized prior to the appearance of the ferrorichterite core of the amphibole. The amphibole incorporated these earlier-formed minerals. Below the solidus, the sanidine grains underwent exsolution. Narsarsukite and elpidite also seem to have crystallized at a subsolidus temperature. Arfvedsonite crystallized as a mantle on the amphibole grains, along with aenigmatite and astrophyllite. The arfvedsonite-albite intergrowth along grain margins is attributed to late codeposition from an intergranular fluid phase. This relationship, the appearance of arfvedsonite needles in the perthite, and the coarsening and modification of the exsolution texture, are the product of interaction of the primary minerals with a peralkaline hydrothermal pore-fluid. Another result of this interaction is the conversion of a monoclinic K-feldspar to microcline (Chapter 3).

Transsolvus granite

The term "transsolvus", initially coined by Bonin (1972) and later described by Martin & Bonin (1976), refers to rocks that are texturally intermediate between hypersolvus and subsolvus granites. This texture illustrates a transition from early crystallization as a hypersolvus rock and late crystallization as a subsolvus rock (see below). This unit occurs in the southeastern portion of the complex as wisps and isolated lenses up to one meter across within the hypersolvus granite. Such lenticular xenoliths seem to have behaved plastically. This rock is fine-grained, grey to greenish grey, hypidiomorphic, and slightly porphyritic, with phenocrysts of euhedral perthite, subhedral to euhedral quartz, and less abundant prisms of arfvedsonite. The melanocratic appearance of the granite is entirely due to the fine-grained nature of arfvedsonite grains distributed within the matrix and not to an increase in modal arfvedsonite. In fact, the bulk composition of the transsolvus granite is similar to that of the hypersolvus granite (Table 1), as confirmed by Pillet *et al.* (1992; Table 3, his "chilled margin" and "feldspathic" facies, respectively).

The transsolvus granite also occurs as cm-sized, roundish enclaves or xenoliths throughout the subsolvus granite. Such enclaves commonly possess a thin rim of felsic material devoid of mafic constituents. Such a rim probably arose as a result of rapid nucleation of feldspar and quartz on the xenoliths upon their incorporation in the melt, and may be taken to indicate that these xenoliths were relatively cool when they were incorporated.

The transsolvus granite shares mineralogical characteristics with both the

hypersolvus and subsolvus granites. It is porphyritic, with phenocrysts of mesoperthite up to 12 mm across in a matrix of discrete microcline and albite grains (Fig. 2c) that thus is subsolvus. The microcline is grid-twinned, subhedral, and 0.3 mm across on average. Subhedral laths of albite in the matrix rarely exceed 0.2 mm. Both microcline and albite laths are found as inclusions in grains of interstitial arfvedsonite, which average 0.2 mm across. The anhedral quartz grains display a sharp extinction.

Subsolvus granite

This unit defines an arcuate pattern (Fig. 1) that almost completely wraps around the hypersolvus granite. It more or less coincides with Currie's (1985) and Pillet's (1989) quartz-rich facies and with the altered granite of Salvi & Williams-Jones (1990). Outcrops occur on ridges partly concealed by moraine deposits. Macroscopically, the granite typically is cream to reddish brown, hypidiomorphic, and inequigranular. Two feldspars and quartz comprise the matrix of this unit; two types of arfvedsonite are present, euhedral phenocrysts and fine-grained crystals in the matrix. Inclusions of fine-grained transsolvus granite are ubiquitous.

Quartz (30 to 40%) is more abundant here than in the hypersolvus granite. It appears earlier in the sequence of crystallization, as euhedral to subhedral crystals up to 4 mm across (Fig. 2d). Grains have a core generally devoid of inclusions, and a rim that is marked by the presence of fluid and mineral (albite and K-feldspar) inclusions. These may delineate an internal pseudohexagonal to subcircular core (Fig. 2e). The presence of discrete albite and K-feldspar trapped in magmatic quartz shows that both

minerals are magmatic in origin. Quartz also is entrapped in arfvedsonite.

The feldspar fraction consists of isolated subhedral grains of K-rich feldspar and albite (Fig. 2d). Growth twins are rare. The grid-twinned grains of microcline perthite (20 to 35%) attain 2.5 mm. Albite occurs as an exsolved phase (less than 5%) in the host microcline, and less commonly, as an overgrowth. The presence of limpid laths of primary albite (10 to 15 vol%; up to 0.3 mm) distinguishes this unit from the hypersolvus rocks. The albite is found especially at quartz and arfvedsonite grain margins and as inclusions in these minerals. It cocrystallized with K-feldspar following the appearance of euhedral quartz and arfvedsonite phenocrysts.

Arfvedsonite amounts to 10% of the rock unit, on average. It occurs as subhedral to euhedral phenocrysts whose grain margins are irregular. These crystals attain 1 cm across. Inclusions of quartz, K-feldspar, and albite are typical in the arfvedsonite, mostly near grain boundaries. The arfvedsonite grains are not zoned and lack a calcic core. In certain areas, near the contact with hypersolvus granite, this unit contains rocks with up to 50% modal arfvedsonite. Lacroix (1923) first described such a rock in the Evisa Complex, Corsica, as "lindinosite". A second generation of arfvedsonite, generally monocrystalline, occupies interstices among the felsic minerals in the subsolvus granite. These arfvedsonite oikocrysts contain quartz, microcline and albite laths as inclusions. Arfvedsonite, therefore, seems to have crystallized over the entire interval between liquidus and extending below the solidus, first as euhedral phenocrysts incorporating inclusions at grain edges, and subsequently at the end stage of crystallization, as interstitial grains that mold and envelop previously formed phases.

Aegirine (0 to 10%) occurs as primary grains interstitial to the felsic minerals and as a replacement of arfvedsonite at grain margins and along cleavage traces. Such aegirine commonly is associated with a ferruginous stain and polycrystalline quartz in hydrothermally altered granite. A possible reaction that accounts for this replacement (Bonin 1986) is:

$$3\ Na_3Fe^{2+}_4Fe^{3+}Si_8O_{22}(OH)_2 + 5/2\ O_2 \rightleftharpoons 9\ NaFe^{3+}Si_2O_6 + 2\ Fe_3O_4 + 6\ SiO_2 + 3\ H_2O$$

arfvedsonite + oxygen $\rightleftharpoons$ aegirine + iron oxide + quartz + water

The degree of such oxidation-induced replacement increases toward the periphery of the complex.

As in the hypersolvus granite, the accessory mineral phases in this unit are late to crystallize, and occur interstitially. Those found in the altered subsolvus granite include calcite, prehnite, kainosite, and purple fluorite, which are all calciferous. Zircon occurs as radiating fibres in "hematized" aggregates and is closely associated with gittinsite, $CaZrSi_2O_7$, which occurs as isolated rosettes that are partially intergrown with hematite.

The presence of isolated microcline and albite laths shows that the magma that produced this unit crystallized under subsolvus conditions (Tuttle & Bowen 1958). Because of their original composition and the relatively low temperature of initial formation, the two separate feldspars later underwent minimal exsolution (in the case of albite, probably none). Quartz crystallized as a liquidus phase. Arfvedsonite appears throughout the course of crystallization, as phenocrysts and oikocrysts. The accessory

minerals seem to have appeared largely at the subsolidus stage, although some authors have concluded otherwise (Birkett *et al* 1992).

Pegmatite bodies

The bodies of granitic pegmatite are the latest to crystallize in the Strange Lake complex. An exceptional 12-cm-wide hypersolvus pegmatitic lens was found in the southern part of the hypersolvus granite unit. It shows no signs of hydrothermal alteration. Arfvedsonite crystals free of aegirine coexist with perthite and a quartz-rich core. On the other hand, numerous small bodies of subsolvus granitic pegmatite occur, mostly in the subsolvus granite and as dykes intruding the Aphebian gneisses to the north. Pegmatite bodies in the subsolvus granite are subvertical, and trend east-west. They appear as pods and irregular lenses up to 40 cm wide Their mineralogy is similar to that of the host granite, i.e , they are essentially composed of only slightly perthitic K-rich feldspar, quartz, arfvedsonite ± aegirine. Miarolitic cavities are associated with the pegmatite pods; they are are lined with the same minerals.

Most of the quartz is euhedral, its habit is typical of the low-temperature modification (Fig 2f). Quartz also occurs as a product of the oxidation-induced breakdown of arfvedsonite to aegirine. The K-rich feldspar is prominently grid-twinned, consistent with its highly ordered state (Chapter 3); the albite and pericline twin-lamellae coarsen toward the grain boundaries. Discrete laths of albite are rare, ranging from 0 to 5 volume % of the pegmatites

The replacement of arfvedsonite by aegirine in subsolvus-granite-hosted pegmatites

is extensive. The arfvedsonite in the host granite adjacent to these pegmatites also is replaced by aegirine, at grain margins and along cleavage traces. Non-pseudomorphic aegirine forms sprays of hematite-stained crystals (Fig. 2f) associated with polycrystalline quartz.

The accessory minerals that give Strange Lake its economic potential are associated with these pegmatites: gittinsite, monazite, zircon, kainosite and pyrochlore. In the ore zone, pegmatite bodies are associated with aplite, which form the lower part of pegmatite-aplite sheets. The aplite is characterized by the presence of, in order of decreasing abundance, quartz, gittinsite, K-feldspar, albite, aegirine, arfvedsonite, and narsarsukite. Both massive and lineated variants occur in the ore zone. The lineated aplite is characterized by albite, narsarsukite, and aegirine, which define a lineation. Albite accounts for a maximum of 15 vol.% of total feldspar in the aplite (Miller 1990). Thus, we may conclude that the albite component "missing" in the subsolvus granitic pegmatites is not accounted for in an aplitic fraction (*cf.* Jahns & Tuttle 1963).

Analytical Methods

Representative samples of the units, devoid of inclusions, were analyzed for major elements, Zn, Rb, Sr, Nb, Zr and Y by X-ray fluorescence (XRF) at McGill University. The analyses were performed with a Philips PW 1400 using fused discs and an σ-coefficient technique (Ahmedali 1983). Fe^{2+} was determined by titration. Concentrations of the rare earths, Ta, Hf, Th, and U were determined by instrumental neutron activation analysis (INAA) at Ecole Polytechnique, as described by Bouly *et al.* (1989).

Geochemistry

Major-element chemistry

In addition to the representative samples chosen for study, a representative cross-section of the pegmatite bodies was sampled to avoid any heterogeneity in composition that could be caused by unrepresentative abundances of the minerals. Average whole-rock compositions and normative mineralogy are presented in Table 1. The full data-set on fifteen samples of hypersolvus, four of transsolvus, three of fresh subsolvus, twenty-one of altered subsolvus, and four of pegmatites is provided in Appendix I. Chemical trends of the different units are illustrated in plots of selected major elements *versus* Al_2O_3 from this data-set in Figure 3.

The silica content in the different units shows little variation (70.3 to 71.0 wt.% SiO_2), with the exception of the pegmatites (65.1 wt.% SiO_2). The concentration of Al remains constant in the hypersolvus, transsolvus and fresh subsolvus granites (11.5 to 11.9 wt.% Al_2O_3). There is a markedly lower level of Al in the altered subsolvus granites and pegmatites (8.7 and 5.8 wt% Al_2O_3, respectively), due to the appearance of Al-free phases. Na/K is greater than unity in the first four units, ranging from 1.20 to 1.61. The pegmatites, however, show a marked decrease in Na/K, with a value of 0.53. Also, the Strange Lake units are highly enriched in iron, the proportion of ferric iron increasing with degree of evolution. The first three units have values of $Fe^{3+}/(Fe^{2+}+Fe^{3+})$ ranging from 0.70 to 0.76, as expected in unaltered A-type granites (Whalen *et al.* 1987) whereas the altered subsolvus granites and pegmatites have values of 0.44 and 0.13, respectively. The concentration of Ti is fairly constant in the four

TABLE 1. AVERAGE COMPOSITION AND NORMATIVE MINERALOGY OF THE STRANGE LAKE UNITS.

unit	hyp(15)	± 1σ	trans(4)	± 1σ	fsub(3)	± 1σ	asub(21)	± 1σ	peg(4)	± 1σ
SiO_2wt %	70.50	1 48	70 66	0.60	70 27	0 84	71 00	0 65	65 11	1 86
TiO_2	0 30	0 09	0.24	0 08	0 21	0 08	0 32	0 10	2 45	1 22
Al_2O_3	11.55	0.63	11 86	0 45	11 54	1 05	8 67	0 45	5 77	0 15
Fe_2O_3	2 63	0 96	2 54	0 33	2.05	0 47	4 15	1 16	3 93	1 78
FeO	2 77	1 28	2 71	0 58	2 87	0 23	1 47	0 88	0 27	0 21
MnO	0 11	0.03	0.11	0 02	0 10	0 01	0 14	0 03	0 10	0 05
MgO	0.02	0 04	0 01	0 00	0 01	0 00	0 23	0 18	0 73	0 36
CaO	0 64	0.34	0 54	0.17	0 77	0 04	1 56	0 70	6 57	3 52
Na_2O	5.08	0 60	4 80	0.34	4 49	0 88	3 96	0 47	1 39	0 97
K_2O	4 81	0.26	5 03	0.19	5 70	2 11	3 88	0 35	3 96	0 40
P_2O_5	0.02	0 02	0 01	0.00	0 02	0 01	0 02	0 01	0 01	0 01
F	0 56	0 18	0 62	0 12	0 70	0 02	0 44	0 26	0 42	0 46
LOI	0.48	0.23	0 47	0 02	0 41	0 02	0 84	0 31	2 14	0 60
	99 47		99.59		99 14		96 68		92 84	
O=F	0.23		0 26		0 29		0 18		0 18	
Total[1]	99 24		99 33		98 85		96 50		92 17	
Q	22 91		23.01		23.34		32 38		34 34	
Z	0 68		0 89		0 65		2.64		2 45	
Or	28.43		29.73		33 69		22.93		23 41	
Ab	32.63		33.00		27 63		23 00		7 63	
Ac	7 61		6.70		5.93		9 26		3 64	
Ns	0.40		0 00		0 85		0.00		0 00	
Di	0.64		0.00		0 25		4 33		3 92	
Wo	0.00		0.00		0.00		0.17		7 66	
Hy	4.51		4 62		5 00		0.00		0 00	
Mt	0 00		0.32		0 00		1 38		0 00	
Hm	0 00		0.00		0 00		0 00		2 67	
Tn	0.00		0 00		0 00		0 00		5 00	
Il	0 57		0.46		0 40		0 61		0 78	
Ap	0.05		0 02		0 05		0.05		0 02	
Fl	1 97		2 54		2 87		1 80		1 72	
Total	100.38		101 30		100 65		98 54		93 25	
(Na+K)/Al	1 17		1.13		1 17		1 24		1 13	
Na/K	1 61		1.45		1 20		1 55		0 53	
$Fe^{2+}/(Fe^{2+}+Fe^{3+})$	0 70		0.70		0 76		0 44		0 13	

Abbreviations used hyp, hypersolvus granite, trans, transsolvus granite, fsub, fresh subsolvus granite, asub, altered subsolvus granite, peg, pegmatite, ± 1σ, ± one standard deviation Numbers in brackets refer to number of analyses

[1] The low totals for the compositions are a result of the enrichment of trace elements (see Table 2)

Figure 3. Selected major elements (expressed as oxides) *versus* Al_2O_3 (wt.%) for the different units in the Strange Lake complex. Symbols used: open squares, hypersolvus granite; solid squares, transsolvus granite; open circles, fresh subsolvus granite; solid circles, altered subsolvus granite; triangles, pegmatites.

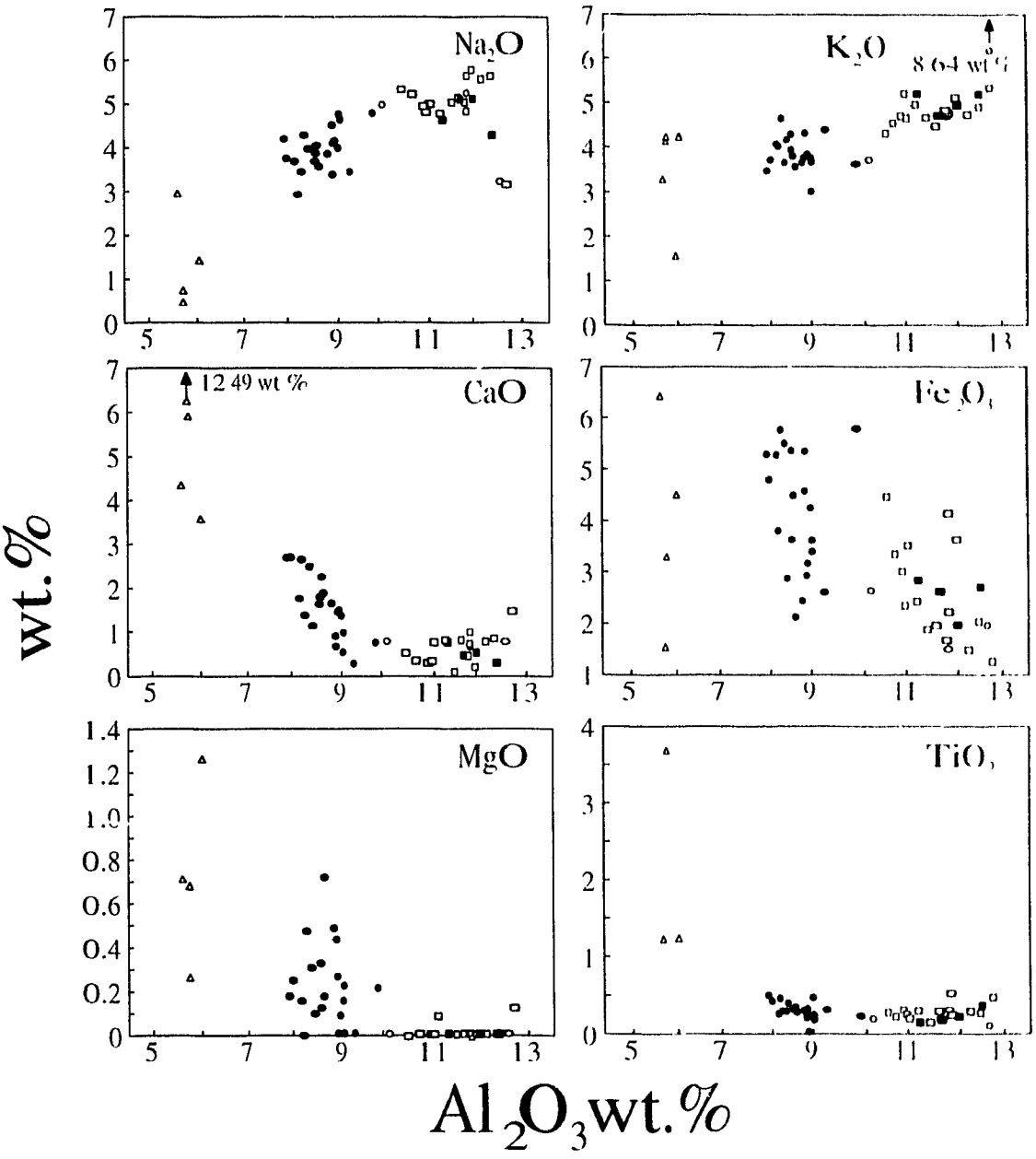
Na2O
K2O
8.64 wt %
CaO
12.49 wt %
Fe2O3
MgO
TiO2
wt.%
Al2O3wt.%

earlier units (0.21 to 0.30 wt.% TiO_2), and shows a large increase in the pegmatites (2.45 wt.% TiO_2). Mg is a trace element in the early units (<0.02 wt.% MgO), but levels increase in the altered subsolvus granites (0.23 wt.% MgO) and the pegmatites (0.73 wt.% MgO). Similarly, Ca increases from 0.54 - 0.77 wt.% CaO in the three earlier units to 1.56 and 6.57 wt.% CaO in the altered subsolvus granites and pegmatites, respectively. These elevated values are most unusual for highly evolved peralkaline granite. For example, Whalen *et al* (1987) reported 0.75 wt.% CaO for the average A-type granite.

All units are peralkaline, with an agpaitic index in the range 1.13 - 1.24. The peralkaline nature of the Strange Lake alkali feldspar granites is consistent with their mineralogy (i.e., presence of arfvedsonite, aegirine, astrophyllite, aenigmatite, and exotic alkali zirconosilicates), and is expressed by the amount of normative acmite (3.64 to 9.26%, Table 1) and sodium disilicate (up to 0.85%).

Quartz, orthoclase and albite are the dominant normative minerals. In a Qtz-Ab-Or diagram (Fig. 4), the hypersolvus granites are located in the feldspar field of the haplogranite system shown for a $P(H_2O)$ of 1 kbar. Most samples plot along the predicted "liquid line of descent" from the Ab-Or join toward the minimum along the quartz-feldspar cotectic (Fig. 4). The initial progression of liquids toward the minimum-melt composition was clearly the result of fractionation of alkali feldspar (sanidine solid-solution). Pillet *et al* (1992, Fig. 9) also showed this by plotting bulk-composition data for these units in a diagram of Si-Al-(Na+K). Sanidine fractionation caused the granitic magma to increase in agpaitic index as it approached the minimum. The

Figure 4. The composition of the different units in terms of normative Qtz-Ab-Or. The 0.5 and 1 kbar quartz-feldspar cotectics also are shown (Tuttle & Bowen 1958). The plus signs represent thermal minima of the haplogranite system (0 wt% F, Tuttle & Bowen 1958), with 1, 2 and 4 wt.% F (Manning 1981) added to the haplogranite system. The thermal minimum of the haplogranite system a) with 4.5% acmite and 4.5% sodium disilicate added, and b) with 8.5% acmite and 8.5% sodium disilicate added (Carmichael & MacKenzie 1963) is progressively shifted (in projection) toward the Qtz-Or sideline. Symbols used are the same as those in Figure 3.

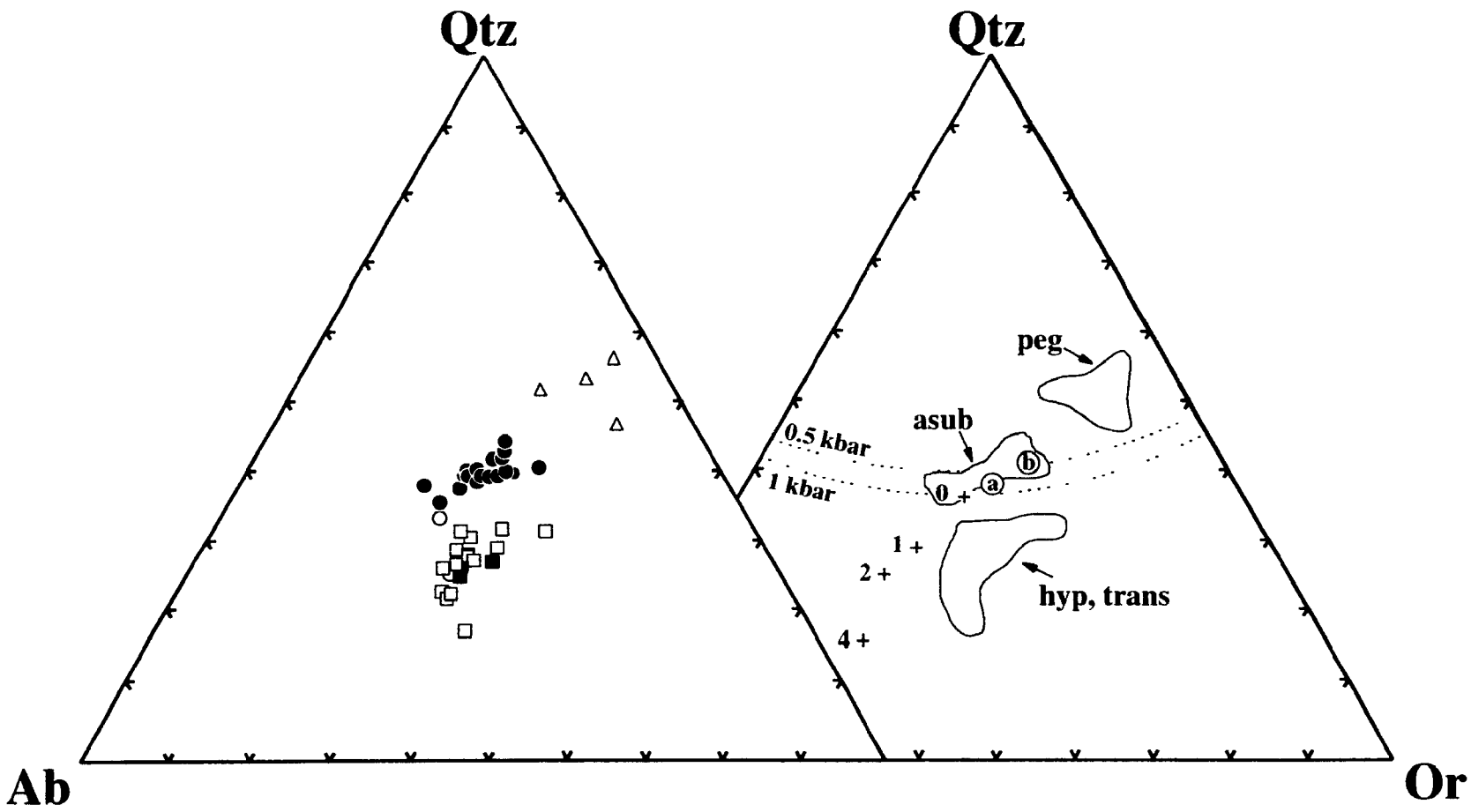
Qtz
Qtz
peg
asub
0.5 kbar
1 kbar
b
a
0 +
1 +
2 +
4 +
hyp, trans
Ab
Or

transsolvus granite and fresh subsolvus granite plot near the cluster of points for hypersolvus granite, confirming their very similar composition in terms of major elements. In projection, the compositions of the granites shift progressively toward the Qtz-Or join. Samples of altered subsolvus granite, clustered at the granite minimum (1.0 kbar), also show a shift away from the Ab apex. They are positioned closer to the minimum in the haplogranite system plus 4.5% each of *ac* + *ns* (Carmichael & MacKenzie 1963) shown as "a" on Figure 4. The pegmatites plot near the Qtz-Or join, indicative of their albite-poor mineralogy. The shift of compositions away from the haplogranite minimum toward the Qtz-Or join is not an artifact of allotment of the alkalis in the norm calculation: the recasting of all sodic normative minerals to the Ab apex of the Qtz-Ab-Or plot does not remove this shift.

What little Ca is in the rocks is expressed in the norm as fluorite and diopside rather than anorthite. The diopside component expresses the presence of ferronchteritic cores of arfvedsonite (Pillet 1989) in the hypersolvus granite, and gittinsite, calcite, and other minor Ca-bearing phases in the subsolvus unit. The late buildup in normative diopside, up to 6.0 wt.% in altered subsolvus granite (Appendix I), clearly is highly anomalous in such an evolved granite.

The average levels of F in the complex gradually increase from hypersolvus granite (0.56 wt.% F) to transsolvus granite (0.62 wt.%) to fresh subsolvus granites (0.70 wt.% F). However, in the altered subsolvus granites (0.44 wt.% F) and pegmatites (0.42 wt.% F) this pattern of enrichment with evolution is reversed.

Trace-element chemistry

Average concentrations of trace elements are presented for each unit in Table 2. An enrichment in Zn, Rb, Ta, Nb, Hf, Zr, Y, Th and U characterizes the sequence hypersolvus granite (least evolved) to subsolvus granitic pegmatites (most evolved) (Fig. 5). This pattern of enrichment is characteristic of peralkaline granites (Tauson 1967, Harris & Marriner 1980). The presence of F and the peralkalinity of the melt promote the formation of alkali-fluoride complexes, which are considered essential to concentrate these elements in the melt (Watson 1979, Collins *et al* 1982).

The earlier units contain low levels of Sr (15-35 ppm Sr), as is typical of peralkaline granites, it is noteworthy that Sr is enriched in the altered subsolvus granite (79 ppm Sr) and pegmatites (294 ppm Sr) (Fig. 5). Sr thus follows both Ca and Mg in their pattern of late enrichment (Table 1). Perhaps as a reflection of the same phenomenon, a Be-bearing mineral (gadolinite) is present in the more altered rocks and the ore zone. Also, Pillet (1989) noted higher concentrations of Ba (754-2079 ppm) in his "quartz-rich" facies (subsolvus granite) relative to his "feldspar-rich" facies (hypersolvus granite; 344-1309 ppm).

The rare-earth elements

The Strange Lake granites and pegmatites are highly enriched in *REE*. Their total concentration increases from 1733 ppm in hypersolvus granite to 7650 ppm in the pegmatites (Table 2). Chondrite-normalized patterns (Fig. 6, chondrite values after Evensen *et al* 1978) graphically demonstrate this enrichment, as well as the marked

TABLE 2. AVERAGE CONCENTRATIONS OF SELECTED TRACE ELEMENTS IN THE STRANGE LAKE GRANITE

unit	hyp	trans	fsub	asub	peg
Zn ppm	442	465	552	1022	----
Rb	600	666	1067	995	1109
Sr	35	15	30	79	294
Ta	18	9	26	25	127
Nb	356	333	327	926	1631
Hf	80	109	113	429	631
Zr	3456	4408	3214	13115	12171
Y	445	574	705	1373	3091
Th	82	46	63	252	689
U	10	101	6	36	100
La	414 6	352.5	736 0	831.2	1263 9
Ce	749.5	671 5	1278.0	1511 1	2872 0
Nd	310.5	277 1	515 6	652 9	1244 5
Sm	72.8	69.4	118 5	174 4	200 0
Eu	3.7	4 2	5 8	9.4	20 4
Gd	64.7	68 2	95 8	207 3	573 4
Tb	10.5	12.2	14 9	57 7	101 6
Dy	49.2	71.7	92 4	166 0	636 6
Tm	6.0	6 2	6 7	23.9	76 7
Yb	47.2	44.4	52.6	183 7	590 9
Lu	4.5	5.8	6 8	23.0	70 3
ΣREE	1733	1583	2923	3841	7650
Eu/Eu*	0 16	0.18	0.16	0 15	0 17
$(La/Yb)_N$	5.8	5 2	9 2	3 0	1 4

Concentrations of Zn, Rb, Sr, Nb, Zr, and Y determined by XRF. Concentrations of Ta, Hf, Th, U, and *REE*s determined by INAA. Raw data are provided in Appendix I.

Figure 5. Selected trace element *versus* Al for the different units of the Strange Lake complex. Symbols used are the same as those in Figure 3.

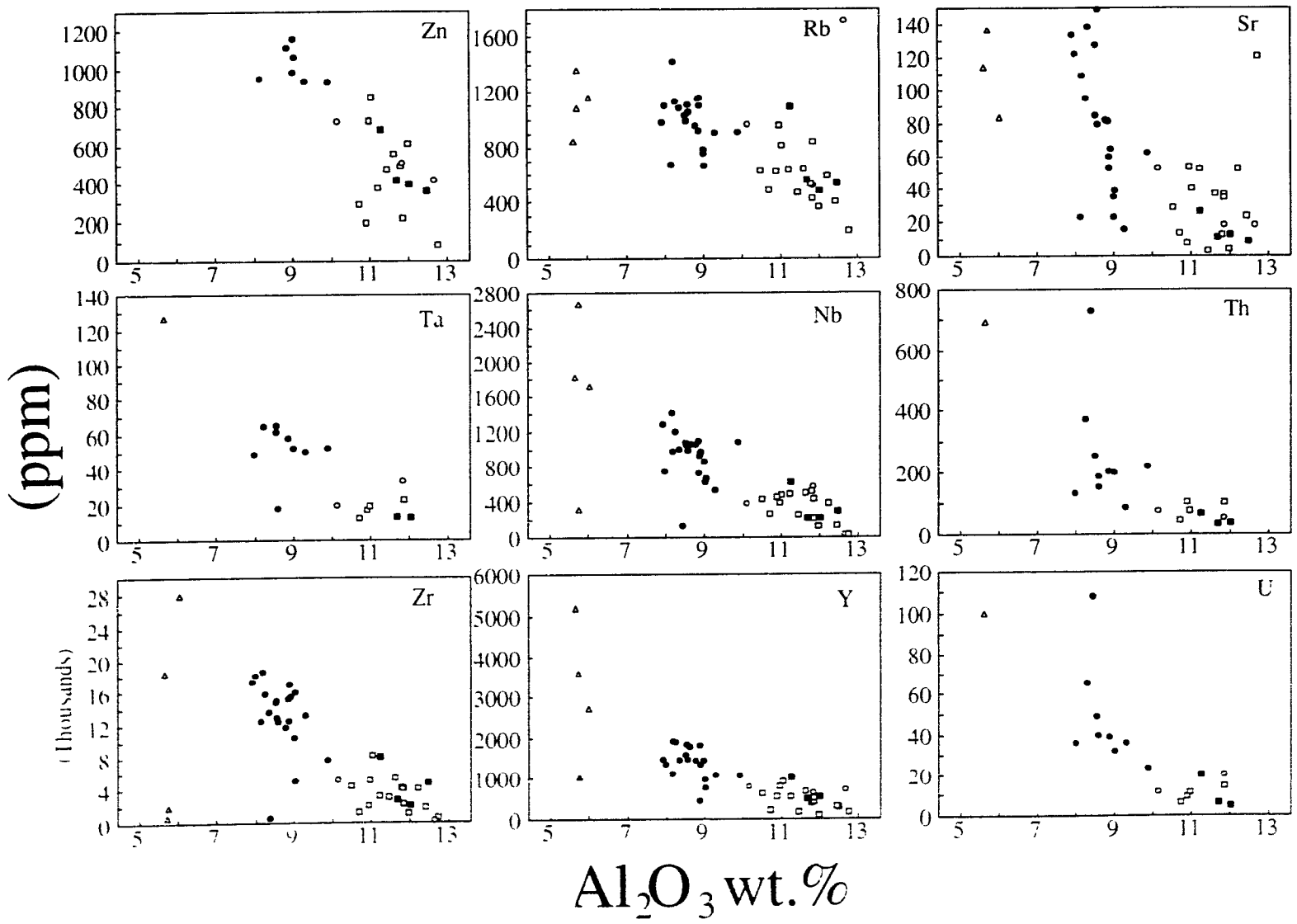
Zn
Rb
Sr
Ta
Nb
Th
Zr
Y
U
(ppm)
(Thousands)
Al_2O_3 wt.%

Figure 6. *REE* chondrite-normalized plots of the different units of the Strange Lake complex. Chondrite values are from Evensen *et al* (1978).

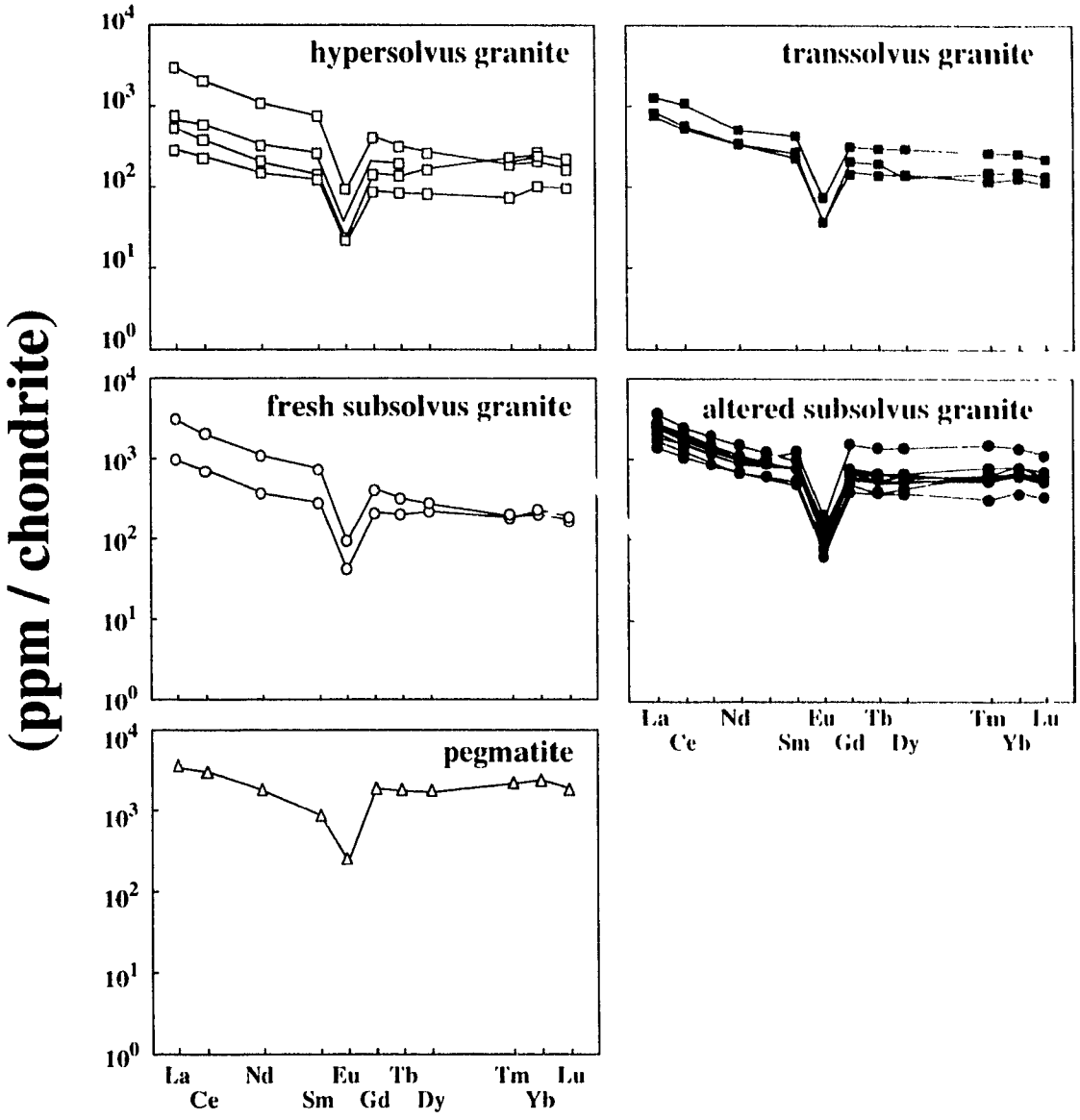
(ppm / chondrite)
hypersolvus granite
transsolvus granite
fresh subsolvus granite
altered subsolvus granite
pegmatite
10^4
10^3
10^2
10^1
10^0
La Ce Nd Sm Eu Gd Tb Dy Tm Yb Lu

increase in *HREE* with evolution: $(La/Yb)_N$ decreases from 9.2 to a value of 1.4 in the pegmatites. All units possess a significant Eu anomaly, Eu/Eu^* ranging from 0.15 to 0.18. With these elevated absolute concentrations, relatively flat patterns and negative Eu anomalies, the units possess *REE* trends typical of A-type granites (Collins *et al.* 1982, Jackson *et al.* 1984, Whalen *et al.* 1987).

Discussion

Pressure of crystallization

According to Tuttle & Bowen (1958), a water-saturated haplogranitic melt can be expected to crystallize with a hypersolvus mineralogy at a confining pressure less than approximately 3.5 kbar, whereas a subsolvus mineralogy is expected above this pressure. Martin & Bonin (1976) proposed that a $P(H_2O) = P$total greater or equal to 2.5 kbar, instead of 3.5 kbar, was required for a metaluminous haplogranitic liquid to yield a subsolvus mineralogy. In addition, a number of igneous complexes have been found to show evidence of a transition from hypersolvus to subsolvus granites (Bonin 1972, 1973, Kamel & Bertraam 1972, Martin & Bonin 1976, Martin 1977, Jackson *et al.* 1985). Confining pressure in these instances can be assumed to have been constant during crystallization, suggesting that factors other than pressure are important. In each case above, the hypersolvus variant was considered to have crystallized from a H_2O-undersaturated granitic melt, resulting in the presence of a single alkali feldspar, whereas the subsolvus granite crystallized from a lower-temperature melt that had become enriched in H_2O, the solidus of which had intersected the alkali feldspar critical

curve (crest of the solvus), resulting in the coexystallization of two distinct alkali feldspars. The Strange Lake intrusive complex is considered to have been emplaced at a shallow crustal level; a semiquantitative estimate of 0.7 kbar is based on inclusions of aqueous fluid in quartz in the mineralized pegmatite (Salvi & Williams-Jones 1992). Even if a confining pressure double their inferred value is proposed, it seems clear that confining pressure at the time of crystallization was more or less constant, and likely less than 2.5 kbar. Thus, variables other than *P*total and *P*(H$_2$O) are required to lower the field of stability of subsolvus granite in terms of *P*total and T.

Constraints imposed by felsic minerals present

The assemblage of felsic minerals in the different units places constraints on the solidus temperatures of the granitic melts from which they crystallized. In terms of pressure and temperature (Fig. 7), relevant solidi are shown, along with the critical curve for alkali feldspar (Luth *et al.* 1974) and the curve for the displacive transformation of α quartz to β quartz (Ghiorso *et al.* 1979).

In the case of the hypersolvus granite at Strange Lake, the presence of a single mesoperthitic feldspar and of "drop" quartz (β-quartz morphology) places its solidus in field H (>650°C, 0.7 kbar; >662°C, 1.5 kbar). The transsolvus granite, with early-formed mesoperthite in a two-feldspar groundmass, has its solidus in field I, which intersects the alkali feldspar solvus (at the temperatures and pressures quoted above). The similarity in bulk composition and the degree of Al-Si order of perthite grains from these two units (Chapter 3) suggests that the transsolvus granite represents

Figure 7. Pressure (kbar) *versus* temperature (°C) diagram showing the likely locations of the solidi for the different units of the Strange Lake pluton. Fields are constrained by isobars of 0.7 and 1.5 kbar. The position of these fields is based on the textures of the felsic minerals in the different units: H, hypersolvus granite; T, transsolvus granite; S, subsolvus granite, P, pegmatite. Other symbols include: AFc, alkali feldspar critical curve, αQ/βQ, α quartz - β quartz displacive transformation. Solidus for the haplogranite system, Hap; the Kûngnât riebeckite granite, ◆; the St. Austell pluton, SA, proposed solidus for the Strange Lake pegmatites, SL, and an ongonite with 1.67% F, ✪, are provided for comparison. Liquidi for the haplogranite system plus 4.5% *ac* + 4.5% *ns*, ▼, plus 4.5% *ns*, ◘ also are shown; the solidi for these compositions were not provided by Carmichael & MacKenzie (1963). Note that the liquidi for the haplogranite system with excess alkalis are even lower than the solidus of the haplogranite system. References are cited in the text.

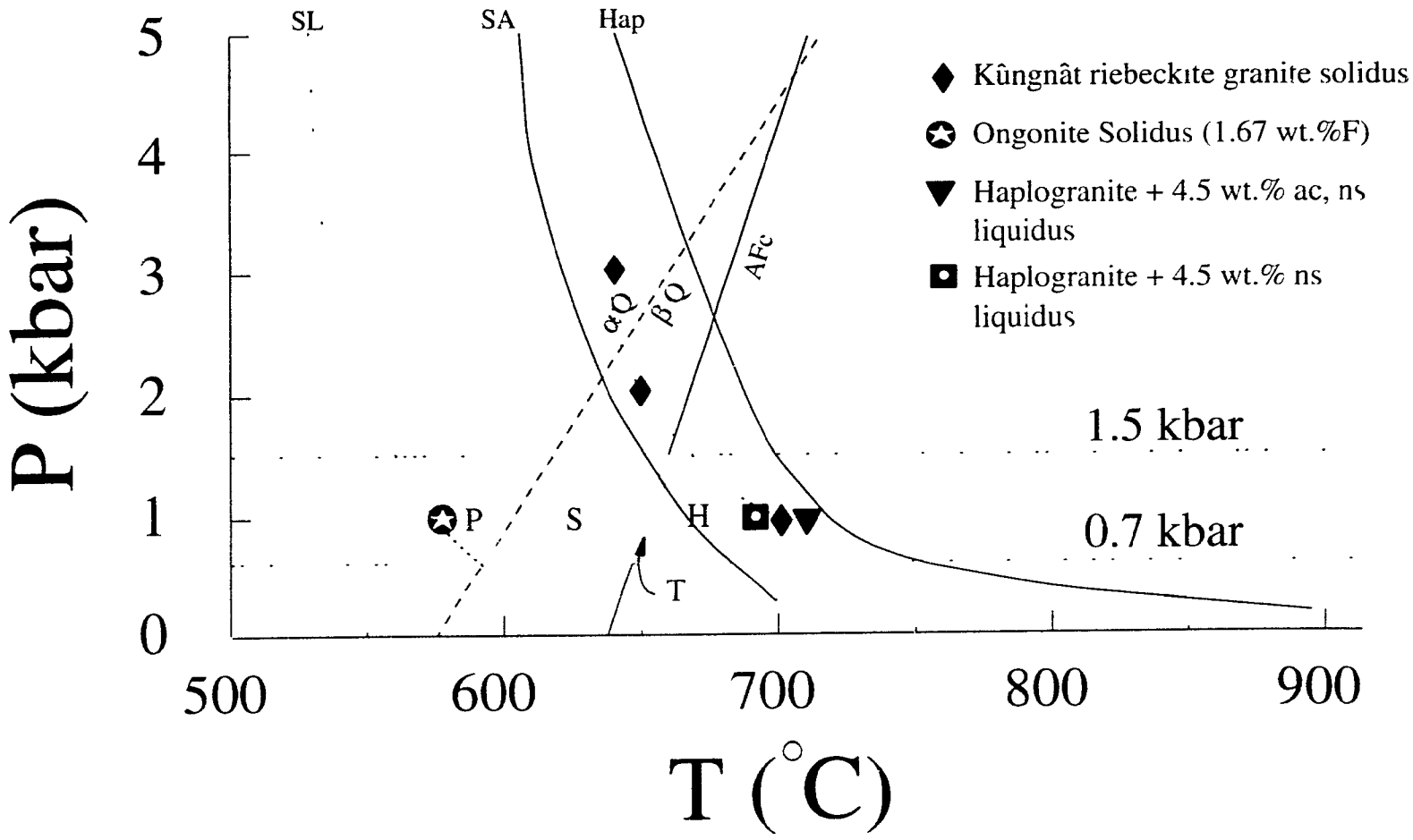
SL
SA
Hap
αQ
βQ
AFc
P
S
H
T
1.5 kbar
0.7 kbar
Kûngnât riebeckite granite solidus
Ongonite Solidus (1.67 wt.%F)
Haplogranite + 4.5 wt.% ac, ns liquidus
Haplogranite + 4.5 wt.% ns liquidus
P (kbar)
0
1
2
3
4
5
500
600
700
800
900
T (°C)

the apical portion of the body of hypersolvus granite. The difference in texture of the two units may be explained by considering the path of crystallization of a granitic melt with increasing volatile content (Whitney 1988). In the case of the coarse-grained hypersolvus granite, a H_2O-undersaturated melt crystallized over a relatively large interval of temperature. Volatiles, including fluorine in this case, migrated to the upper portion of the magma chamber, contributed to a lowering of the solidus, and promoted the crystallization of the fine-grained transsolvus granite over a short interval of temperature. Most of the fluorine seems to have escaped upon crystallization. Next, the subsolvus granite, with its two primary feldspars and β-quartz, has a solidus in field S, which is bounded by the alkali feldspar critical curve and α-β quartz reaction. Finally, the assemblage two-feldspar + α-quartz typical of the pegmatite places its solidus within field P (590°C, 0.7 kbar, <615°C, 1.5 kbar).

The role of excess alkalis

Experimental studies on peralkaline granitic systems have demonstrated that the temperature of the liquidus surface (Carmichael & MacKenzie 1963, Thompson & MacKenzie 1967) and of the solidus (McDowell & Wyllie 1971) of these melts are lower than those of the haplogranite system. Carmichael & MacKenzie (1963) determined a minimum liquidus temperature of 715°C for the haplogranite system with 4.5% $NaAlSi_3O_8$ (*ab*) + 4.5% Na_2SiO_3 (*ns*) added at a $P(H_2O)$ of 1 kbar (Fig. 7) and noted a progressive shift of the minima towards the Qtz-Or join ("a" in Fig. 4). Thompson & MacKenzie (1967) determined a liquidus minimum of 693°C for the

haplogranite system with 5% *ns* added at the same pressure (Fig. 7) (haplogranite liquidus minimum 730°C, 1kbar). McDowell & Wyllie (1971) determined the following solidus temperatures for the Küngnât riebeckite granite: 700°C at 1 kbar, 650°C at 2 kbar, and 640°C at 3 kbar (Fig. 7) (haplogranite solidus 715°C, 1 kbar). These experiments demonstrate that the presence of excess alkalis in a granitic melt extends the course of crystallization to lower temperatures (Bailey & Schairer 1966) by promoting the formation of non-bridging bonds in the granitic melt (Onorato *et al.* 1985). Consequently, higher diffusivities of cations result and account, in part, for the higher levels of *HFSE*s and *LIL*s in the more evolved melts.

The addition of alkalis to the granite system also enhances the solubility of water in the liquid and the proportion of dissolved silicates in a coexisting vapour (Luth & Tuttle 1969, Mustart 1972) such that a continuous transition from peralkaline magma to a hydrothermal solution may exist in some natural systems. This increased solubility between liquid and vapour phases suggest reduced temperatures of solidi for peralkaline systems (Luth 1976). This relationship may ensure that the granitic liquid remains undersaturated in H_2O until close to the solidus.

Constraints imposed by mafic mineralogy

Relative temperatures of formation and $f(O_2)$ conditions for the different granitic magmas may be inferred from the experimentally determined fields of stability of mafic minerals. In a plot of $f(O_2)$ *versus* temperature (Fig. 8) for a $P(H_2O)$ of 1 kbar, stability fields of end-member ferrorichterite (Charles 1975) and end-member arfvedsonite (Ernst

Figure 8 Log $f(O_2)$ *versus* temperature (°C) diagram showing the stability fields of ferroriehterite (Charles 1975) and arfvedsonite (Ernst 1962). Symbols used: Rbk, riebeckite; Rbk-Arf, riebeckite-arfvedsonite solid solution; Fe Rt, ferroriehterite, Fe Pa, ferropargasite Symbols for oxygen fugacity buffers: HM, hematite-magnetite, NNO, nickel-nickel oxide, QFM, quartz-fayalite-magnetite; MW, magnetite-wüstite; IW, iron-wüstite; MI, magnetite-iron, and FQI, fayalite-quartz-iron.

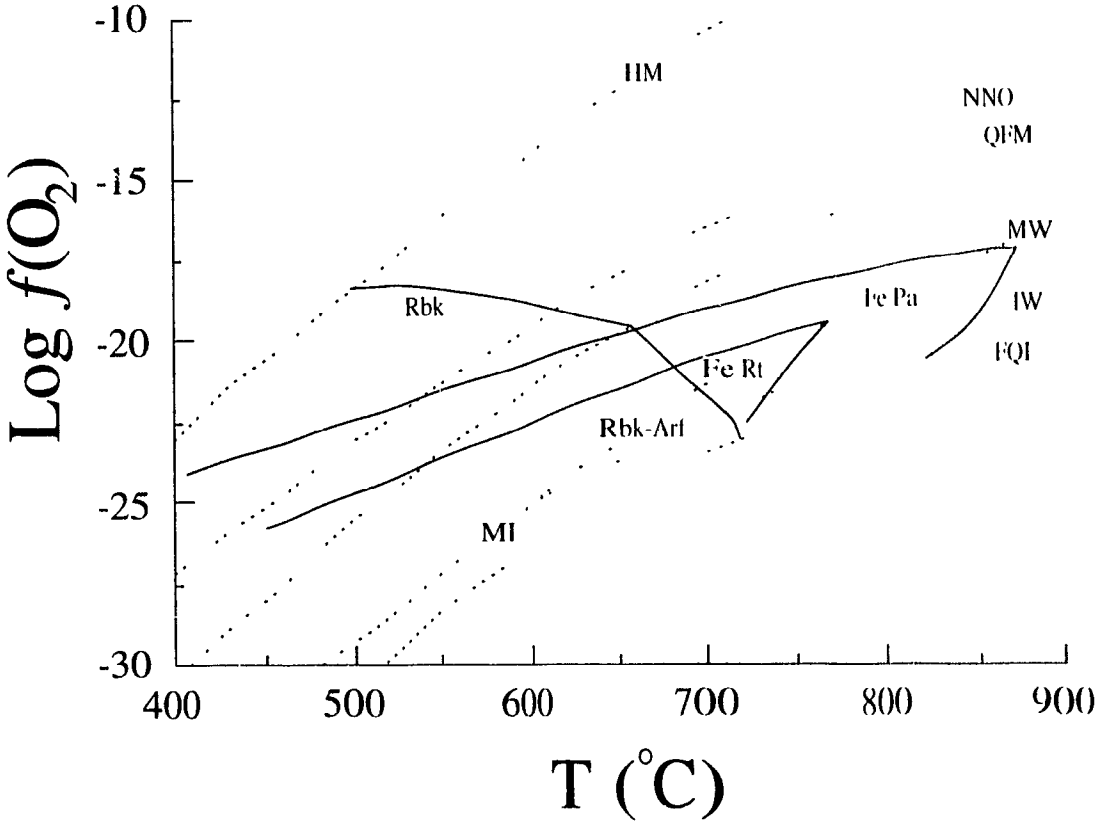
-10
-15
-20
-25
-30
Log $f(O_2)$
400
500
600
700
800
900
T (°C)
HM
NNO
QFM
MW
IW
FQI
Rbk
Fe Pa
Fe Rt
Rbk-Arf
MI

1962) are shown.

In the hypersolvus granite, the amphibole has a ferrorichteritic core and an arfvedsonitic rim (Pillet 1989). This zonation is marked by a decrease in Ca, an increase in Na and Si, and an inferred increase in Fe^3. The sequential crystallization of the Na-Ca (ferrorichterite) and Na (arfvedsonite) amphiboles in the hypersolvus granite reflects mostly the progressive depletion of calcium in the melt and is consistent with a decrease in temperature. An increase in Fe^3 would normally indicate an increase rather than a decrease in oxygen fugacity, but the amphibole assemblage suggests the latter. Thornber *et al* (1980) have shown that Fe^{3+} activity increases with the peralkalinity of a magma. In such a case, Fe^{3+} may increase as oxygen fugacity falls.

At 1 kbar, the upper stability-limit of end-member ferrorichterite is 535°C and 760°C for the QFM and MW buffers, respectively (Charles 1975). Riebeckite-arfvedsonite solid solutions are stable up to 650°C and 695°C for the QFM and MW buffer, respectively (Ernst 1962). On the assumption that the arfvedsonite rims crystallized at a lower temperature than the ferrorichterite cores, they would have crystallized closer to the MW buffer than to QFM. As for the associated aenigmatite, it has a lower stability limit of 700°C at $P(H_2O)$ of 0.7 kbar at the magnetite-wüstite buffer (Ernst 1962). The feldspar, having crystallized prior to much of the amphibole and aenigmatite, would therefore have formed at least above 700°C, which is consistent with its hypersolvus character. The albite-arfvedsonite "swapped margins", albite overgrowths and secondary mafic minerals, are indicative of subsolidus circulation of sodium- and iron-bearing intergranular pore fluids.

Arfvedsonite and aegirine occur as both early phenocrysts and late grains in the subsolvus granite. The absence of albite and microcline in the cores of these phenocrysts suggests that the mafic minerals crystallized, in part, prior to the feldspars. Although the presence of near-end-member arfvedsonite (Salvi & Williams-Jones 1990, Pillet 1989) is consistent with low $f(O_2)$ conditions, the late appearance of quenched crystals of aegirine coexisting with hematite (Fig. 21), and the replacement of arfvedsonite by aegirine, are consistent with the striking late increase of the fugacity of oxygen. One mechanism that could explain this phenomenon is sudden degassing upon saturation of the magmatic system in water, with preferential loss of hydrogen over oxygen.

The role of F

The progressive decrease in solidus temperatures of the granitic units and the pegmatites may be ascribed mostly to the F enrichment in the Strange Lake complex. Experimental work has shown that addition of F to water-saturated granitic melts reduces their solidus to a temperature below 570°C at low pressure (Koster van Groos & Wyllie 1968, Anfilogov *et al* 1973, Kovalenko 1977, Manning & Henderson 1981, Webster *et al* 1987). Manning (1981) obtained a minimum liquidus temperature of 630°C and detected the coexistence of two separate alkali feldspars, quartz, glass, and vapour at temperatures as low as 550°C at 1 kbar for the haplogranitic system with 4 wt.% F added. Other studies demonstrated significant lowering of the solidus to 663°C for natural systems containing 1.15 wt% F (Fig. 7) (*cf* Weidner & Martin 1987)

Fluorine depolymerizes the silicate network of granitic melts. As a result, liquidus and solidus temperatures are reduced, and the liquidus field of quartz expands at the expense of that of feldspar (Manning 1981, Dingwell 1988). Fluorine also reduces melt viscosity, enhances the diffusivity of cations, and thus favours the concentration of HFS elements in granitic systems

Based on the F and Zr content of unaltered hypersolvus granite at Strange Lake and the positive correlation of F and Zr in pantelleritic obsidians (Bailey & Macdonald 1975), Boily & Williams-Jones (pers. comm., 1992) extrapolated a fluorine content of 3.7 wt.% for the subsolvus granitic melt. This value is close to the predicted amount of F required to lower the granite minimum to 630°C (Manning 1981) assuming that only F (and not other fluxing agents like excess Na and K) is responsible for the lower solidus. This would result in the intersection of the solidus and solvus, and the ensuing crystallization of two separate feldspars from a melt. It is interesting to note that both the Slip fluorite granite (1.15 wt.% F; Weidner & Martin 1987) and a topaz-bearing ongonite (2.25 wt.% F, Kovalenko *et al.* 1971) also contain a subsolvus assemblage (K-feldspar and albite)

The "hypersolvus" and "transsolvus" granitic melts crystallized in the field of alkali feldspar, whereas the melts that gave the subsolvus granites crystallized in the field of quartz. This transition is ascribed to the evolution along a liquid line of descent as alkali feldspar crystallized. The crystallization of quartz as a liquidus phase in the subsolvus granite attests to the expansion of the primary field of quartz owing to increased F content of the evolving melt (much of it ultimately lost during degassing).

The *HREE* enrichment in the altered subsolvus granite and pegmatites reflects 1) the tendency for *HREE* to form more stable alkali-*REE*-fluoride complexes than *LREE* (Herrmann 1969, Christiansen *et al* 1983) and 2) the interaction of these rocks with a subsolidus F-enriched fluid (Kontak 1990) released upon degassing

Origin of the enrichment in K in the pegmatites

The elevated K/Na values of the pegmatites (Table 1) are consistent with the elevated Or content of the bulk feldspar separates of the pegmatites (Chapter 3) The sodium in the pegmatites is mostly incorporated in arfvedsonite and aegirine, not albite Even by assigning all normative sodium minerals to Ab, the bulk compositions of the pegmatites plot away from the granite minimum toward the Qtz-Or join in the haplogranite system. What causes such a shift?

Jahns & Burnham (1969) suggested that a water-saturated melt was required to crystallize coexisting albite-enriched aplite and K-feldspar-enriched pegmatite, the bulk composition of which corresponds to the pseudoternary minimum in the granite system (Jahns & Tuttle 1963). In their model, any K-enriched pegmatite, usually near the hanging wall, is "matched" by an albite-rich aplite, near the footwall contact They proposed that circulating bubbles could redistribute the alkalis in the melt and thereby cause its freezing (by so-called compositional quenching) London *et al* (1989) and London (1992), on the other hand, contended that an initially vapour-undersaturated melt can crystallize K-enriched pegmatite under disequilibrium conditions London (1992) suggested that the decreasing density of K-feldspar nuclei and the increasing

concentrations of melt-interactive, crystal-incompatible components like fluorine seem to be the key to pegmatite formation. The experiments from which these models were formulated were performed in the presence of thermal gradients. London (1992) reasoned that the evidence for early saturation in an aqueous fluid in most granitic pegmatites is weak, and that no role should thus be attributed to the fluid phase to explain either textural features of the pegmatites or, in this context, their anomalous enrichment in K. The peralkalinity of the system is another reason to discount the hypothesis of early saturation in a free aqueous phase.

The dilemma is perhaps resolvable, in the case of Strange Lake at least, by proposing that although early saturation (i.e., in hypersolvus granite) in a free aqueous phase likely did not occur, saturation must have occurred once the solidus of the most evolved granitic liquid was intersected, possibly at 575°C or so (Fig. 7). In view of the melt's peralkalinity and near-surface emplacement, large volumes of water must have been expelled upon saturation, probably explosively, leading to brecciation and fluidization along the main fractures. One is tempted to attribute to this event of catastrophic degassing the important loss of Na (and F?) from the bulk composition of the final products of magmatic crystallization. The hypothesis of massive degassing of the magma chamber could be tested by an investigation of the stable isotope geochemistry of the complex.

Salvi & Williams-Jones (1992) have demonstrated the presence of what was considered to be inclusions of the primary orthomagmatic fluid in quartz from the pegmatites. They reported salinities ranging from 23 to 27 wt. % NaCl eq., the presence

of NaCl as the only solid phase in the decrepitated primary inclusions, and inferred a trapping temperature of approximately 600°C. With the solidus temperature of the pegmatite-forming melt constrained to just below 600°C, vapour saturation may indeed have begun to occur above the solidus, as recorded by the presence of miarolitic cavities.

This fluid, coexisting initially with Na- and K-rich feldspars, is known to be very sodic [i.e., Na/(Na+K) = 0.95 at 1 kbar, 500°C] in the presence of fluoride (Pichavant 1983). This Na enrichment confirms the empirical data of Salvi & Williams-Jones (1992). The alkali feldspar in equilibrium with this sodic fluid remains very K-rich (up to 90 mol.% Or; Pichavant 1983). In light of these experimental results, the quantitative evacuation of the system near its solidus could thus lead to massive loss of Na and F, and explain the anomalous buildup in K in the final products of magmatic crystallization.

Conclusions

The Strange Lake peralkaline complex offers an example of the influence of chemical composition on granitic textures. The granites have crystallized at a shallow depth, possibly less than 5 km (*i.e.*, ~1.5 kbar), and yet the most evolved subsolvus granite possesses a two-feldspar magmatic assemblage. In the haplogranite system, a $P(H_2O)$ of 2.5 kbar is required to crystallize two separate alkali feldspars (Tuttle & Bowen 1958, Luth 1976). The addition of fluorine and excess alkalis to the water-saturated melt has lowered the liquidus and solidus, thereby extending the course of

crystallization for the subsolvus granite to lower-than-expected temperatures. The additive effects of these extra components promoted the intersection of the solidus and the alkali feldspar solvus at relatively low confining pressures. The solidus temperature for the subsolvus peralkaline granite probably was lowered to temperatures below 600°C. By comparison, the least evolved hypersolvus granite crystallized from a water-undersaturated melt at temperatures in the vicinity of 700°C.

The presence of miarolitic cavities in the subsolvus granites and the pegmatites shows that the granitic magma at Strange Lake did reach water saturation at the latest stages of magmatic crystallization, in spite of enhanced solubility of H_2O in a peralkaline melt. Alteration haloes as well as pervasive alteration of entire outcrops in the form of "hematization" and "aegirinization" (Salvi & Williams-Jones 1990) also suggest the involvement of an oxygenated (owing to the loss of hydrogen during degassing) and alkaline fluid. Evacuation of the system at this stage can explain the anomalous buildup in K over Na in the granitic pegmatites. The alkaline fluid probably is responsible for the efficient redistribution of the ore constituents within the complex, and may well have promoted efficient recrystallization (fenitization?) in the more calcic and magnesian wallrocks. The Ca, Mg, Sr, Ba and Be(?) so released were reintroduced at low temperature into the pluton by circulation along fractures expected by thermal contraction. This proposal successfully accounts for the anomalous buildup in Ca and Mg in the most evolved granites, and seems much more plausible than the pattern of magmatic enrichment in Ca and Mg expressed by Birkett *et al.* (1992).

References

Ahmedali, T. (1983) XRF procedures, circular no.1, Department of geological sciences, McGill University

Anfilogov, V.N., Glyuk, D.S. & Frufanova, L.G. (1973). Phase relations in interaction between granite and sodium fluoride at water vapour pressure of 1000 kg/cm^2. *Geochem Int* **10,** 30-33.

Bailey, D.K. & Macdonald, R. (1975). Fluorine and chlorine in peralkaline liquids and the need for magma generation in an open system *Mineral Mag* **40,** 405-414

_____ & Schairer J.F (1966): The system Na_2O - Al_2O_3 - Fe_2O_3 - SiO_2 at 1 atmosphere, and the petrogenesis of alkaline rocks. *J Petrol* **7,** 114-170.

Birkett, T.C., Miller, R.R., Roberts, A.C. & Mariano, A.N. (1992) Zirconium-bearing minerals of the Strange Lake intrusive complex, Quebec-Labrador *Can Mineral* **30,** 191-205.

Boily, M., Brooks, C., Ludden, J.N. & James, D.E. (1989): Chemical and isotopic evolution of the Coastal Batholith of southern Peru. *J Geophys Res* **95,** 12483-12498.

Bonin, B. (1972): Le complexe granitique annulaire de la région de Tolla-Cauro (Corse). Thèse 3^e cycle, Univ. Paris VI, France.

_____ (1973): Les complexes granitiques subvolcaniques de Corse. *1ère Réunion ann Sci. Terre, Paris, France,* 88 (abstr.).

_____ (1986): Ring complex granites and anorogenic magmatism. Elsevier, New York, 188 pp.

Bowden, P., Black, R., Martin, R.F., Ike, E.C., Kinnaird, J.A. & Batchelor, R.A. (1987): Niger - Nigerian alkaline ring complexes, a classic example of African Phanerozoic anorogenic mid-plate magmatism. *In* Alkaline Igneous Rocks (J.G.

Fitton & B.G.J. Upton, eds.). *Geol Soc London Spec. Publ.* **30,** 357-379.

Carmichael, I.S.E. & MacKenzie, W.S. (1963): Feldspar - liquid equilibria in pantellerites: an experimental study. *Am J. Sci.* **261,** 382-396.

Charles, R W (1975): The phase equilibria of richterite and ferrorichterite. *Am. Mineral* **60,** 367-374.

Christiansen, E.H., Burt, J.V., Sheridan, M.F. & Wilson, R.T. (1983): The petrogenesis of topaz rhyolites from the western United States. *Contrib Mineral. Petrol* **83,** 16-30.

Collins, W.J., Beams, S.D., White, A.J.R. & Chappell, B.W. (1982): Nature and origin of A-type granites with particular reference to southeastern Australia. *Contrib. Mineral Petrol* **80,** 189-200.

Currie, K.L. (1985): An unusual peralkaline granite near Lac Brisson, Quebec-Labrador *Geol. Surv. Can., Pap* **85-1A,** 73-80.

Dingwell, D.B (1988): The structures and properties of fluorine-rich magmas: a review of experimental studies. *In* Recent advances in the geology of granite-related mineral deposits (R.P. Taylor & D.F. Strong, eds.). *Can. Inst. Min Metall., Spec Vol* **39,** 1-12.

Drysdall, A R , Jackson, N.J., Ramsay, C.R., Douch, C.J. & Hackett, D. (1984): Rare element mineralization related to Precambrian alkali granites in the Arabian Shield. *Econ Geol.* **79,** 1366-1377.

Ernst, W.G. (1962). Synthesis, stability relations, and occurrence of riebeckite and riebeckite-arfvedsonite solid solutions. *J Geol.* **70,** 689-736.

Evensen, N.M., Hamilton, P.J. & O'Nions, R.K. (1978): Rare-earth abundances in chondritic meteorites. *Geochim Cosmochim. Acta*, **42,** 1199-1212.

Ghiorso, M.S., Carmichael, I.S.E. & Moret, L.K. (1979): Inverted high-temperature quartz. Unit cell parameters and properties of the α-β quartz inversion. *Contrib Mineral. Petrol* **68**, 307-323.

Harris, N.B.W. & Marriner, G.F. (1980): Geochemistry and petrogenesis of a peralkaline granite complex from the Midian Mountains, Saudi Arabia *Lithos* **13**, 325-337.

Herrmann, A.G. (1969): Yttrium and lanthanides, sect 39. *In* Handbook of Geochemistry 2, pt. 5 (K.H. Wedepohl, ed.). Springer-Verlag, Berlin.

Hoffman, P.F. (1988): United plates of America, the birth of a craton, early Proterozoic assembly and growth of Proto-Laurentia. *Rev Earth Planet Sci* **16**, 71 p

Jackson, N.J., Drysdall, A.R. & Stoeser, D.B. (1985): Alkali granite-related Nb-Zr-REE-U-Th mineralization in the Arabian Shield. *In* High Heat Production granites, hydrothermal circulation and ore genesis, IMM, London, 470-487.

_____, Walsh, J.N. & Pegran, E. (1984): Geology, geochemistry and petrogenesis of the late Precambrian granitoids in the Central Hijaz Region of the Arabian Shield *Contrib. Mineral Petrol* **87**, 205-219.

Jahns, R.H. & Burnham, C.W. (1969): Experimental studies of pegmatite genesis: I A model for the derivation and crystallization of granitic pegmatites. *Econ Geol* **64**, 843-864.

_____, R.H. & Tuttle, O.F. (1963): Layered pegmatite-aplite intrusives. *Mineral Soc Am. Spec. Pap.* **1**, 78-92.

Karner, F.R. & Bertraam, R.E. (1982): Modal variation in granitic units of the White Mountain plutonic - volcanic series, New Hampshire. *24th Int Geol Congr*, Sect. **2**, 164-170.

Kontak, D.J. (1990): The East Kempville topaz-muscovite leucogranite, Nova Scotia. I. Geological setting and whole-rock geochemistry. *Can Mineral* **28**, 787-825.

Koster van Groos, A.F. & Wyllie, P.J. (1968): Melting relationships in the system $NAlSi_3O_8$ - NaF - H_2O to 4 kilobars pressure. *J. Geology* **76,** 50-70.

Kovalenko, N.I. (1977): The reactions between and aqueous hydrofluoric acid in relation to the origin of fluorine-bearing granites. *Geokhimiya* **4,** 503-515.

_____, Kuz'man, M.I., Antipin, V.S. & Petrov, L.L. (1971): Topaz-bearing keratophyre (ongonite), a new variety of subvolcanic igneous vein rock. *Dokl Akad. Sci. USSR, Earth Sci Sect* **199,** 132-135.

Lacroix, A. (1923). La signification des granites alcalins très riches en soude. C.R. Acad. Sci Paris, **177,** 417-422.

London, D. (1992). The application of experimental petrology to the genesis and crystallization of granitic pegmatites. *Can Mineral* **30,** 498-540.

_____, Morgan, G.B., VI & Hervig, R. L. (1989): Vapor-undersaturated experiments with Macusani glass + H_2O at 200 MPa, and the internal differentiation of granitic pegmatites. *Contrib Mineral Petrol.* **102,** 1-17.

Luth, W.C. (1976). Granitic Rocks. *In* The evolution of the crystalline rocks (D.K. Bailey & R. Macdonald, eds.). Academic Press, London (335-417).

_____, Martin, R.F. & Fenn, P.J. (1974): Peralkaline alkali feldspar solvi. *In* The feldspars: Proc. NATO advanced studies institute. (W.S. Mackenzie & J. Zussman, eds.). Manchester University Press, Manchester (297-312).

_____ & Tuttle, O.F. (1969): The hydrous vapour phase in equilibrium with granite and granite magmas *Geol Soc Am Mem* **115,** 513-548.

Manning, D.A.C. (1981): The effect of fluorine on liquidus phase relationships in the system qz-ab-or with excess water at 1 kb. *Contrib Mineral. Petrol* **76,** 206-215.

_____ & Henderson, C.M.B. (1981): The effect of the addition of fluorine on liquidus phase relationships in the system Qz-Ab-Or with excess water at 1 kb. *N.E.R.C.*

Rep Prog. Exper Petrol **5,** 16-23

Martin, R.F. (1977): The association hypersolvus granite - subsolvus granite - "Solvsbergite" at Andrew's Point, Cape Ann, Massachusetts: a case of localized fenitization. *Am J Sci* **277,** 273-287

_____ & Bonin, B. (1976) Water and magma genesis: the association hypersolvus granite - subsolvus granite. *Can Mineral* **14,** 228-237

McDowell, S.D. & Wyllie, P.J. (1971): Experimental studies of igneous rock series the Kûngnât syenite complex of southwest Greenland *J Geol* **79,** 173-194

Miller, R.R. (1986). Geology of the Strange Lake alkalic complex and the associated Zr-Y-Nb-Be-REE mineralization. *Newfoundland Dep Mines and Energy Mineral Development Div., Rep* **86-1,** 11-19.

_____ (1990): The Strange Lake pegmatite-aplite hosted rare-metal deposit, Labrador. *Newfoundland Dep Mines and Energy, Geol Surv Branch, Rep* **90-1,** 171-182

Mustart, D.A. (1972) Phase relations in the peralkaline portion of the system Na_2O - Al_2O_3 - SiO_2 - H_2O. Ph.D. thesis, Stanford University, Stanford, California

Onorato, P.I.K., Alexander, M.N., Struck, C.W. & Tasker, G.W. (1985) Bridging and nonbridging oxygen atoms in alkali aluminosilicate glasses. *J Am Ceram Soc* **68,** C148-150.

Pichavant, M. (1983): (Na, K) exchange between alkali feldspars and aqueous solutions containing borate and fluoride anions; experimental results at P = 1 kbar 3rd NATO advanced study institute on feldspars, feldspathoids and their paragenesis, Rennes, France, 102. (abstr.).

Pillet, D. (1989): Le granite peralcalin du Lac Brisson, Labrador Central (province du Québec, Canada): pétrologie, géochronologie, et relations avec les minéralisations internes à Zr, Y, Nb. Thèse de doctarat, Université Claude Bernard-Lyon I, Lyon, France.

_____, Bonhomme, M.G., Duthou, J.L. & Chenevoy, M. (1989): Chronologie Rb/Sr et K/Ar du granite peralcalin du lac Brisson, Labrador central, Nouveau-Québec. *Can. J. Earth Sci.* **26,** 328-332

Pillet, D., Chenevoy, M. & Bélanger, M. (1992). Pétrologie du granite peralcalin du lac Brisson, Labrador central, Nouveau-Québec. 1. Mode de mise en place et évolution chimique. *Can. J. Earth Sci.* **29,** 353-372

Salvi, S. & Williams-Jones, A.E. (1990): The role of hydrothermal processes in the granite-hosted Zr, Y, REE deposit at Strange Lake, Quebec/Labrador: evidence from fluid inclusions. *Geochim. Cosmo. Acta* **54,** 2403-2418.

_____ & _____ (1992): Reduced orthomagmatic C-O-H-NaCl fluids in the Strange Lake rare-metal granitic complex, Quebec/Labrador, Canada. *Eur. J. Mineral.* **4,** 1155-1174

Streckeisen, A. (1976). To each plutonic rock its proper name. *Earth Sci. Rev.* **12,** 1-23.

Tauson, L.V. (1967): Geochemical behaviour of rare elements during crystallization and differentiation of granitic magmas. *Geochem. Int.* **4,** 1067-1074

Thompson, R.N. & MacKenzie, W.S. (1967): Feldspar - liquid equilibria in peralkaline acid liquids: an experimental study. *Am. J. Sci.* **265,** 714-734

Thornber, C.R., Roeder, P.L. & Foster, J.R. (1980): The effect of composition on the ferric-ferrous ratio in basaltic liquids at atmospheric pressure. *Geochim. Cosmochim. Acta* **44,** 525-532

Tuttle, O.F. & Bowen, N.L. (1958): Origin of granite in the light of experimental studies in the system $KAlSi_3O_8$ - $NaAlSi_3O_8$ - SiO_2 - H_2O. *Geol. Soc. Am. Mem.* **74,** 153 pp

Watson, E.B. (1979). Zircon saturation in felsic liquids: experimental results and applications to trace element geochemistry. *Contrib. Mineral. Petrol.* **70,** 407-419.

Webster, J.D., Holloway, J.R. & Hervig, R.L. (1987): Phase equilibria of Be, U and F-enriched vitrophyre from Spor Mountain, Utah. *Geochim Cosmochim Acta* **51,** 389-402.

Weidner, J.R. & Martin, R.F. (1987): Phase equilibria of a Be, U and F-enriched vitrophyre from Spor Mountain, Utah. *Geochim Cosmochim Acta* **51,** 1591-1597

Whalen, J.B., Currie, K.L. & Chappell, B.W. (1987): A-type granites, geochemical characteristics, discrimination and petrogenesis. *Contrib Mineral Petrol* **95,** 407-419.

Whitney, J.A. (1988): The origin of granite, the role and source of water in the evolution of granitic magmas. *Geol Soc Am Bull* **100,** 1886-1897

Zajac, I.S., Miller, R.R., Birkett, T.C. & Nantel, S. (1984): Le gîte de Zr, Y, Nb et Be du complexe alcalin de Strange Lake, Québec - Labrador. Ministère de l'Energie et des Ressources, Québec, DV 84-18, 127-142.

CHAPTER 3

Feldspar Mineralogy and Geochemistry of the Strange Lake Peralkaline Complex

Abstract

The structural state and geochemistry of the alkali feldspars from the various intrusive units of the Strange Lake peralkaline complex (Quebec-Labrador) were investigated. The high degree of order of the feldspars, *i.e.*, low microcline and low albite ($t_1O > 0.98$), is attributed to the presence of an alkaline fluid phase in the cooling pluton. Near-end-member compositions of the feldspars (albite, $X_{Or} < 0.03$; microcline, $X_{Or} > 0.96$), consistent with compositions obtained from electron-microprobe analysis, indicate temperatures of equilibration below 300°C. The Ca content of the feldspars is extremely low. Anomalously high *b* unit-cell dimensions in K-feldspar are consistent with the incorporation of Rb and Fe^{3+} in the structure. The mol % Or of the bulk feldspar increases with evolution; this trend can be explained by degassing of the magma near or at the solidus, and ensuing forced crystallization upon massive loss of Na to the fluid phase. The incompatible elements Li, Rb, Cs and Tl in the feldspar fraction show marked increases from hypersolvus to pegmatitic samples (Li, 1 to 45 ppm; Rb, 500 to 4600; Cs, 1 to 6.5; Tl, 2.6 to 15), which is consistent with the fractionation of a single batch of magma. The concentration of the compatible elements (Ba, Sr) in general decreases (Ba, 99 to 18 ppm; Sr, 29.5 to 0), with minor exceptions due to late-stage alteration. By and large, the rare-earth elements are not structurally bound in the feldspar. Most of the Ca in the most evolved rocks was introduced at the hydrothermal stage, presumably as a result of contamination from the wall rocks.

Introduction

The Strange Lake anorogenic granitic pluton, of Middle Proterozoic age, is located on the Labrador-Québec border 250 km north of Schefferville (Fig. 1). The pluton has strategic importance, in view of the significant levels of Zr, Y, and *REE* mineralization near its centre ("Ore zone", Fig. 1). A lively debate has developed recently over the timing of the mineralization. Proponents of a *magmatic* process of Zr, Y, *REE* enrichment in the ore zone (Birkett *et al.* 1992) claim that crystallization of primary alkali zirconosilicates like dalyite, vlasovite and elpidite efficiently led to an increase in the content and activity of calcium in the residual magma, to the extent that calciferous zirconosilicates like armstrongite, and possibly calcium catapleiite and gittinsite as well, were stabilized instead of the alkali-bearing zirconosilicates (Birkett *et al.* 1992, p. 201). Protagonists of a *metasomatic* model of mineralization (Salvi & Williams-Jones 1990, 1991) contend that the Strange Lake pluton, though indeed strange, most likely followed a normal path of igneous fractionation, and that calcium was introduced, possibly from the country rocks *via* an aqueous phase at a low subsolidus temperature. The latter view is well documented by evidence from fluid inclusions trapped in quartz that accompanied the formation of gittinsite ($CaZrSi_2O_7$) and other ore minerals. This investigation of the feldspar mineralogy of representative fresh and hydrothermally altered samples of the Strange Lake granitic complex was undertaken to characterize the compositional and structural evolution of the dominant rock-forming mineral in the pluton. Along with the textural descriptions provided in Chapter 2, this information allows an evaluation of the conditions of magmatic crystallization.

Figure 1. Geological map of the Strange Lake peralkaline complex, astride the Quebec-Labrador border, showing the major intrusive phases and the country rocks. The map units are modified from Miller (1986) and Salvi & Williams Jones (1990). The granite classification is based on the petrographic descriptions given in Chapter 2. The location of the samples selected for this study is shown.

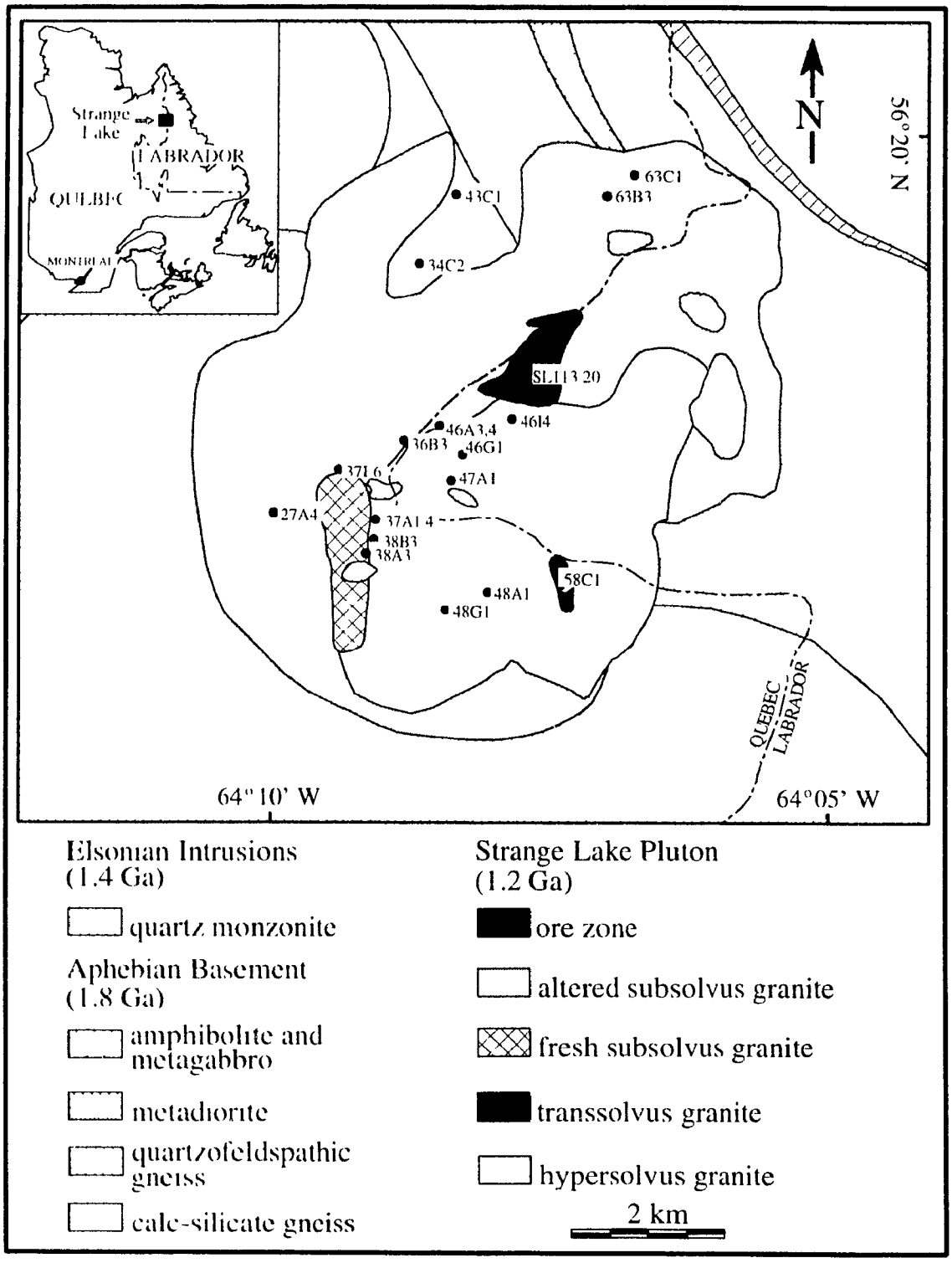
Strange Lake
LABRADOR
QUEBEC
MONTREAL
N
56°20' N
43C1
63C1
63B3
34C2
SL113 20
46A3,4
46I4
36B3
46G1
37L6
47A1
27A4
37A1 4
38B3
38A3
58C1
48A1
48G1
QUEBEC
LABRADOR
64°10' W
64°05' W
Elsonian Intrusions
(1.4 Ga)
quartz monzonite
Aphebian Basement
(1.8 Ga)
amphibolite and metagabbro
metadiorite
quartzofeldspathic gneiss
calc-silicate gneiss
Strange Lake Pluton
(1.2 Ga)
ore zone
altered subsolvus granite
fresh subsolvus granite
transsolvus granite
hypersolvus granite
2 km

and the subsequent postmagmatic evolution of the Strange Lake complex. Our results allow a definitive statement to be made concerning the behaviour of calcium throughout the evolution of the complex.

Details About the Intrusive Units

This study of the detailed mineralogy of feldspar-group phases at Strange Lake builds on the detailed textural and compositional characterization that allows the distinction of the various intrusive units (Chapter 2). The *hypersolvus granite* is exposed in the southeastern portion of the complex (Fig. 1). It represents the earliest and geochemically least evolved intrusive phase. When the magma froze, the resulting granite consisted of a single alkali feldspar (now mesoperthitic), as well as quartz, and late sodic-calcic to sodic amphibole. The *transsolvus granite*, found only at the periphery of the hypersolvus granite, represents the apical portion of this unit. It is characterized by the former presence of single-phase feldspar (now mesoperthitic) as phenocrysts in a subsolvus matrix, as well as quartz and amphibole. The *subsolvus granite*, exposed in an arcuate unit that almost completely girds the complex (Fig. 1), is geochemically the most evolved main unit. It is characterized by early arfvedsonite ± aegirine, quartz, and discrete laths of magmatic albite and K-feldspar. This unit possesses fresh and altered variants, the latter characterized by the replacement of arfvedsonite by aegirine ± hematite. *Granitic pegmatite* is found as lenses in the subsolvus granite and as dykes in the country rocks. Pegmatitic and associated minor aplitic facies occupy the ore zone. The pegmatites consist of coarse-grained K-feldspar,

minor albite, arfvedsonite, aegirine, and exotic Zr-, Y- and *REE*-bearing minerals. Figure 1 shows the distribution of the samples selected for study.

Previous Work

In addition to the detailed petrographic descriptions reported in Chapter 2, other descriptions have been provided by Miller (1986), Pillet (1989), Pillet *et al* (1989), Salvi & Williams-Jones (1990) and Birkett *et al* (1992). Only Pillet (1989) provided compositional information on the feldspars, obtained by wavelength-dispersion electron-microprobe analysis. He reported compositions in terms of Ab, Or and An (over 200 determinations), and provided concentrations of Ba, Sr and Fe for about one-quarter of these. On the whole, the albite was found to contain less than 0.5 mol.% An (maximum recorded, 1.2 mol % An). Pillet (1989) found discrete grains of the two feldspars in the subsolvus granite to be close to end-member compositions ($Ab_{100}Or_0$ to $Ab_{98}Or_2$ for the albite, and Ab_5Or_{95} to Ab_1Or_{99} for the K-feldspar). In perthitic grains typical of the hypersolvus granite, he found a greater spread in composition, between $Ab_{100}Or_0$ and $Ab_{67}Or_{33}$ for the sodic phase, and between Ab_2Or_{98} and $Ab_{49}Or_{51}$ for the potassic phase. The latter ranges of composition are not confirmed in this investigation (see below). He found the Fe content of the K-feldspar to be highest (in excess of 1.1 wt % Fe_2O_3) in the subsolvus rocks (his "quartz-rich" facies). Ba and Sr concentrations are both invariably less than 0.5 wt.% BaO or SrO, and generally below the limits of detection.

Analytical Methods

Electron-microprobe analyses

Some of the feldspar grains analyzed in 54 representative samples are variably turbid, with microinclusions of alkali amphibole and accessory minerals. With the use of the electron microprobe, it was possible to position the electron beam (diameter 5 μm) away from these heterogeneities. Concentrations of Na, K, Ca, Si, Al and Fe were recorded using wavelength-dispersion spectrometry (Cameca CAMEBAX microprobe instrument, accelerating voltage 15 kV, beam current 8 nA). Albite (Na), orthoclase (K, Al, Si) and andradite (Ca, Fe) were used as standards. Alkali loss was minimized by using a 5-μm beam and a counting time of 25 s. Spot analyses were repeated at least once to ensure representative results for each grain analyzed. The ZAF data-reduction package (Goldstein *et al.* 1992) was utilized. The concentrations determined are considered accurate to approximately 3% of the amount present.

Mineral separation

Representative samples were separated from each unit for trace-element analysis. Rocks were initially crushed to a 0.5-cm grain size with a BICO jaw crusher. Samples were ground and sieved; material was then hand-picked from the +60, -16 mesh fraction. Grains were observed in denatured alcohol, which allowed the selection of grains devoid of micro-inclusions. A 75-mg feldspar separate for each sample was pulverized in an agate mortar, then rinsed in distilled water and denatured alcohol before digestion prior to analysis.

Perthite grains were sampled from four samples of hypersolvus granite. Only the perthite phenocrysts were separated from the three samples of transsolvus granite. The separates of subsolvus granite contain discrete grains of both feldspars. Discrete grains of albite are rare in the pegmatites, so that the data reported pertain to the K-feldspar megacrysts, which may or may not be slightly perthitic.

Atomic absorption spectroscopy

Part of the separated feldspar (50 mg) was digested with 2.5 mL of nitric, 2.5 mL of hydrofluoric, and 0.5 mL of perchloric acid, and analyzed for Na and K by atomic absorption spectroscopy, using the method of Abbey (1965) with matrix-matched standards. The results, recast in terms of mol % Or, provide a bulk composition of the feldspar in the various units.

Inductively coupled plasma - mass spectrometry

The remaining 25 mg of the same separates were analyzed for their trace-element content using the Sciex ELAN model 250 inductively coupled plasma - mass spectrometer (ICP-MS) at the Department of Earth Sciences, Memorial University of Newfoundland. This material was digested in HF + HNO_3, and the solution was analyzed using the method of standard addition to correct for matrix effects (Jenner *et al.* 1990).

X-ray diffraction

A powder X-ray-diffraction pattern was recorded for each separate and of selected other samples using a Guinier-Hagg focusing camera (CuKα_1 radiation, synthetic spinel internal standard, a = 8.0833 Å at room temperature). The cell parameters were refined using the program of Appleman & Evans (1973), as modified by Garvey (1986).

Degree of Al-Si Order of the Feldspars

The unit-cell parameters of 28 samples of alkali feldspar are reported in Appendix II. The data are plotted in terms of b *versus* c (Fig. 2) and α^* *versus* γ^* (Fig. 3).

All samples encountered in this investigation contain very well-ordered microcline and albite. Also, the two feldspars have near-end-member compositions (Tables 1, 2). Figure 2a shows that most samples have b and c cell dimensions greater than those of ideal low microcline (Kroll & Ribbe 1983, Table 4), and thus plot outside the b-c quadrilateral. Similarly, most of the albite data-points in Figure 2b have slightly larger b and c dimensions than expected for end-member, fully ordered albite. The anomalous positions of the microcline data-points in Figure 2a may be explained by an enrichment of the microcline in Fe^{3+} and Rb, vectors for which are shown, based on the cell dimensions of $KFeSi_3O_8$ (Wones & Appleman 1963) and $RbAlSi_3O_8$ (Pentinghaus & Henderson 1979). If these two elements are indeed the only two "contaminants", then it seems clear that the resultant vector expressing enrichment in both elements must have as its origin a point consistent with a less-than-perfect degree of Al-Si order than fully ordered microcline. The data points for albite (Fig. 2b) are shifted along a different

Figure 2. Plot of *b versus c* cell dimensions of feldspar samples X-rayed in this study. The coordinates for low microcline and low albite were obtained from Kroll & Ribbe (1983). Symbols used: open square, hypersolvus granite; grey square, feldspar phenocryst, transsolvus granite; filled square, matrix, transsolvus granite; open circle, subsolvus granite; and triangle, pegmatite. (a) Portion of the plot showing the location of the microcline data-points. The Rb vector was derived from cell dimensions of Rb-end-member microcline (Pentinghaus & Henderson 1979); each tick mark on the Rb vector represents the incorporation of 10 mol.% Rb in K-feldspar. The Fe^{3+} vector was derived from cell dimensions of Fe^{3+}-end-member microcline (Wones & Appleman 1963); each tick mark on the Fe^{3+} vector represents 2 mol % $KFeSi_3O_8$. σ = maximum error ($\Delta\sigma_b = \pm 0.0030$, $\Delta\sigma_c = \pm 0.0018$), δ = minimum error ($\delta_b = \pm 0.0010$, $\Delta\delta_b = \pm 0.0006$), in Å. (b) Portion of the plot showing the location of the albite data-points. σ = maximum error ($\Delta\sigma_b = \pm 0.0030$, $\Delta\sigma_c = \pm 0.0019$), δ = minimum error ($\delta_b = \pm 0.0010$, $\Delta\delta_b = \pm 0.0007$), in Å.

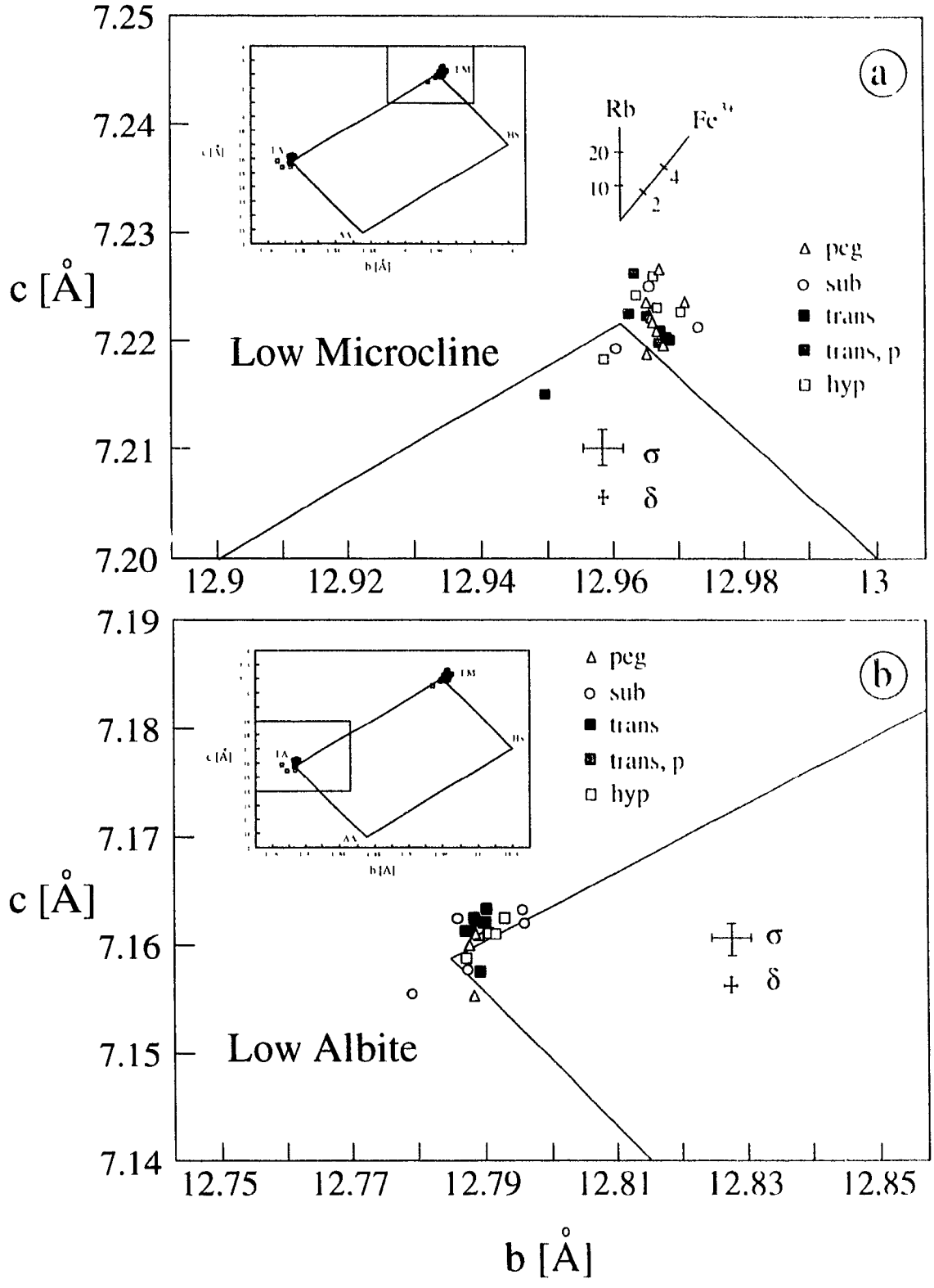
a
Low Microcline
peg
sub
trans
trans, p
hyp
σ
δ
Rb
Fe
20
10
4
2
7.25
7.24
7.23
7.22
7.21
7.20
12.9
12.92
12.94
12.96
12.98
13
b
Low Albite
peg
sub
trans
trans, p
hyp
σ
δ
7.19
7.18
7.17
7.16
7.15
7.14
12.75
12.77
12.79
12.81
12.83
12.85
c [Å]
b [Å]

Figure 3. Plot of α^* *versus* γ^* cell dimensions of feldspar samples X-rayed in this study. The coordinates of low microcline and low albite were obtained from Kroll & Ribbe (1983). Symbols are the same as those in Figure 2. (a) Portion of the plot showing the location of the microcline data-points with respect to the LM corner. σ = maximum error ($\Delta\sigma_{\alpha^*} = \pm 0.030$, $\Delta\sigma_{\gamma^*} = \pm 0.027$). δ = minimum error ($\delta_{\alpha^*} = \pm 0.010$, $\Delta\delta_{\gamma^*} = \pm 0.008$), in degrees. (b) Portion of the plot showing the location of the albite data-points with respect to the LA corner. σ = maximum error ($\Delta\sigma_{\alpha^*} = \pm 0.030$, $\Delta\sigma_{\gamma^*} = \pm 0.023$), δ = minimum error ($\delta_{\alpha^*} = \pm 0.010$, $\Delta\delta_{\gamma^*} = \pm 0.007$), in degrees.

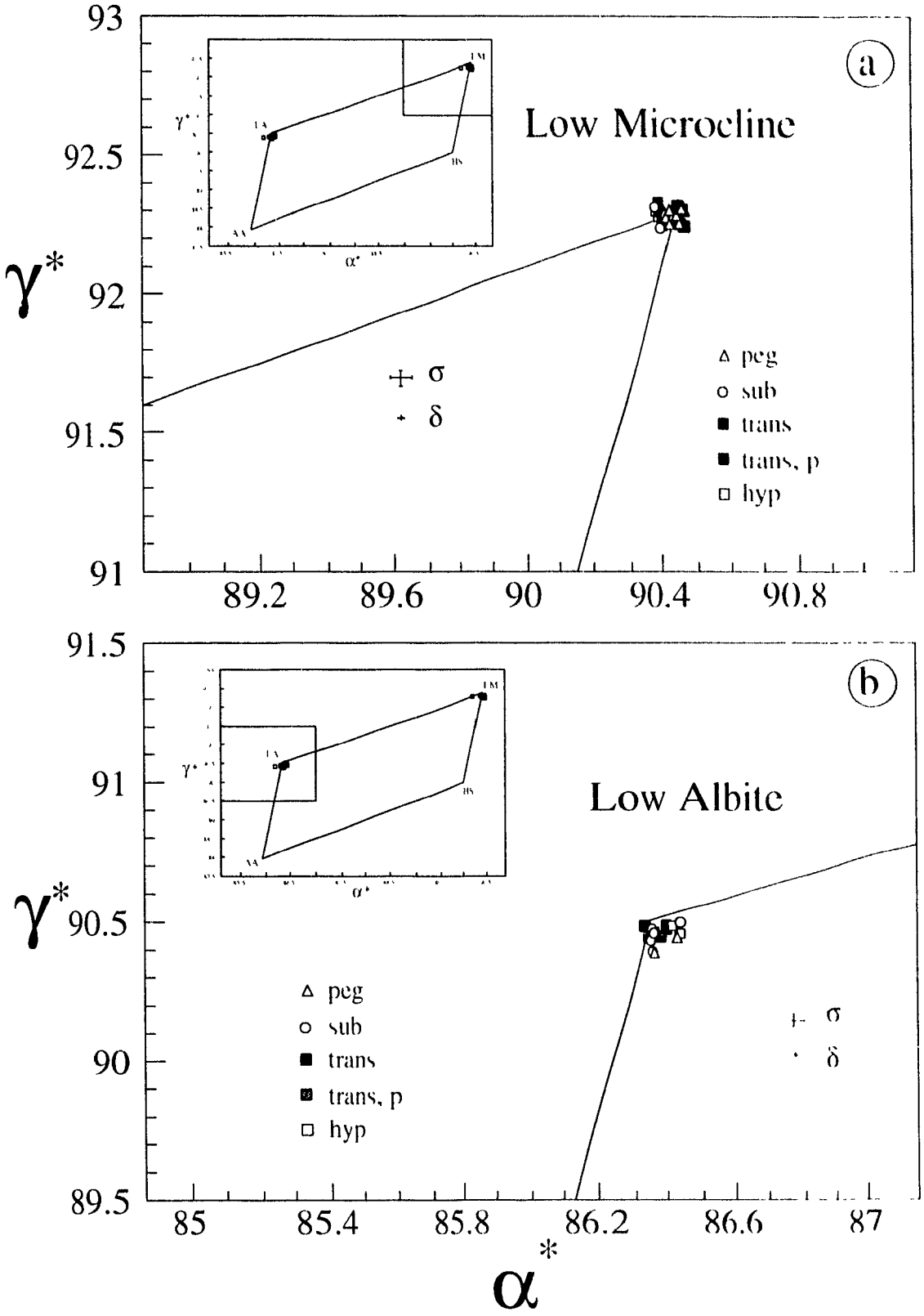
a
Low Microcline
93
92.5
92
91.5
91
γ*
89.2
89.6
90
90.4
90.8
σ
δ
peg
sub
trans
trans, p
hyp
b
Low Albite
91.5
91
90.5
90
89.5
85
85.4
85.8
86.2
86.6
87
α*

TABLE 1 COMPOSITION AND DEGREE OF Al-Si ORDER IN K-FELDSPAR

	N_{Or}	t_1O+t_1m	t_1O-t_1m	t_1O
Hypersolvus granite				
37A1	1.00	1.020	0.975	1.00
38B3	0.96	0.984	1.001	0.99
48A1	0.99	1.014	1.005	1.01
48G1	1.00	0.985	1.016	1.00
57C1	1.00	0.997	1.010	1.00
Transsolvus, phenocrysts				
37A4	0.98	1.031	0.986	1.01
47A1A	0.97	0.973	1.030	1.00
58C1	0.99	1.004	1.003	1.00
Transsolvus, matrix				
36B3	0.99	0.980	0.992	0.99
37A4	0.99	0.971	1.010	0.99
37D1	0.96	0.985	0.967	0.98
47A1A	0.99	0.973	0.995	0.98
58C1	0.97	0.996	1.015	1.01
Subsolvus granite				
38A3	1.00	0.968	1.026	1.00
46A3	0.96	0.984	0.980	0.98
46A4	1.00	1.015	1.000	1.01
Pegmatite				
34C2	0.97	0.969	1.000	0.98
36B3	0.99	1.004	1.006	1.01
37I-6	0.99	0.997	0.998	1.00
43C1	1.01	1.021	0.997	1.01
46G1	1.00	0.989	0.981	0.99
46I4	0.99	0.970	0.996	0.98
63B3	1.01	0.989	1.007	1.00
63C1	1.00	0.995	1.002	1.00
SL113	0.99	0.981	0.975	0.98
SI 120	1.00	0.993	0.994	0.99

Composition is calculated from cell volume using the equation of Kroll & Ribbe (1983). Degree of Al-Si order, expressed as t_1O, is calculated using the expressions of Blasi (1977).

TABLE 2 COMPOSITION AND DEGREE OF Al-Si ORDER IN Na-FELDSPAR

	N_{Or}	t_1O+t_1m	t_1O-t_1m	t_1O
Hypersolvus granite				
37A1	0.02	1.004	1 005	1 00
38B3	0.00	1.000	0 994	1 00
48A1	0.01	1.011	0 991	1 00
48G1	0 01	1.011	1 006	1 01
57C1	0 01	1 008	1 005	1 01
Transsolvus, phenocrysts				
37A4	0.01	1 015	0 998	1 01
47A1A	0.00	0 988	0 999	0 99
58C1	0.01	1 015	0 998	1 01
Transsolvus, matrix				
37A4	0 01	1 014	1 018	1 02
37D1	0.01	1.011	1 010	1 01
46A4	0.02	1 021	1 004	1 01
47A1A	0.01	1 022	1 003	1 01
58C1	0 02	1 015	1 001	1 01
Subsolvus granite				
38A3	0.02	1 004	1 001	1 00
46A3	----	0 997	1 006	1 00
46A4	0 01	1 026	1 004	1 01
Pegmatite				
34C2	0 01	1 007	0 974	0 99
46A4	0 01	0 994	0 977	0 99
46G1	----	1 035	1 021	1 03
46I4	0 01	0 977	0 984	0 98
63B3	0 03	1 007	1 005	1 01

Composition is calculated from cell volume using the equation of Kroll & Ribbe (1983) Degree of Al-Si order, expressed as t_1O, is calculated using the expressions of Blasi (1977)

vector than in the case for microcline, consistent with the presence of structurally bound Fe^{3+} but not Rb. Values of t_1O, the proportion of Al in the T_1O position, have been inferred from the cell dimensions b, c, α^* and β^* (Blasi 1977). Both the microcline and albite are highly ordered, with t_1O values close to 1.00 (Tables 1, 2). Note, however, that the t_1O value is slightly larger than it should be, possibly on account of the expansion of the unit cell by Rb in the alkali position and Fe^{3+} in the tetrahedrally coordinated position. Two samples of hypersolvus granite, 47A1A and 48A1 (Fig. 1), were found to contain a small proportion of orthoclase along with the microcline, which is consistent with the proposal that the coexisting microcline is less well ordered that would appear from Figure 2a.

Values of N_{Or} are based on unit-cell volume of the feldspars. They were obtained with the polynomial of Kroll & Ribbe (1983) for the series low albite - low microcline (Tables 1, 2). The albite has an inferred composition N_{Or} in the range 0 to 0.03, with most of the values being 0.01 (Table 2). In view of the asymmetry of the solvus (the albite limb is vertical at N_{Or} 0 below the solidus of these granites: see, *e.g.*, Smith & Brown 1988, Fig. 1.2), it seems clear that 1) the N_{Or} of the albite really is 0, as indicated by the electron-microprobe data (see below), and 2) the expansion of the unit-cell volume reflects the structural incorporation of Fe^{3+}, as documented above. By the same token, a negative correction of 0.01 to 0.02 should be applied to the N_{Or} data for the microcline (Table 1), because of the incorporation of Rb and Fe^{3+}, which brings the compositions in Table 1 into close agreement with the electron-microprobe results (see below).

Chemical Composition of the Feldspars

Major elements electron-microprobe data

Results of electron-microprobe analyses were recalculated on the basis of eight atoms of oxygen, and expressed in terms of molar proportions of the end members Or, Ab, FeOr and FeAb (Table 3). These results indicate that both feldspars are even closer to their end-member compositions than claimed by Pillet (1989). In particular, the intermediate compositions that he reported in some samples of hypersolvus granites can now be attributed to intersection of exsolution-related domains of microcline and albite by the electron beam. The compositions encountered here, in the range Or_{95-96} (Fe^{3+} arbitrarily assigned to the Ksp end-member), are in close agreement with corrected values of N_{Or} derived from the XRD data.

The albite has a composition between $Ab_{98.7}$ and $Ab_{99.3}$ (Fe^{3+} arbitrarily assigned to the Ab end-member), in agreement with corrected values of N_{Or} based on XRD data. In the albite as well as the microcline, the concentration of calcium is very low (0.12 wt.% CaO is a maximum), as is typical of Na- and K-feldspars from other peralkaline complexes (Carmichael 1962, Noble *et al.* 1971, Mahood & Stimac 1990). There is a hint that the amount of Ca is marginally higher in the latest units of the complex to crystallize. The iron content of both feldspars attains up to 0.72 wt.% Fe_2O_3 on average, it seems to vary by a factor of two among grains of a given specimen. The highest iron contents are in material from the altered subsolvus granite (Appendix III), as noted by Pillet (1989). The concentrations of Fe^{3+} attained are typical of feldspar found in rapidly quenched peralkaline systems [0.96 wt.% Fe_2O_3 in sodic sanidine from type-locality

TABLE 3 AVERAGE CONCENTRATIONS OF Fe, Ca, Na AND K IN MICROCLINE AND ALBITE, STRANGE LAKE COMPLEX.

	Microcline		Albite	
	ave	± 1σ	ave	± 1σ
Hypersolvus granite				
Fe_2O_3 wt.%	0 45	0 25	0 51	0.30
CaO	0 00	0 00	0.01	0 01
Na_2O	0 44	0 21	11.41	0 23
K_2O	16.36	0 54	0.16	0 16
Or mol.%	94 49		0.95	
Ab	3 97		97 30	
FeOr	1 54		----	
FeAb	----		1.75	
Transsolvus porphyritic granite				
Fe_2O_3	0.62	0 12	0.72	0.32
CaO	0 00	0 00	0 01	0.01
Na_2O	0 56	0 15	11.41	0 14
K_2O	16 25	0 51	0.13	0 02
Or	92 89		0 75	
Ab	4 99		96.81	
FeOr	2.12		----	
FeAb	----		2.44	
Fresh subsolvus granite				
Fe_2O_3	0.61	0.37	0.71	0 33
CaO	0 00	0 00	0 00	0 01
Na_2O	0.46	0.13	11 35	0 20
K_2O	16 32	0 17	0.14	0 06
Or	93.73		0 81	
Ab	4 15		96.79	
FeOr	2 12		----	
FeAb	----		2 41	
Altered subsolvus granite				
Fe_2O_3	0.72	0 31	0 55	0.21
CaO	0 00	0 01	0 01	0.01
Na_2O	0.48	0.13	11.41	0.12
K_2O	16 31	0 35	0 17	0 05
Or	93 21		0.87	
Ab	4 29		97 45	
FeOr	2 50		----	
FeAb	----		1.69	
Pegmatite				
Fe_2O_3	0.36	0 14	0.58	0.24
CaO	0 01	0 03	0.01	0.01
Na_2O	0 53	0 31	11.37	0.23
K_2O	16.17	0.48	0.23	0.04
Or	94 02		1.31	
Ab	4 74		96.76	
FeOr	1 24		----	
FeAb	----		1.94	

Symbols used: Or, orthoclase; Ab, albite; FeOr, iron-orthoclase; FeAb, iron-albite. Fe^{3+} was arbitrarily assigned to FeOr end-member in microcline and FeAb end-member in albite. Number of analyses performed on microcline and albite, respectively: hypersolvus, 31, 16; transsolvus, 10, 6; fresh subsolvus, 15, 9; altered subsolvus, 43, 9; pegmatite, 19, 7.

pantellerite: Mahood & Stimac (1990); 0.68 wt.% Fe_2O_3 in sanidine from comendite from the Great Basin of the western United States Noble *et al.* (1971)] The structural incorporation of Fe^{3+} is responsible for a homogeneous bright red cathodoluminescence in both Na- and K-feldspar

Na and K in the feldspar separates AAS data

The proportion of Or in the feldspar separates ranges from 41.2 to 48.4% in four samples of hypersolvus granite (Table 4). In the transsolvus granite, the perthite cortains between 45.0 and 53.9% Or, it was impossible to obtain a clean separate of the groundmass assemblage in these porphyritic rocks. One sample of fresh subsolvus granite contains two feldspars of aggregate composition of 63.1% Or, whereas in two altered samples of the same unit, the total feldspar fraction contains 59.3 and 63.3% Or In the samples of pegmatite, the easiest to sample, the total feldspar fraction contains between 75.4 and 98.0% Or. As these data indicate, some samples of microcline consist almost completely of a single phase; as a result, some entries describing microcline in Table 1 do not have a corresponding entry for albite in Table 2 The progressive increase in potassium in these four units constitutes a recurrent theme in studies of granitic pegmatites, and will be addressed in the Discussion section

The trace elements ICP-MS data

Of the trace elements detected in the purified concentrates submitted for analysis by ICP-MS, some (*e.g.*, Rb, Cs, Tl) are expected to occupy the alkali site, whereas others

TABLE 4a TRACE-ELEMENT CONCENTRATIONS IN FELDSPAR SEPARATES

Sample	37A1	38B3	48A1	48G1	37A4	47A1	58C1	38A3	27A4	46A3
unit	hyp	hyp	hyp	hyp	trans	trans	trans	fsub	asub	asub
mol % Or	41 2	43 8	46 8	48 4	45 0	53 9	49 8	63 1	63 3	59 3
Trace elements (ppm)										
Li	5 4	2 0	20 6	0 8	1 3	0 9	1 2	2.2	2 7	5 5
Rb	561 3	815 7	840 0	1281 9	1609 7	905 9	690 5	1802 4	1854.8	1327 5
Sr	5 4	10 3	6 6	1 7	7 9	2 0	1 9	4.8	8 3	4 0
Cs	0 9	1 4	6 5	2 6	1 6	1 9	1 9	1 6	0 9	1 9
Ba	36 0	31 6	26 3	98 6	53 0	31 2	75 0	23.5	55 1	60 3
Tl	2 8	2 6	4 5	6 0	7 2	4 7	7 6	8 6	4.1	5 5
Pb	5 7	11 5	65 4	84 3	112 4	23 3	52 6	30 6	108 1	32 9
Th	6 3	2 4	10 2	47 2	10 3	6 4	23 2	9 3	5 7	22 3
U	0 7	0 4	5 8	6 2	8 2	0 7	2.2	2 7	1 8	2 4
Y	21 4	16 8	122 1	97 1	180 3	34 2	22 6	62 5	64 6	121 3
Zr	66 8	29 7	440 5	499 3	4381 2	102 0	109 2	345 2	448 3	171 5
Rare-earth elements (ppm)										
La	8 36	5 49	43 34	25 59	254 17	12 08	16 14	31 60	87 56	18 81
Ce	17 89	12 11	114 05	76 25	470 98	28 16	36 51	69.51	197 12	43 35
Pr	2 19	1 44	13 07	7 95	55 85	4 05	4 28	7 61	20 85	4 91
Nd	7 54	5 36	43 68	27 04	192 99	18 64	13 92	26.13	66 59	19 95
Sm	2 08	1 13	12 65	8 07	38 93	5 41	3 17	6 95	14 03	8 91
Eu	0 20	0 29	0 69	0 54	2 23	0 37	0 24	0 49	0 63	0 77
Gd	2 47	1 22	13 11	9 57	35 63	5 57	2 50	7 91	14 05	14 79
Tb	0 56	0 25	2 92	2 61	5 01	0 93	0 55	1 59	2 19	2 95
Dy	3 63	2 04	23 28	22 23	29 40	6 03	4 34	11 79	12 97	19 39
Ho	0 81	0 46	5 75	5 40	5 87	1 30	0 99	2 40	2 61	4 07
Er	2 76	1 62	21 73	19 82	16 53	3 90	3 54	7 87	7 69	11 06
Tm	0 40	0 30	4 14	3 43	2 36	0 59	0 60	1 18	1 06	1 46
Yb	2 48	1 86	30 32	22 28	13 82	3 81	3 54	7 96	6 56	9 05
Lu	0 29	0 22	4 31	2 58	1 73	0 44	0 45	1 06	0 95	1 14
K/Rb	105 1	74 9	83 3	52 9	39 2	85 3	105 0	49 6	39 0	59 6
ΣREE	51 66	33 79	333 02	233 36	1125 52	91 27	90 77	184 04	434 84	160 60
$(La/Yb)_N$	2 23	1 95	0 94	0 76	12 13	2 09	3 01	2 62	8 81	1 37
Eu/Eu*	0 27	0 76	0 16	0 19	0 18	0 20	0 25	0 20	0 14	0 20

Trace-element and rare-earth-element analyses by ICP-MS. Or mol % determined by atomic absorption

TABLE 4b. TRACE-ELEMENT CONCENTRATIONS IN FELDSPAR SEPARATES

Sample	34C2	36B3	37I 6	43C1	46A4	46G1	46I4	63B3	63C1	SI 113	SI 120
unit	peg	peg	peg	peg	peg	peg	peg	peg	peg	peg	peg
mol.% Or	75 4	94 6	98 0	82 0	83 6	87 0	80 1	89 2	95 6	87 0	91 3
Trace elements (ppm)											
Li	1 8	1 0	11 1	16 7	0 7	8 7	5 9	1 2	1 1	24 9	30 7
Rb	2732 9	3047 3	2116 3	2509 9	1942.7	3652 2	2351 8	4483 9	4594 5	4706 0	3943 7
Sr	----	----	0 5	2 5	1 2	----	0.1	0 4	----	12 3	2 9
Cs	1 9	1 7	1 0	1 2	1 7	3 1	3 1	2 7	2 6	6 6	3 5
Ba	17 7	25 3	23 5	28 7	57 8	64 2	39 8	18 3	34 1	109 0	58 2
Tl	7.0	8 1	4 7	6 1	6 3	9 8	7 4	6 3	9 2	14 8	11 2
Pb	24 6	8 0	16 8	10 3	17 0	18 9	16 8	19 3	7 6	79 3	17 7
Th	2 8	1 4	6 2	1 3	2 2	2 0	0 4	0 3	0 5	1 7	0 2
U	0 5	0 4	0 8	0 5	0 5	0 9	0 9	0 2	1 4	32 7	0 6
Y	7 2	1 8	6 3	14 3	25 5	2 1	2 8	2 0	11 1	139 8	10 9
Zr	22 2	14 1	8 3	22 0	11 6	8 2	16 2	2 4	148 3	19 1	4 7
Rare-earth elements (ppm)											
La	1 90	9 46	3 39	3 38	5 32	1 08	0 99	1 61	8 09	71 91	13 17
Ce	5 08	20 46	7 79	8 10	12 37	2 33	5 39	3 11	13 81	31 15	9 85
Pr	0 55	1 94	0 88	1 10	1 45	0 29	0 39	0 43	1 69	13 88	1 76
Nd	2 02	5 94	3 12	5 73	5.41	0 85	1 33	1 47	5 91	45 31	5 09
Sm	0 62	1 00	0 65	1 86	1 82	0 42	0 37	0 30	1 15	13 13	0 89
Eu	0 05	0 04	0 04	0 12	0 17	0 02	0 02	0 02	0 05	0 69	0 05
Gd	0 72	0 60	0 70	2 13	2 74	0 31	0 38	0 31	1 06	14 02	0 91
Tb	0 16	0 08	0 15	0 41	0 55	0 07	0 06	0 05	0 19	3 38	0 20
Dy	1 20	0 41	1 14	2 84	3 92	0 61	0 44	0 31	1 46	21 49	1 57
Ho	0 28	0 09	0 27	0 55	0 79	0 09	0 10	0 07	0 36	5 52	0 40
Er	0 90	0 35	1 00	1 49	2.12	0 37	0 33	0 16	1 18	16 62	1 31
Tm	0 14	0 07	0 14	0 20	0 21	0 08	0 05	0 02	0 20	2 15	0 18
Yb	0 79	0 46	0 94	1 06	1 02	0 49	0 30	0 11	1 60	10 75	0 87
Lu	0 11	0 05	0 10	0 13	0 10	0 06	0 04	0 01	0 26	1 17	0 11
K/Rb	37 3	39 4	63 5	43 3	57 4	30 7	44 5	25 0	26 2	25 7	31 1
ΣREE	14 51	40 95	20 30	29 09	37 99	7 06	10 20	7 98	37 02	254 45	36 35
$(La/Yb)_N$	1 59	13 66	2 39	2 10	3 43	1 45	2 21	10 13	3 34	4 41	9 96
Eu/Eu*	0 23	0 15	0 17	0 18	0 24	0 16	0 14	0 19	0 14	0 15	0 15

Trace-element and rare-earth-element analyses by ICP-MS, Or mol % determined by atomic absorption

(*e.g.*, Zr, U, Th), smaller and more highly charged, are largely held in unavoidable microinclusions, as reviewed below

Lithium, because of its small ionic radius (0.92 Å for ^{VIII}Li), normally does not constitute an important occupant of the alkali site Tens of ppm commonly are found, especially in albite (Lagache & Sebastian 1991), with higher concentrations in feldspar formed from late solutions (Smith 1974) At Strange Lake, the feldspar concentrates contain from less than 1 to 31 ppm (Fig 4). These values are well within the levels of concentrations documented in evolved granitic systems (*e.g.*, 200 ppm: Černý *et al.* 1985a). The highest concentrations of Li are indeed found in the latest unit to crystallize, but the important host mineral is K-feldspar, not albite Note, however, the virtual absence of Li in the feldspar of some samples of pegmatite

Rubidium, with its relatively large ionic radius (1.61 Å) and unit valence, follows K in the feldspar structure Concentrations range from 560 ppm in the feldspar fraction of the hypersolvus granite 37A1 (K/Rb = 105: Table 4a) to 4700 ppm in microcline in the pegmatite SL120 (K/Rb = 31 Table 4b). The data points (Fig. 4) indicate progressive buildup of Rb with increasing proportion of K-feldspar in the felsic rocks. The drop in K/Rb ratio over the transition hypersolvus → transsolvus → subsolvus → subsolvus pegmatite (Fig 4), to a value of 25 in pegmatite 63B3, is progressive, which indicates that the samples are interrelated by an efficient process of fractionation. There is thus no evidence in this suite for the late injection of an unrelated batch of magma Note that the level of enrichment in Rb is much greater in some peraluminous rare-element-enriched granitic pegmatites. Černý *et al.* (1985b) found microcline with up

Figure 4. Concentration (ppm) of Li, Rb and Cs, and ratio K/Rb *versus* Or mol% for alkali feldspar bulk separates. Symbols used: open square, hypersolvus granite, filled square, transsolvus granite; open circle, fresh subsolvus granite; filled circle, altered subsolvus granite; and triangle, pegmatite.

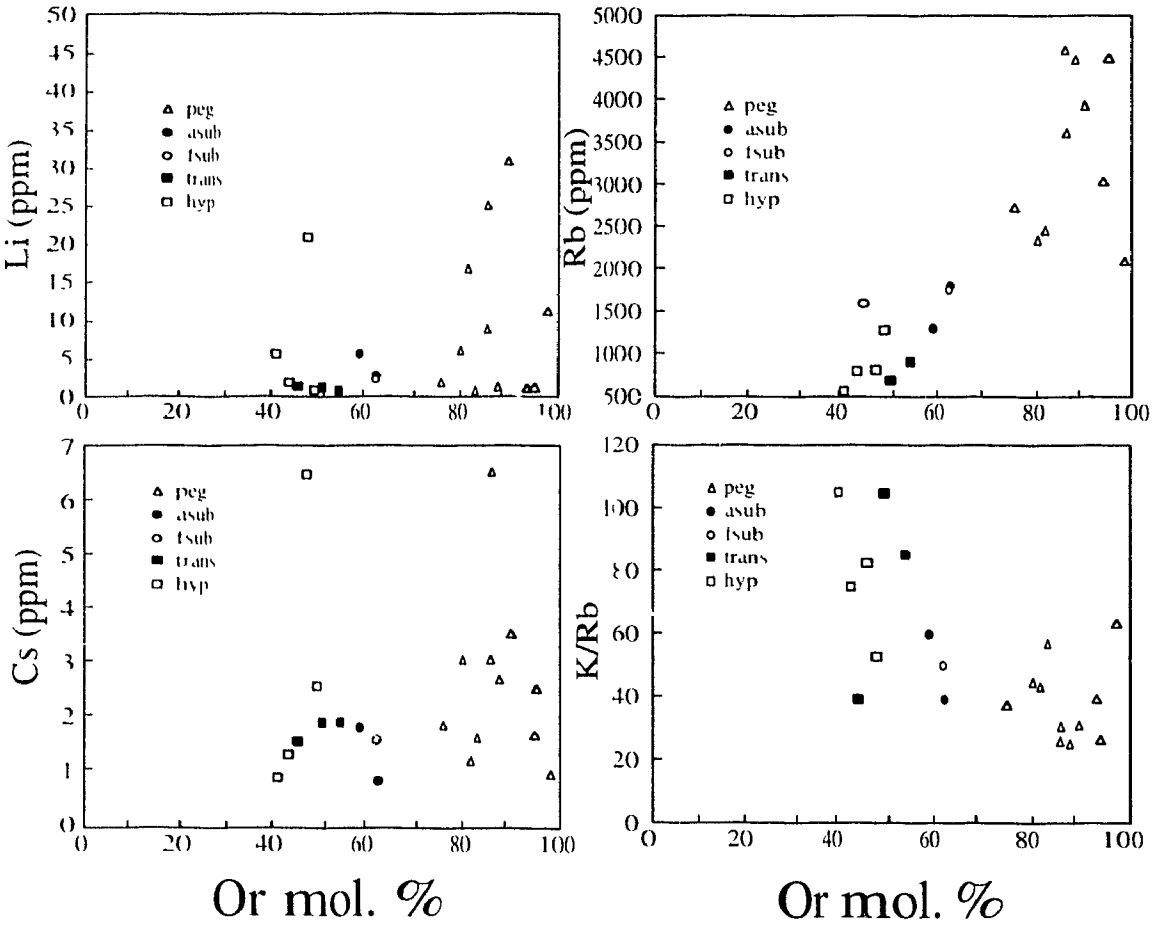
Li (ppm)
Rb (ppm)
Cs (ppm)
K/Rb
peg
asub
fsub
trans
hyp
Or mol. %
Or mol. %

49800 ppm Rb at Red Cross Lake, in northeastern Manitoba

Concentrations of *cesium* in the feldspar concentrates range from less than 1 to 6.6 ppm (Fig. 4). The progressive increase in Cs concentrations with fractionation is less regular than that of Rb, possibly in part owing to the very low levels of Cs in this complex. Černý *et al.* (1984) documented a progressive increase to 68 ppm in the feldspar fraction from Věžná, Czechoslovakia (ion-microprobe data). Shmakin *et al.* (1975) recorded up to 1.5 wt.% Cs in K-feldspar from a pollucite-bearing pegmatite.

Thallium (1.59 Å) is of the same size and valence as Rb, but because of its greater electronegativity, it should form stronger, more covalent bonds with oxygen. As a result, Tl, like Cs, is most concentrated in the latest-formed units. The feldspar fraction at Strange Lake ranges from 2 to 15 ppm (Fig. 5). Concentrations at Strange Lake are much lower than in the feldspar fraction of some Norwegian granitic pegmatites (maximum of 140 ppm, Heier & Taylor 1959).

At Strange Lake, the concentration of *strontium* in feldspar is very low (below limit of detection to a maximum of 30 ppm), as is usually the case in evolved anorogenic felsic complexes. The proportion of Sr generally decreases with increasing degree of fractionation (Fig. 5). "Contamination" with radiogenic Sr is expected in the evolved, Rb-rich rocks (Clark & Černý 1987), in other words, the very small amounts recorded thus have to be reduced further to take into account the proportion of ^{87}Sr produced *in situ* since the time of intrusion. It seems clear that the process of magmatic fractionation led to the very efficient removal of almost all the Sr *via* the early-formed magmatic minerals, and that the removal was still proceeding to bring the granitic melt from

Figure 5. Concentration (ppm) of Tl, Sr, Ba, and Pb *versus* Or mol.% for alkali feldspar bulk separates. Symbols used: open square, hypersolvus granite; filled square, transsolvus granite; open circle, fresh subsolvus granite; filled circle, altered subsolvus granite; and triangle, pegmatite.

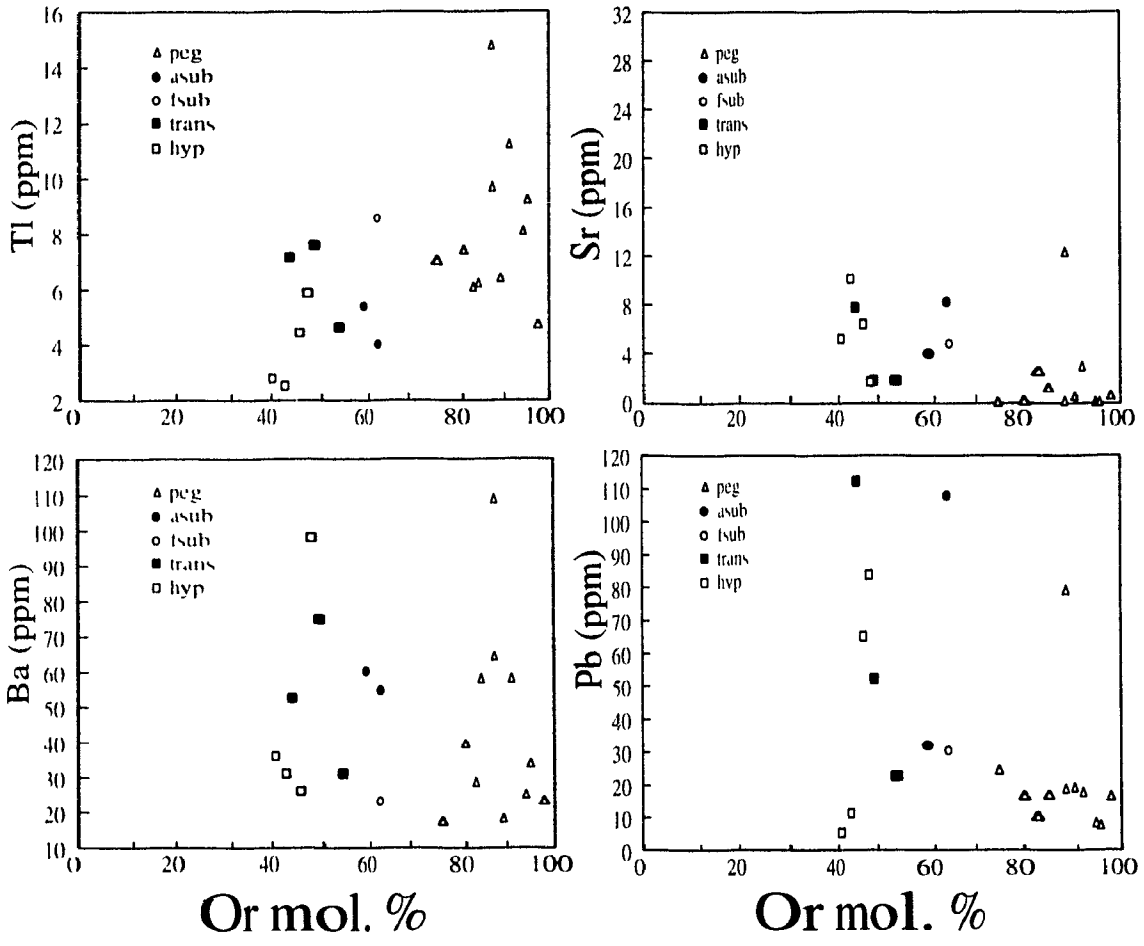
Tl (ppm)
Sr (ppm)
Ba (ppm)
Pb (ppm)
peg
asub
fsub
trans
hyp
Or mol. %
Or mol. %

the "hypersolvus granite" stage to the "subsolvus granite" stage. The pattern of behaviour of calcium can be expected to have been identical to that of nonradiogenic Sr. Both elements evidently were progressively depleted in the Strange Lake granitic system at the magmatic stage.

The pattern of behaviour of *barium* in evolved granitic systems is generally one of efficient removal *via* early-formed K-rich feldspar. At Strange Lake, the concentration of Ba is lowest in the feldspar fraction of some pegmatite samples, but there is much overlap with the more primitive granites of the suite. Concentrations range from 18 to 109 ppm; the most enriched feldspar separate was taken from a pegmatite. The Strange Lake granites are barium-poor, as is typical of evolved peralkaline granites (Whalen *et al.* 1987). The scatter in the data points in Figure 5 may well indicate that some of the barium was added to these rocks at the hydrothermal stage from outside the system, or was remobilized internally.

In a sulphur-deficient environment like at Strange Lake, *lead* enters the structure of both K-rich and Na-rich feldspars (Stevenson & Martin 1986), where it occupies the alkali site. The feldspar concentrates at Strange Lake contain between 6 and 112 ppm, in general, the feldspar fraction in the pegmatitic samples contains less Pb than that from the other units. The distribution of data points is less erratic than that of barium (Fig. 5), possibly owing to greater mobility of the lead, part of which can be expected to be radiogenic. As the pegmatite-bearing ore zone has anomalous levels of uranium and thorium [up to 2570 ppm Th, 212 ppm U in Miller's "exotic rich" facies (1986)], one might expect the pegmatites to be the most enriched in lead if the scale of

mobilization was strictly local.

Neither *uranium* nor *thorium* can be accepted in the feldspar structure. Instead, the small concentrations of U and Th likely are held in grains of impurity phases (*e.g.*, thorite), the presence of which could not be avoided in spite of painstaking hand-picking. Typical ranges of concentration in perthite from the hypersolvus granites (Table 4a) are from 0.4 to 5.8 ppm U, and from 2.4 to 47 ppm Th. The average concentrations decrease with increasing grain-size of the feldspar separate, as would be expected of elements hosted by accessory phases.

Zirconium and *yttrium* also can not be accepted by the feldspar structure. Measured concentrations are erratic, and as for U and Th, highest in the fine-grained separates (Table 4). As the Strange Lake pluton is Zr- and Y-mineralized, it is not surprising that submicroscopic impurities rich in these elements abound in the feldspar host, which develops secondary pore-space as a result of subsolidus recrystallization (see below).

Concentrations of *rare-earth-elements* in the bulk feldspar separates of the Strange Lake pluton are presented in Tables 4a and b. Chondrite-normalized concentrations are illustrated in Figure 6, along with average patterns for each unit (data from Chapter 2). The sum of *REE* concentrations in the feldspar separates decreases with an increase in mol.% Or: hypersolvus feldspars, 33.8-333.0 ppm; transsolvus, 91.3-1125.5 ppm; subsolvus, 160.6-434.8 ppm; pegmatite, 7.1-254.5 ppm. All separates show a negative Eu anomaly, with Eu/Eu^* ranging from 0.14 to 0.27 except for 38B3, where it is 0.76. A slight decrease in Eu/Eu^* values is noted in the pegmatite separates. On average, the feldspar fraction becomes *HREE*-depleted [i.e., increases in $(La/Yb)_N$] with evolution:

Figure 6. Range of chondrite-normalized plots for the rare earth element concentrations (ppm) of the alkali feldspar bulk separates from the different units. Number of samples, n, in each plot is given. Average chondrite-normalized pattern for each unit is provided. Chondrite values are from Evensen *et al* (1978). Note Sample SL113 was not plotted in view of the elevated concentrations of *REE* relative to other pegmatite separates.

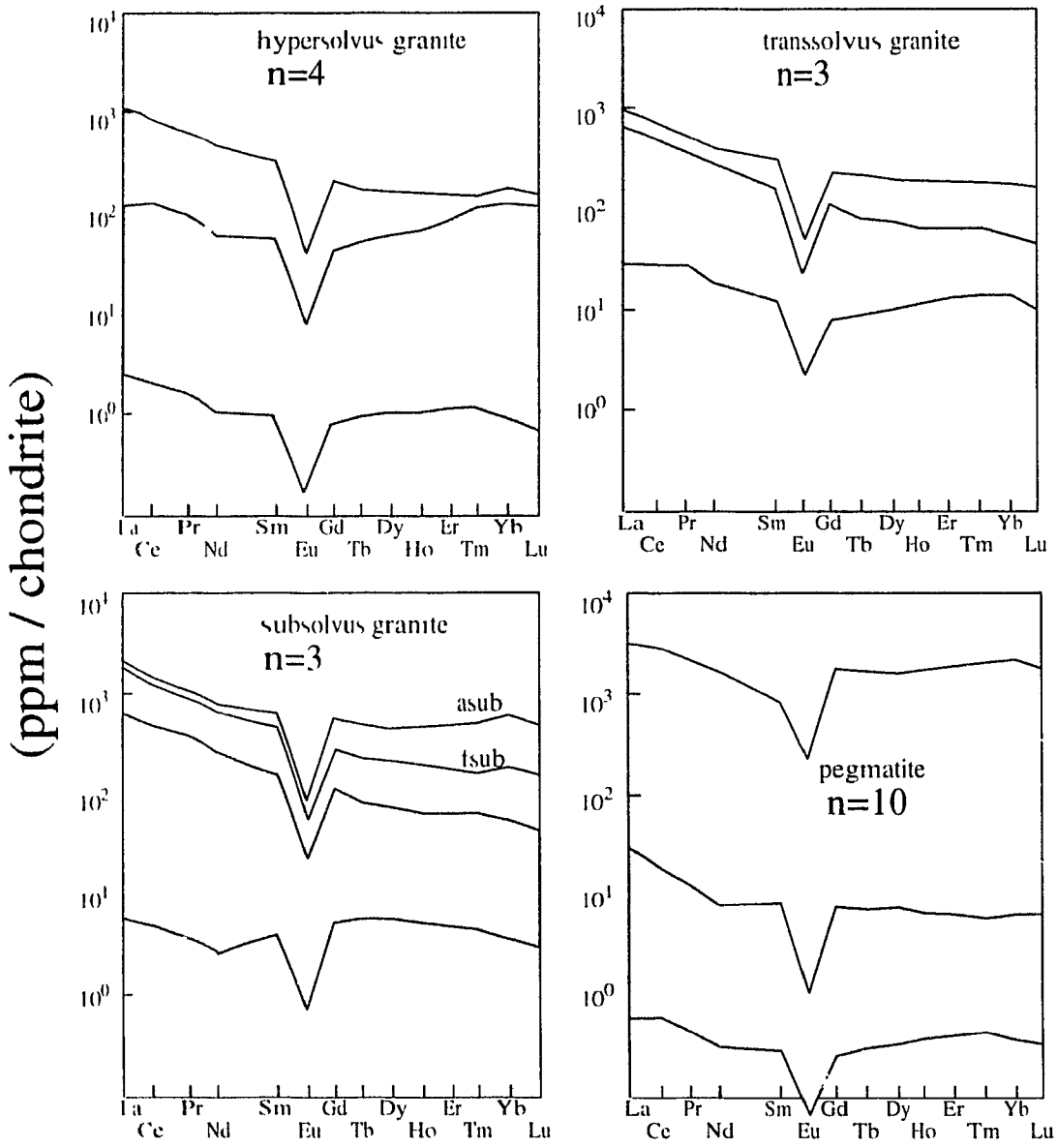
(ppm / chondrite)
hypersolvus granite
n=4
transsolvus granite
n=3
subsolvus granite
n=3
asub
tsub
pegmatite
n=10
La Ce Pr Nd Sm Eu Gd Tb Dy Ho Er Tm Yb Lu

hypersolvus feldspars, 0.9-2.2; transsolvus, 2.1-12.1; subsolvus, 1.4-8.8, pegmatite, 1.5-13.7. In view of published partition coefficients and the low levels of the rare earths typical of clean separates of feldspar (*e.g.*, Kontak *et al.* 1991), the high concentrations of rare earths recorded here largely reside in the micro-inclusions rather than in the feldspar structure.

Discussion & Conclusions

The feldspar minerals of the Strange Lake granite retain an excellent record of a magmatic trend of crystallization, followed by extensive recrystallization during their cooling. In terms of their chemical composition (Table 3), the samples now contain whatever the unit, almost pure microcline (95% Or + FeOr) and virtually pure albite. These compositions indicate a low temperature near 300°C on the basis of the phase diagram of Brown & Parsons (1989). A significantly lower temperature of equilibration (~100°C) is indicated, however, if the values of N_{Or} calculated from unit-cell volume (Table 1) are taken at face value. The two values of N_{Or} can be partly (but not completely) reconciled if it is assumed that the unit-cell volume of the coexisting feldspars are reduced to compensate for the structurally bound Fe^{3+} and Rb. A reduction of 0.01 or 0.02 in N_{Or} would bring the inferred value of N_{Or} of albite (Table 2) to the expected value of 0. An equivalent correction must be applied to the K-feldspar data, as well as an additional correction to reflect the amount of Rb present in the structure (Fig. 4). For some reason, perhaps attributable to the level of Cs, Tl, Pb, Ba and Sr (Fig. 5), the departure of the microcline data-points from the expected location of pure

microcline exceeds that expected for the amounts of Fe^{3+} and Rb recorded (see tick marks on the vectors in Fig. 2a). Although it is not possible to be more specific about the closure temperature of the two-feldspar system, it probably was close to 200°C. Such values are consistent with fluid-inclusion data obtained on quartz (Salvi & William-Jones 1990).

One important aspect of the compositional data obtained on the feldspar separates relates to the progressive increase of the K/Na value from least evolved to most evolved unit. The bulk composition of the perthite in the hypersolvus granite falls in the range Or_{41} - Or_{18}, very close to the composition expected from a haplogranitic composition at the pseudoternary minimum at 1 kbar $P(H_2O)$ (Tuttle & Bowen 1958). One might predict, on the basis of contours on the quartz-feldspar cotectic, that the liquid will remain at the minimum until crystallization is complete. The location of the isobaric pseudoternary minimum will shift slightly in response to the buildup in dissolved water until the point of saturation in H_2O (*e.g.*, Steiner *et al.* 1975, Holtz & Johannes 1991), and possibly drift in the direction of the Ab corner owing to progressive buildup of F in the system. Instead, the feldspar separates indicate a striking increase in K-feldspar, to the point that some samples of pegmatite are devoid of coexisting albite. At Strange Lake, this enrichment in K-feldspar does not seem matched by the development of complementary albite-enriched aplitic rocks, such as are encountered in some zoned bodies of granitic pegmatite (*e.g.*, Jahns & Tuttle 1963).

The progressive buildup in K without Na is not easy to explain. It may be a reflection of the phase equilibria in a haplogranite system with excess alkalis.

Carmichael & MacKenzie (1963) found that the addition of 4.5 wt% each of $NaFeSi_2O_6$ and Na_2SiO_3 shifts the minimum and the "thermal valley" measurably toward the Qtz-Or sideline, in projection. Also, the feldspar coexisting with the peralkaline melt is consistently more potassic than the melt, as noted in experiments by Bailey & Schairer (1964) and in nature by Mahood & Stimac (1990). However, the shift to the Or-Qtz sideline is more extreme in the Strange Lake pluton than predicted experimentally; furthermore, the agpaitic index of the melt is less than that modeled experimentally, and it does not seem to have increased markedly with fractionation, if average bulk compositions of the four units are compared (Chapter 2, Table 1).

Another mechanism that explains the progressive enrichment in K over Na involves the preferential loss of Na by degassing. It seems clear that saturation of the melt in a strongly peralkaline fluid began to occur before the solidi of the transsolvus granite, the subsolvus granite, and the pegmatite were reached. In view of 1) the shallow level of emplacement of this pluton, 2) an initial period of crystallization of the peralkaline melt in an H_2O-undersaturated state, abetted by the enhanced solubility of water due to peralkalinity, 3) the efficient fractionation of anhydrous minerals (quartz, K-feldspar, albite), and 4) the rapid growth of these minerals toward the end stage of consolidation, the magma at Strange Lake likely vesiculated and lost its fluid phase. This fluid, coexisting initially with Na- and K-feldspars, is inferred to have been very sodic. For example, the Na/(Na+K) value of such a fluid would be 0.95 at 1 kbar, 500°C in the presence of fluoride (Pichavant 1983). The high degree of Na enrichment matches the fluid-inclusion compositions inferred to be samples of orthomagmatic fluid by Salvi &

Williams-Jones (1992): loss of such a fluid could account for the levelling off in agpaitic index and fluorine content in the most evolved rocks, and for the local metastable preservation of disordered K-feldspar (orthoclase) in a sample of hypersolvus granite and another of transsolvus granite. The possibility of massive degassing and the ensuing "compositional quenching" of the magma (Jahns & Tuttle 1963) could be tested by stable isotope geochemistry of this plutonic suite, especially by monitoring the ratio D/H (Taylor 1988)

The successful conversion of orthoclase-bearing assemblages to the assemblage low albite + low microcline, except in the two samples mentioned earlier, indicates that an alkaline fluid later re-entered the system and catalyzed the ordering of the K-feldspar to low microcline, stable below 450°C or so (Brown & Parsons 1989) A high degree of order of the sodic and potassic feldspars is found regardless of the unit sampled. This finding is not at all surprising in the case of albite, but is worthy of discussion in the case of the K-feldspar. Well-ordered microcline is prevalent in this pluton, in spite of its small size, relatively shallow level of emplacement, and inferred rapid rate of cooling There is no evidence of mild reheating in the area, nor of deformation, two factors known to promote the transformation Instead it is the alkalinity of the fluid phase that seems to have promoted the successful conversion of a monoclinic K-feldspar to microcline Although ordering took place over the interval 450°-100°C (?), the reaction did not quite reach completion. This can be seen by correction of the microcline data-points for Fe^3 and Rb in Figure 2.

The geochemical evolution of the K-feldspar separated from the various samples

(Fig. 4, 5) is consistent with efficient fractionation of a single batch of evolved granitic magma. The Ca content of the albite and K-feldspar is extremely low (Table 3), as is consistent with the efficient early fractionation of sodic-calcic amphibole and fluorite at the hypersolvus granite stage, and of plagioclase and other mafic minerals at an even earlier stage, which resulted in the development of a negative Eu anomaly. It thus seems clear that the important buildup in Ca and Sr recorded in the most evolved rocks occurred entirely at the subsolidus stage, as proposed by Salvi & Williams-Jones (1990) on the basis of fluid-inclusion data.

Mineralization in the complex is attributed to the late redistribution of ore constituents *via* a contaminated peralkaline fluid, which gained Ca, Sr and Mg by interaction with country rocks. The fluid phase became saturated in a suite of accessory minerals, including some rich in Ca, and deposited these along cleavages and in vacuoles in the shrinking feldspar minerals. The resultant chondrite-normalized profile of the perthite in the hypersolvus granite resembles the profile of the altered subsolvus granite (relatively flat, *HREE* enrichment). Residence time of the late fluid phase in the hypersolvus granite probably was brief, as the microcline in the perthite did not recrystallize to visibly grid-twinned microcline, in spite of deuteric coarsening (Parsons 1978). Residence time must have been much greater in the core of the complex

References

Abbey, S. (1965) Determination of potassium, sodium and calcium in feldspars. *Can Mineral* **8,** 347-353

Appleman, D.E. & Evans, H.T., Jr. (1973): Job 9214: indexing and least-squares refinement of powder diffraction data. *U.S Geol. Surv., Comput Contrib* **20** (*NTIS Doc* **PB2-16188**).

Bailey, D.K. & Schairer, J.F. (1964): Feldspar-liquid equilibria in peralkaline liquids - the orthoclase effect *Am J Sci* **262,** 1198-1206.

Birkett, T.C., Miller, R.R., Roberts, A.C. & Mariano, A.N. (1992): Zirconium-bearing minerals of the Strange Lake intrusive complex, Quebec-Labrador. *Can Mineral* **30,** 191-205

Blasi, A. (1977): Calculation of T-site occupancies in alkali feldspar from refined lattice constants *Mineral Mag* **41,** 525-526.

Brown, W.L. & Parsons, I. (1989): Alkali feldspars: ordering rates, phase transformations and behaviour diagrams for igneous rocks. *Mineral Mag* **53,** 25-42.

Carmichael, I.S.E. (1962): Pantelleritic liquids and their phenocrysts. *Mineral Mag.* **33,** 86-113.

_____ & MacKenzie, W.S. (1963): Feldspar-liquid equilibria in pantellerites: an experimental study. *Am. J Sci* **261,** 382-396.

Černý, P., Smith, J.V., Mason, R.A. & Delaney, J.S. (1984): Geochemistry and petrology of feldspar crystallization in the Věžná pegmatite, Czechoslovakia. *Can Mineral* **22,** 631-651

_____, Meintzer, R.E. & Anderson, A.J. (1985a): Extreme fractionation in rare-element granite pegmatites. Selected examples of data and mechanisms. *Can. Mineral* **23,** 381-421.

_____, Pentinghaus, H & Macek, J.J (1985b) Rubidian microcline from Red Cross Lake, northeastern Manitoba *Bull Geol Soc Finland* **57,** part 1-2, 217-230

Clark, G.S. & Černy, P. (1987) Radiogenic (87)Sr, its mobility, and the interpretation of Rb-Sr fractionation in rare-element granitic pegmatites *Geochim Cosmochim Acta* **51,** 1011-1018.

Evensen, N.M., Hamilton, P.J & O'Nions, R.K (1978) Rare-earth abundances in chondritic meteorites *Geochim Cosmochim Acta* **42,** 1199-1212

Garvey, R. (1986): LSUCRIPC, least squares unit-cell refinement with indexing on the personal computer *Powd Diff* **1**(1), 114

Goldstein, J.I., Newbury, D.E., Echlin, P., Joy, D.C., Romig, A.D., Lyman, C.L., Fiori, C. & Lifshin, E. (1992). Scanning electron microscopy and X-ray microanalysis: a text for biologists, material scientists and geologists 2nd ed Plenum Press, New York, 820 pp.

Heier, K.S. & Taylor, S.R. (1959): Distribution of Li, Na, K, Rb, Cs, Pb, and Tl in southern Norwegian pre-Cambrian alkali feldspars. *Geochim Cosmochim Acta* **15,** 284-304.

Holtz, F. & Johannes, W. (1991): Genesis of peraluminous granites I Experimental investigation of melt compositions at 3 and 5 kbar and various H_2O activities *J Petrol* **32,** 935-958.

Jahns, R.H. & Tuttle, O.F. (1963): Layered pegmatite-aplite intrusives *Mineral Soc Am Spec Pap* **1,** 78-92

Jenner, G.A., Longerich, H.P, Jackson, S.E. & Fryer, B.J (1990) ICP - MS - a powerful tool for high precision trace element analysis in earth sciences: evidence from analysis of selected USGS reference samples. *Chem Geol* **83,** 133-148

Kontak, D.J., Kerrich, R., & Strong, D.F (1991): The role of fluids in the late-stage evolution of the South Mountain Batholith, Nova Scotia: further geochemical and

oxygen isotopic studies *Atlant Geol* **27,** 29-47.

Kroll, H & Ribbe, P H. (1983): Lattice parameters, composition and Al-Si order in alkali feldspars *In* Feldspar Mineralogy (P.H. Ribbe, ed.). *Mineral Soc. Am., Rev Mineral* **2,** 57-99.

Lagache, M. & Sebastian, A (1991): Experimental study of Li-rich granitic pegmatites. II. Spodumene + albite + quartz equilibrium. *Am Mineral* **76,** 611-616.

Mahood, G. & Stimac, J.A. (1990): Trace-element partitioning in pantellerites and trachytes *Geochim Cosmochim Acta* **54,** 2257-2276.

Miller, R R. (1986): Geology of the Strange Lake alkalic complex and the associated Zr-Y-Nb-Be-REE mineralization. *Newfoundland Dep Mines and Energy, Mineral Development Div., Rep* **86-1,** 11-19.

Noble, D C., Korringa, M.K. & Haffty, J. (1971): Distribution of calcium between alkali feldspar and glass in some highly differentiated silicic volcanic rocks. *Am. Mineral.* **56,** 2088-2097.

Parsons, I (1978): Feldspars and fluids in cooling plutons. *Mineral Mag* **42,** 1-17.

Pentinghaus, H & Henderson, C.M B. (1979): Rubidium-aluminosilikat-feldspat ($Rb(AlSi_3O_8)$; stabilitat strukturelle Zustande und Schmelzverhalten: chemische und thermische Ausdehnung des ($AlSi_3O_8$)-Gerustes. *Fortschr Mineral* **57,** Beiheft 1, 119-120

Pichavant, M (1983). (Na, K) exchange between alkali feldspars and aqueous solutions containing borate and fluoride anions; experimental results at P = 1 kbar. 3rd NATO advanced study institute on feldspars, feldspathoids and their paragenesis, Rennes, France, 102. (abstr.)

Pillet, D (1989) Le granite peralcalin du Lac Brisson, Labrador Central (province du Québec, Canada): pétrologie, géochronologie, et relations avec les minéralisations internes à Zr, Y, Nb. Thèse de doctorat, Université Claude Bernard-Lyon I, Lyon,

France.

_____, Bonhomme, M.G., Duthou, J.L. & Chenevoy, M. (1989): Chronologie Rb/Sr et K/Ar du granite peralcalin du lac Brisson, Labrador central, Nouveau-Québec. *Can J Earth Sci* **26,** 328-332.

Salvi, S. & Williams-Jones, A.E. (1990): The role of hydrothermal processes in the granite-hosted Zr, Y, REE deposit at Strange Lake, Quebec/Labrador: evidence from fluid inclusions *Geochim Cosmochim Acta* **54,** 2403-2418.

_____ & _____ (1991): Reply to comment by T.C. Birkett and R.R. Miller on "The role of hydrothermal processes in the granite-hosted Zr, Y, REE deposit at Strange Lake, Quebec/Labrador: evidence from fluid inclusions" *Geochim Cosmochim Acta* **55,** 3447-3449.

_____ & _____ (1992). Reduced orthomagmatic C-O-H-NaCl fluids in the Strange Lake rare-metal granitic complex, Quebec/Labrador, Canada. *Eur J Mineral* **4,** 1155-1174.

Shmakin, B.M. (1979): Composition and structural state of K-feldspars from some U.S. pegmatites. *Am Mineral.* **64,** 49-56.

Smith, J.V. (1974): Feldspar minerals. 1. Crystal structure and physical properties Springer-Verlag, Heidelberg, 627 pp.

_____ & Brown, W.L. (1988): Feldspar Minerals. 1. Crystal structures, physical, chemical, and microtextural properties (second ed.). Springer-Verlag, Berlin, 828 pp.

Steiner, J.C., Jahns, R.H. & Luth, W.C. (1975). Crystallization of alkali feldspar and quartz in the haplogranite system $NaAlSi_3O_8$-$KAlSi_3O_8$-SiO_2-H_2O at 4 kb *Geol Soc Am. Bull* **86,** 83-98.

Stevenson, R.K. & Martin, R.F. (1986): Implications of the presence of amazonite in the Broken Hill and Geco metamorphosed sulfide deposits. *Can Mineral* **24,** 729-745.

Taylor, B.E. (1988): Degassing of rhyolitic magmas: hydrogen isotope evidence and implications for magmatic-hydrothermal ore deposits. *In* Recent Advances in the Geology of Granite-Related Mineral Deposits (R.P. Taylor & D.F. Strong, eds.). *Can Inst Min Metall, Spec Vol* **39,** 33-49.

Tuttle, O. F. & Bowen, N. L. (1958): Origin of granite in light of experimental studies in the system $NaAlSi_3O_8$-$KAlSi_3O_8$-SiO_2-H_2O. *Geol Soc. Amer Mem.* **74.**

Whalen, J.B., Currie, K.L. & Chappell, B.W. (1987): A-type granites: geochemical characteristics, discrimination and petrogenesis. *Contrib. Mineral. Petrol* **95,** 407-419.

Wones, D.R. & Appleman, D.E. (1963): Properties of synthetic Triclinic $KFeSi_3O_8$, iron-microcline, with some observations on the iron-microcline ⇌ iron-sanidine transition. *J. Petrol.* **4,** 131-137.

CHAPTER 4

Conclusions

Conclusions

The following are the principal conclusions derived from this research:

1) The Strange Lake granite complex may be subdivided into different petrogenetic units based on its feldspar petrography: hypersolvus granite, a single mesoperthitic alkali feldspar; transsolvus granite, mesoperthitic alkali feldspar set in a matrix of discrete microcline and albite grains; subsolvus granite, isolated grains of microcline and albite; and pegmatite, K-feldspar megacrysts with rare albite.

2) The temperature of crystallization of the least evolved hypersolvus granite through pegmatite units can be monitored *via* the assemblage of felsic minerals and of mafic minerals. There is a progressive decrease in temperature of the respective solidus for each unit. The depth of emplacement is considered to have been less than 4 km.

3) The transition from the least evolved hypersolvus granite through pegmatite is explained by the progressive buildup of added components to the haplogranite system. Progressive increases in excess alkalis (peralkalinity) and volatiles (F, H_2O) with evolution of the Strange Lake system enables the more evolved melts to crystallize at temperatures lower than the haplogranite system. The hypersolvus granite crystallized at a temperature above 650°C, 0.7 kbar; the pegmatites crystallized below 590°C, 0.7 kbar.

4) The XRD data on the alkali feldspars of the different units reflect their highly ordered nature as well as their near-end-member compositions. This suggests that the feldspars have equilibrated over the interval between 300° to 100°C in the presence of a peralkaline fluid.

5) Bulk feldspar compositions (and granitic pegmatites) document an increase in Or mol.% with the evolution of the units. This can best be explained by degassing of the magma near or at the solidus, and ensuing forced crystallization of the magma upon massive loss of Na to the fluid phase.

6) Electron microprobe data indicate that Fe^{3+} enters the feldspar structure (up to 1 wt.% Fe_2O_3), reflecting the peralkaline nature of the parent melt. Very little to no Ca was present in the alkali feldspar at the magmatic stage. The striking buildup in Ca seen in the most evolved parts of the complex occurred at the subsolvus stage.

7) The trace element content of feldspar separates from the different units is typical of evolved peralkaline systems. Li, Rb, Cs and Tl increase, which is consistent with the fractionation of a single batch of magma; the increased Ba and Sr contents of some feldspar separates from pegmatites are consistent with late-stage hydrothermal mobilization, even in the most actionated pegmatites. Mineralization in the complex is attributed to the late redistribution of ore constituents *via* a contaminated peralkaline fluid, which gained Ca, Sr and Mg by interaction with country rocks.

APPENDIX I

Whole-rock geochemistry

APPENDIX I

WHOLE-ROCK GEOCHEMISTRY

Sample	38A1	46A1	46B3	46C1	46E1	47A1	48A2	48A3	48A5	49A1	57C10	LB10D1S	LB10D33
unit	hyp	hyp	hyp	hyp	hyp	hyp	hyp	hyp	hyp	hyp	hyp	hyp	hyp
SiO2wt%	70.96	69.94	70.21	70.10	70.54	72.06	72.65	66.31	69.99	72.08	70.92	68.99	70.18
TiO2	0.26	0.30	0.26	0.31	0.21	0.49	0.16	0.24	0.23	0.31	0.32	0.54	0.28
Al2O3	10.97	11.63	11.85	11.23	11.03	12.75	11.45	11.98	10.71	10.90	11.80	11.85	12.11
Fe2O3	2.35	1.96	4.15	2.42	3.51	1.26	1.89	3.63	3.35	3.01	1.66	2.23	2.05
FeO	3.35	2.58	0.41	3.22	1.34	2.83	3.38	5.16	4.31	2.44	2.75	3.23	2.40
MnO	0.11	0.12	0.06	0.15	0.12	0.06	0.09	0.11	0.13	0.08	0.10	0.12	0.10
MgO	0.01	0.01	0.01	0.01	0.09	0.13	0.01	0.01	0.01	0.01	0.01	0.00	0.01
CaO	0.36	0.82	0.69	0.83	0.78	1.48	0.11	0.23	0.37	0.32	0.18	1.00	0.85
Na2O	4.83	5.14	4.85	4.81	5.01	3.16	5.04	5.81	5.24	4.97	5.06	5.67	5.66
K2O	5.21	4.50	4.78	4.96	4.68	5.34	4.67	5.11	4.56	4.70	4.81	4.75	4.92
P2O5	0.01	0.02	0.02	0.03	0.04	0.09	0.01	0.01	0.01	0.01	0.01	0.04	0.02
F	0.53	0.65	0.59	0.77	0.59	0.10	0.26	0.47	0.51	0.49	0.63	0.69	0.69
LOI	0.30	0.53	1.18	0.60	0.67	0.36	0.14	0.28	0.30	0.18	0.11	0.16	0.12
	99.25	98.20	99.06	99.44	98.61	100.11	99.86	99.38	99.72	99.80	98.99	99.57	100.02
O=F	0.22	0.27	0.25	0.32	0.25	0.04	0.11	0.20	0.21	0.21	0.26	0.29	0.29
Total	99.05	97.93	98.81	99.12	98.36	100.07	99.75	99.18	99.51	99.61	98.73	99.28	99.73
A I	1.24	1.15	1.11	1.18	1.21	0.86	1.17	1.26	1.27	1.22	1.15	1.27	1.18
Normative mineralogy													
Q	25.37	23.00	24.74	23.57	24.29	28.89	26.24	14.18	23.28	27.07	24.17	20.36	20.39
C	0.00	0.00	0.00	0.00	0.00	0.00	0.00	0.00	0.00	0.00	0.00	0.00	0.00
Z	0.72	1.09	0.81	0.64	1.67	0.10	0.58	0.23	0.25	0.39	0.84	0.41	0.36
Or	31.08	26.84	28.57	29.56	27.97	31.64	27.78	30.34	27.14	28.02	28.63	28.21	29.23
Ab	27.19	34.57	34.08	29.96	30.43	26.74	32.75	33.07	29.55	29.71	33.75	31.38	36.17
An	0.00	0.00	0.00	0.00	0.00	1.81	0.00	0.00	0.00	0.00	0.00	0.00	0.00
Ac	6.80	5.67	6.12	7.00	10.16	0.00	5.47	10.50	9.69	8.71	1.80	6.15	5.93
Ns	1.39	0.58	0.00	0.65	0.10	0.00	0.86	0.97	0.94	0.57	0.84	1.16	1.09
Di	0.00	0.70	0.05	0.18	0.67	1.37	0.00	0.00	0.00	0.00	0.00	0.14	0.66
Wo	0.00	0.00	0.15	0.00	0.00	0.00	0.00	0.00	0.00	0.00	0.00	0.00	0.00
Hy	5.95	4.12	0.00	5.61	2.21	3.06	6.13	9.36	7.80	4.14	4.73	5.03	3.84
Mt	0.00	0.00	0.76	0.00	0.00	1.83	0.00	0.00	0.00	0.00	0.00	0.00	0.00
Hm	0.49	0.57	1.51	0.00	0.40	0.93	0.30	0.16	0.44	0.59	0.61	1.03	0.53
Il	0.02	0.05	0.49	0.59	0.09	0.21	0.02	0.02	0.02	0.02	0.02	0.09	0.05
Ap	0.00	0.00	0.00	0.00	0.00	0.00	0.00	0.00	0.00	0.00	0.00	0.00	0.00
Fl	2.18	2.67	2.42	3.16	2.41	0.38	1.07	1.93	2.10	2.01	2.59	3.57	2.83
Total	101.19	99.86	99.77	100.98	100.40	99.96	101.20	101.06	101.21	101.23	100.98	101.49	101.35
Proportion of normative components													
Qtz	30.33	27.25	28.31	28.37	29.37	33.10	30.24	18.28	29.13	31.92	27.93	24.54	23.68
Or	37.16	31.80	32.69	35.57	33.83	36.26	32.02	39.10	33.93	33.01	33.08	31.03	33.75
Ab	32.51	40.95	39.00	36.06	36.80	30.64	37.74	42.62	36.94	35.04	38.99	41.43	42.57
Trace-element concentrations													
Zn	728.0	557.0	217.0	370.0	846.0	83.0	473.0	612.0	291.0	196.0	493.0		
Rb	965.0	647.0	845.0	638.0	819.0	199.0	179.0	353.0	489.0	622.0	530.0	434.0	404.0
Sr	53.0	37.0	37.0	52.0	40.0	121.0	3.0	4.0	13.0	8.0	12.0	33.0	23.0
Ta	19.2	-----	23.0	-----	-----	-----	--- -		12.0	17.0			
Nb	384.0	496.0	431.0	485.0	479.0	26.0	254.0	128.0	261.0	450.0	516.0	214.0	145.0
Hf	134.3	-----	111.0	-----	----	-----	-----	- --	33.0	43.0		-	
Zr	5210.0	5427.0	4012.0	3161.0	8292.0	505.0	2861.0	1157.0	1246.0	1956.0	4190.0	2189.0	1767.0
Y	792.0	671.0	490.0	518.0	906.0	162.0	163.0	76.0	206.0	533.0	399.0	411.0	301.0
Th	74.8	-----	102.0	-----	-----	-----	-----	- - -	45.0	104.0			-
U	11.4	-----	14.3	-----	-- --	-----	-----	--	6.0	9.0			
La	1113.0	----	238.8	-----	-----	- ---	-----	----	107.4	199.0		-	
Ce	1884.0	-----	535.0	-----	-----	-----	-----	- ---	224.0	355.0			
Nd	771.0	-----	224.0	-----	-----	-- --	-----	- -	104.8	142.0			
Sm	172.4	-----	57.6	-----	----	-----	-----	-----	28.3	32.8	- -	-	
Eu	7.9	-----	3.1	-----	-----	-----	-----	--- -	1.8	2.0	-		
Gd	127.1	-----	59.9	-----	-----	-----	-----	-----	26.9	44.8	-	-	-
Tb	18.3	-----	10.7	-----	-----	-----	- ---	-- --	4.8	8.0	-- -	-	-
Dy	102.1	-----	-----	-----	-----	-----	-----	--- -	31.1	64.7	--	-	
Tm	6.8	-----	6.7	-----	-----	-----	-- --	----	2.6	8.0	- -	-	
Yb	49.2	----	53.3	-----	-----	-----	-----	---	24.7	61.7	-- -	-	
Lu	6.4	-----	-----	-----	----	-----	-----	-----	3.7	8	---		

APPENDIX I (cont'd)

WHOLE-ROCK GEOCHEMISTRY

Sample	1B9D13	5E13D12	57A1	57E1	58C4	58D1	37A3	38A1	57D1	25B1	25C1	25E1	27A4
unit	hyp	hyp	trans	trans	trans	trans	fsub	fsub	fsub	asub	asub	asub	asub
SiO2wt%	70.68	71.89	70.28	70.10	70.62	71.64	69.38	71.40	70.04	71.24	70.69	70.41	71.25
TiO2	0.30	0.29	0.16	0.38	0.23	0.19	0.12	0.20	0.31	0.20	0.48	0.22	0.27
Al2O3	12.22	10.51	11.26	12.48	12.01	11.69	12.65	10.14	11.84	9.02	9.00	8.86	8.16
Fe2O3	1.50	4.48	2.85	2.70	1.98	2.61	1.98	2.65	1.51	3.41	4.27	4.58	5.30
FeO	3.92	0.26	2.16	3.62	2.81	2.25	2.69	2.73	3.20	2.77	1.45	0.96	0.71
MnO	0.10	0.11	0.13	0.13	0.09	0.08	0.08	0.11	0.11	0.16	0.20	0.15	0.11
MgO	0.01	0.00	0.01	0.01	0.01	0.01	0.01	0.01	0.01	0.23	0.16	0.44	0.16
CaO	0.80	0.52	0.79	0.32	0.55	0.48	0.79	0.80	0.71	0.56	1.40	0.69	1.78
Na2O	5.57	5.33	4.65	4.32	5.13	5.11	3.25	4.99	5.23	4.65	3.98	3.41	3.68
K2O	4.75	4.31	5.20	5.20	4.98	4.73	8.64	3.76	4.71	3.02	3.79	4.36	4.06
P2O5	0.02	0.02	0.02	0.01	0.01	0.01	0.01	0.01	0.03	0.02	0.02	0.02	0.03
I	0.87	0.53	0.76	0.44	0.68	0.59	0.73	0.69	0.67	0.36	0.62	0.22	0.99
LOI	0.45	0.62	0.50	0.44	0.49	0.46	0.38	0.43	0.41	0.54	0.79	0.84	0.62
	101.19	98.91	98.77	100.15	99.59	99.85	100.71	97.92	98.78	96.18	96.85	95.16	97.12
Q-I	0.37	0.23	0.32	0.18	0.29	0.25	0.31	0.29	0.28	0.15	0.26	0.09	0.42
Total	100.82	98.68	98.45	99.97	99.30	99.60	100.40	97.63	98.50	96.03	96.59	95.07	96.70
A/I	1.17	1.28	1.18	1.02	1.15	1.16	1.16	1.21	1.16	1.21	1.18	1.17	1.28
Normative mineralogy													
Q	20.99	27.59	23.65	23.22	22.71	24.19	20.79	28.55	22.51	31.01	32.70	33.31	35.02
C	0.00	0.00	0.00	0.00	0.00	0.00	0.00	0.00	0.00	0.00	0.00	0.00	0.00
Z	0.82	0.89	1.63	0.97	0.39	0.56	0.06	1.05	0.83	3.21	2.09	3.06	2.50
Or	28.30	25.89	31.15	30.94	29.62	28.17	52.96	22.59	28.04	18.14	22.70	26.21	24.25
Ab	36.23	29.71	28.64	35.08	33.90	33.63	16.30	30.93	34.52	29.35	24.95	20.95	19.16
An	0.00	0.00	0.00	0.00	0.00	0.00	0.00	0.00	0.00	0.00	0.00	0.00	0.00
Ac	4.34	12.96	8.25	1.30	5.73	7.55	3.98	7.67	4.37	8.80	7.68	6.96	10.55
Ns	1.39	0.15	0.31	0.00	0.70	0.24	0.00	0.60	1.11	0.00	0.00	0.00	0.00
Di	0.45	0.00	0.09	0.00	0.00	0.00	0.31	0.50	0.07	0.80	2.57	1.76	0.86
Wo	0.00	0.00	0.00	0.00	0.00	0.00	0.00	0.00	0.00	0.00	0.33	0.00	1.14
Hy	6.68	0.20	3.92	4.42	4.97	3.99	4.25	4.65	5.55	4.90	0.00	0.28	0.00
Mt	0.00	0.00	0.00	3.27	0.00	0.00	0.88	0.00	0.00	0.53	2.34	2.94	1.86
Hm	0.57	0.55	0.30	0.72	0.00	0.00	0.00	0.00	0.00	0.00	0.00	0.14	0.37
Il	0.05	0.05	0.05	0.02	0.44	0.36	0.21	0.38	0.59	0.38	0.91	0.42	0.51
Ap	0.00	0.00	0.00	0.00	0.02	0.02	0.02	0.02	0.07	0.00	0.00	0.00	0.00
H	2.81	2.22	3.12	1.81	2.79	2.42	3.00	2.84	2.75	1.48	2.54	0.90	4.06
Total	102.66	100.22	101.11	101.75	101.27	101.43	102.75	99.78	100.41	98.65	98.86	96.98	100.35
Proportion of normative components													
Qtz	21.55	33.17	28.31	27.65	26.34	28.38	23.09	34.79	26.16	39.50	40.70	41.39	44.65
Or	33.09	31.12	37.31	33.91	34.35	32.65	58.81	27.52	32.96	23.11	28.25	32.57	30.92
Ab	42.36	35.71	34.32	38.44	39.31	38.97	18.10	37.69	40.58	37.39	31.05	26.04	24.43
Trace-element concentrations													
Zn	-	-	687.0	359.0	394.0	418.0	419.0	728.0	508.0	1158.0	987.0	1113.0	957.0
Rb	602.0	631.0	1086.0	535.0	481.0	560.0	1714.0	965.0	521.0	757.0	791.0	1148.0	669.0
Sr	52.0	28.0	26.0	9.0	12.0	11.0	18.0	53.0	18.0	35.0	39.0	81.0	23.0
Ta		- -	0.0	- ---	12.8	13.0	-----	19.2	33.0	-----	52.0	58.0	-----
Nb	383.0	436.0	615.0	289.0	213.0	214.0	30.0	384.0	566.0	684.0	862.0	1094.0	979.0
Hf	- ---		192.0	- ---	61.3	75.0	-----	134.3	91.0	-----	352.0	416.0	-----
Zr	8064.0	4448.0	8091.0	4814.0	1957.0	2767.0	307.0	5210.0	4124.0	15974.0	10420.0	15201.0	12424.0
Y	0.0	596.0	1022.0	277.0	513.0	483.0	698.0	792.0	624.0	723.0	1431.0	1822.0	1106.0
Th	---	-	66.0	----	36.5	34.0	-----	74.8	51.0	-----	198.0	203.0	-----
U	-- --	-- --	20.0	---	4.6	6.0	-----	11.4	29.9	-----	32.2	39.0	-----
La	----	-- --	473.3	- ---	311.3	272.8	-----	1113.0	359.0	-----	1003.0	1337.0	-----
Ce	----	- ---	987.0	--- -	534.4	493.0	-----	1884.0	671.9	-----	1913.0	2271.0	-----
Nd	- -	-----	356.0	-----	239.2	236.0	-----	771.0	260.2	-----	774.0	1039.0	-----
Sm	- ---	----	97.5	-----	59.2	51.6	-----	172.4	64.5	-----	166.8	220.9	-----
Eu	-----	- ---	6.2	-----	3.1	3.2	-----	7.9	3.6	-----	11.1	12.3	-----
Gd	-----	-- --	95.8	-----	62.2	46.5	-----	127.1	64.5	-----	168.6	200.5	-----
Tb	- ---	-----	17.1	-----	11.1	8.3	-----	18.3	11.5	-----	30.1	35.8	-----
Dy	---	-----	111.3	-----	49.5	54.3	-----	102.1	82.7	-----	204.8	-- --	-----
Tm	-----	- ---	9.2	----	5.2	4.2	-----	6.8	6.5	-----	18.9	17.5	-----
Yb	-----	-----	63.7	-----	38.0	31.5	-----	49.2	56.0	-----	160.5	133.9	-----
Lu	-----	-----	8.3	-----	5.1	4.1	-----	6.4	7.2	-----	20.3	15.8	-----

APPENDIX I (cont'd)

WHOLE-ROCK GEOCHEMISTRY

Sample	27B1	27B5	46G3	LB11D17	LB13D16	SL8D3	LB13D8	LB15D16	LB5D29	LB5D44	LB7D11	SL16D7
unit	asub	asub	asub	asub	asub	asub	asub	asub	asub	asub	asub	asub
SiO2wt%	71.62	71.01	71.93	71.53	70.36	72.34	70.40	71.18	70.25	70.85	71.13	70.85
TiO2	0.24	0.25	0.32	0.29	0.33	0.04	0.31	0.29	0.30	0.36	0.31	0.32
Al2O3	9.88	9.02	9.29	8.86	8.52	8.91	8.27	8.61	8.35	8.58	8.78	8.53
Fe2O3	5.79	3.62	2.62	5.37	5.37	3.17	5.77	2.13	5.51	4.50	2.11	3.63
FeO	0.20	2.91	2.39	1.03	1.03	1.73	0.32	2.44	0.88	1.06	3.40	2.09
MnO	0.12	0.13	0.14	0.14	0.14	0.13	0.11	0.16	0.16	0.15	0.16	0.16
MgO	0.22	0.01	0.01	0.27	0.33	0.09	0.48	0.72	0.31	0.18	0.49	0.13
CaO	0.77	0.99	0.30	0.92	1.66	1.52	1.39	1.91	2.19	2.27	1.65	1.81
Na2O	4.80	4.76	3.46	4.53	3.69	4.15	3.46	3.58	4.30	4.06	3.85	3.88
K2O	3.65	3.69	4.42	3.78	4.32	3.84	4.64	3.59	3.68	3.85	3.67	3.95
P2O5	0.02	0.01	0.01	0.02	0.02	0.02	0.02	0.03	0.02	0.02	0.03	0.01
F	0.15	0.69	0.19	0.23	0.19	0.27	0.18	0.51	0.59	0.51	0.31	0.44
LOI	0.70	0.77	1.01	0.67	0.66	0.61	0.74	1.22	0.77	0.60	0.83	0.74
	98.16	97.86	96.09	97.41	96.43	97.17	96.09	96.37	97.61	96.99	97.05	96.84
O=F	0.06	0.29	0.08	0.10	0.08	0.11	0.08	0.21	0.25	0.21	0.13	0.18
Total	98.10	97.57	96.01	97.31	96.35	97.06	96.01	96.16	97.36	96.78	96.92	96.36
A/I	1.20	1.31	1.13	1.30	1.26	1.23	1.30	1.14	1.32	1.26	1.17	1.25
Normative mineralogy												
Q	30.44	30.33	33.54	31.44	31.75	32.25	32.20	32.60	30.60	31.59	30.73	31.32
C	0.00	0.00	0.00	0.00	0.00	0.00	0.00	0.00	0.00	0.00	0.00	0.00
Z	1.55	1.01	2.65	2.52	2.97	3.10	3.18	2.47	2.71	2.60	2.37	3.00
Or	21.92	22.06	26.47	22.69	25.93	23.13	27.85	21.62	22.16	23.17	22.06	23.73
Ab	30.22	25.65	22.90	24.25	19.46	24.10	26.36	23.98	22.13	22.36	21.44	21.58
An	0.00	0.00	0.00	0.00	0.00	0.00	0.00	0.00	0.00	0.00	0.00	0.00
Ac	9.15	10.47	5.62	12.40	10.36	9.17	11.38	5.56	12.55	10.56	7.06	9.91
Ns	0.00	0.64	0.00	0.00	0.00	0.14	0.00	0.00	0.00	0.00	0.03	0.00
Di	1.18	1.33	0.45	2.78	2.02	5.40	2.58	5.82	2.51	2.72	5.66	5.98
Wo	0.62	0.00	0.00	0.00	1.96	0.00	1.09	0.00	2.64	2.30	0.00	0.00
Hy	0.00	4.49	3.34	0.07	0.00	0.16	0.00	2.96	0.00	0.00	1.31	0.62
Mt	0.34	0.00	0.98	1.57	2.59	0.00	0.49	0.30	1.70	1.23	0.00	0.30
Hm	2.39	0.00	0.00	0.00	0.00	0.00	1.50	0.00	0.00	0.00	0.00	0.00
Il	0.45	0.47	0.61	0.55	0.63	0.74	0.59	0.55	0.57	0.68	0.59	0.61
Ap	0.00	0.00	0.00	0.00	0.00	0.00	0.00	0.00	0.00	0.00	0.00	0.00
Fl	0.61	2.83	0.78	0.94	0.78	0.10	0.73	2.09	2.42	2.09	1.27	1.81
Total	98.93	99.31	97.37	99.26	98.48	99.35	98.00	98.02	100.05	99.36	98.58	98.87
Proportion of normative components												
Qtz	36.86	38.86	40.45	40.11	41.16	40.58	42.14	41.69	40.86	40.96	39.79	40.87
Or	26.54	28.27	31.93	28.95	33.61	29.10	36.45	27.65	29.59	30.01	28.56	30.97
Ab	36.60	32.87	27.62	30.94	25.23	30.32	21.41	30.66	29.55	29.00	31.65	28.16
Trace-element concentrations												
Zn	936.0	1063.0	937.0	-----	-----	-----	--- -	- - -	-			
Rb	914.0	669.0	911.0	921.0	1031.0	1150.0	1128.0	1057.0	1082.0	1100.0	961.0	997.0
Sr	62.0	23.0	16.0	53.0	127.0	64.0	94.0	79.0	138.0	119.0	82.0	84.0
Ta	52.0	-----	50.0	-----	-----	-----	65.1	17.5		61.7		65.0
Nb	1080.0	629.0	525.0	729.0	1070.0	969.0	1194.0	1062.0	998.0	986.0	1059.0	1055.0
Hf	194.0	-----	514.3	-----	-----	-----	506.2	375.7		427.0		508.0
Zr	7730.0	5016.0	13190.0	12525.0	14762.0	15406.0	15806.0	12312.0	13481.0	12931.0	11797.0	14911.0
Y	1065.0	952.0	1061.0	411.0	1849.0	0.0	1913.0	1799.0	1469.0	1457.0	1128.0	1563.0
Th	216.0	-----	87.6	-----	----	- ---	372.8	151.0		183.2		253.7
U	23.2	-----	36.0	-----	-- -	-----	65.0	0.0		40.0	-	49.0
La	623.4	-----	522.9	-----	- ---	-----	780.9	1021.9	-	971.7		901.1
Ce	1159.0	-----	999.6	-----	-----	----	1418.0	1791.0	-	1686.5	-	1586.0
Nd	474.5	-----	470.9	-----	-----	-----	619.0	700.5		692.5		685.8
Sm	107.2	-----	121.0	--- -	-----	-----	182.1	179.9	- -	181.9		173.0
Eu	5.8	-----	7.0	-----	-----	-----	9.7	9.2	----	8.2	-	8.7
Gd	118.7	-----	145.6	-----	-----	-----	233.0	202.7	-- -	183.1		210.6
Tb	21.2	-----	21.6	-----	-----	-----	37.5	30.7	-	29.2	-	37.6
Dy	141.6	-----	164.7	-----	-----	-----	248.9	242.0	--	195.3		219.8
Tm	11.5	-----	22.9	-----	-----	-----	28.2	19.5	--	20.5		21.7
Yb	98.4	-----	203.4	-----	-----	-----	198.9	153.2	- --	156.6		166.8
Lu	12.2	-----	21.8	-----	-----	-----	25.9	18.6		20.8		22.3

APPENDIX I (cont'd)

WHOLE-ROCK GEOCHEMISTRY

Sample	SL16D1	SL9BD3	SL5D36	SL5D9	SL8D13	37L6	63C1	LB13D12	LB13D43
unit	asub	asub	asub	asub	asub	peg	peg	peg	peg
SiO2wt%	70.41	71.03	70.61	69.68	72.16	63.17	63.86	68.01	65.39
TiO2	0.41	0.47	0.43	0.51	0.34	3.67	3.67	1.24	1.23
Al2O3	8.40	8.20	7.99	7.92	8.89	5.72	5.72	6.02	5.64
Fe2O3	2.88	3.80	4.80	5.30	2.93	1.53	3.29	4.48	6.42
FeO	1.02	0.79	0.63	1.14	2.02	0.00	0.16	0.26	0.65
MnO	0.14	0.08	0.15	0.18	0.15	0.02	0.16	0.10	0.11
MgO	0.10	0.00	0.25	0.18	0.01	0.68	0.26	1.26	0.70
CaO	1.16	2.66	2.72	2.71	1.46	12.49	5.90	3.57	4.31
Na2O	3.98	2.94	3.76	4.22	4.10	0.72	0.45	1.42	2.95
K2O	4.17	4.04	3.73	3.49	3.84	4.23	4.15	4.20	3.27
P2O5	0.05	0.03	0.01	0.02	0.02	0.01	0.01	0.00	0.00
F	0.24	1.15	0.59	0.52	0.24	-----	-----	0.57	1.11
LOI	1.86	1.45	0.72	0.78	0.60	2.87	1.27	2.46	1.97
	94.84	96.64	96.39	96.65	96.76	95.11	88.90	93.59	93.75
O=F	0.10	0.48	0.25	0.22	0.10	---	-----	0.24	0.47
Total	94.74	96.16	96.14	96.41	96.66	95.11	88.90	93.35	91.31
A/I	1.32	1.12	1.28	1.35	1.23	1.01	0.91	1.14	1.49
Normative mineralogy									
Q	34.15	36.62	33.08	30.78	32.21	28.20	36.08	37.58	33.14
C	0.00	0.00	0.00	0.00	0.00	0.00	0.00	0.00	0.00
Z	0.00	3.74	3.65	3.47	3.41	0.14	6.23	5.60	3.68
Or	23.65	24.42	22.46	21.00	23.12	25.41	25.04	25.26	19.65
Ab	19.99	19.25	20.00	21.01	24.01	5.54	3.81	7.23	10.55
An	0.00	0.00	0.00	0.00	0.00	0.00	1.11	0.00	0.00
Ac	8.33	1.96	10.41	12.95	8.48	0.49	0.00	4.22	12.70
Ns	0.98	0.00	0.00	0.00	0.25	0.00	0.00	0.00	0.00
Di	3.27	0.00	1.34	2.67	5.32	3.66	1.40	6.77	3.76
Wo	0.22	3.12	3.71	3.21	0.00	18.73	6.19	1.40	4.10
Hy	0.00	0.00	0.00	0.00	0.63	0.00	0.00	0.00	0.00
Mt	0.00	1.41	1.27	1.20	0.00	8.96	8.13	2.06	0.94
Hm	0.00	1.09	0.32	0.00	0.00	1.36	3.29	3.02	2.03
Il	0.78	0.89	0.82	0.97	0.65	0.01	0.68	0.76	1.61
Ap	0.00	0.00	0.00	0.00	0.00	0.00	0.00	0.00	0.00
H	0.97	4.71	2.43	2.13	0.98	0.00	0.00	2.34	4.58
Total	93.46	100.31	99.51	99.13	99.09	92.55	91.98	96.24	96.74
Proportion of normative components									
Qtz	43.33	45.61	43.79	42.29	36.39	47.68	55.57	53.63	52.32
Or	31.29	30.11	29.73	28.85	6.12	42.96	38.56	36.05	31.02
Ab	25.37	23.98	26.48	28.86	57.49	9.37	5.87	10.32	16.66
Trace-element concentrations									
Zn	---	-	-	--	-----	---	-----	-----	-----
Rb	--	1126.0	1099.0	986.0	1102.0	1076.0	1357.0	1158.0	845.0
Sr	- -	109.0	122.0	133.0	60.0	841.0	136.0	83.0	114.0
Ta	--	-	18.6	- --	-----	-----	-----	-----	126.8
Nb	125.9	1404.0	735.0	1278.0	924.0	310.0	2664.0	1726.0	1823.0
Hf	-	- - -	569.0	- --	-----	-----	-----	-----	631.0
Zr	533.5	18606.0	18148.0	17280.0	16959.0	709.0	1784.0	27870.0	18321.0
Y	- -	1918.0	1330.0	1471.0	1319.0	993.0	3479.0	2688.0	5203.0
Th	727.0	- -	131.2	- ---	-----	-----	-----	-----	689.1
U	108.0	-	36.0	-----	-----	-----	-----	-----	100.0
La	686.2	- -	654.9	- ---	-----	-----	-----	-----	1263.9
Ce	1453.0	--	1113.7	---	-----	-----	-----	-----	2872.0
Nd	618.9	-	501.3	-----	-----	-----	-----	-----	1244.5
Sm	286.4	--	130.1	-----	-----	-----	-----	-----	200.0
Eu	15.7	-- -	6.3	-----	-----	-----	-----	-----	20.4
Gd	160.3	- ---	145.6	-----	-----	-----	-----	-----	573.4
Tb	79.2	-- --	20.1	-----	-----	-----	-----	-----	101.6
Dy	529.8	-----	152.7	-----	-----	-----	-----	-----	636.6
Tm	53.4	- ---	20.8	-----	-----	-----	-----	-- --	76.7
Yb	345.5	- ---	189.0	-----	-----	-----	-----	-----	590.9
Lu	42.4	----	25.7	-----	-----	-----	-----	-----	70.3

APPENDIX II

Unit-cell parameters of K- and Na-feldspars in representative samples of the Strange Lake Complex

APPENDIX II
UNIT-CELL PARAMETERS OF K-FELDSPAR(S) IN REPRESENTATIVE SAMPLES OF THE STRANGE LAKE COMPLEX

	a	b	c	α	β	γ	V	#	a*	b*	c*	α*	β*	γ*
SL113	8.5857	12.9668	7.2311	90.579	115.946	87.725	722.30	63	0.129628	0.077184	0.154010	90.463	64.056	92.248
@	0.0009	0.0013	0.0008	0.012	0.009	0.010	0.10		0.000017	0.000008	0.000019	0.011	0.009	0.010
SL120	8.5871	12.9658	7.2224	90.608	115.934	87.682	722.56	79	0.129593	0.077192	0.153968	90.451	64.069	92.282
@	0.0008	0.0010	0.0006	0.010	0.008	0.009	0.08		0.000012	0.000006	0.000013	0.010	0.008	0.009
34C2	8.5791	12.9678	7.2198	90.628	115.954	87.667	721.59	60	0.129740	0.077180	0.154049	90.438	64.050	92.289
peg seg	0.0011	0.0013	0.0010	0.013	0.010	0.011	0.11		0.000017	0.000008	0.000019	0.013	0.010	0.011
36B3	8.5857	12.9675	7.2213	90.619	115.938	87.687	722.38	54	0.129621	0.077181	0.153997	90.437	64.066	92.272
@ trans	0.0011	0.0013	0.0009	0.011	0.011	0.010	0.12		0.000017	0.000008	0.000023	0.014	0.011	0.010
36B3	8.5841	12.9652	7.2237	90.656	115.942	87.653	722.35	75	0.129648	0.077196	0.153949	90.413	64.062	92.291
@ peg	0.0009	0.0013	0.0008	0.011	0.008	0.009	0.09		0.000014	0.000008	0.000016	0.011	0.008	0.009
37A1	8.5828	12.9664	7.2263	90.576	115.916	87.725	722.55	44	0.129672	0.077186	0.153900	90.467	64.056	92.250
	0.0016	0.0016	0.0011	0.619	0.013	0.018	0.15		0.000023	0.000009	0.000025	0.016	0.013	0.016
37A4	8.5746	12.9632	7.2268	90.639	115.912	87.700	721.74	29	0.129792	0.077206	0.153884	90.408	64.062	92.246
pheno	0.0018	0.0023	0.0014	0.021	0.024	0.021	0.23		0.000037	0.000014	0.000039	0.023	0.025	0.024
37A4	8.5796	12.9686	7.2203	90.612	115.869	87.645	722.24	33	0.129641	0.077177	0.153927	90.462	64.134	92.320
matrix	0.0018	0.0021	0.0010	0.017	0.016	0.015	0.16		0.000031	0.000012	0.000027	0.019	0.016	0.016
37D1	8.5828	12.9498	7.2154	90.549	115.823	87.746	721.36	34	0.129525	0.077284	0.153960	90.481	64.188	92.239
	0.0023	0.0030	0.0018	0.029	0.021	0.024	0.23		0.000038	0.000018	0.000040	0.027	0.022	0.021
37F6	8.5818	12.9647	7.2226	90.641	115.927	87.673	722.09	72	0.129669	0.077198	0.153953	90.419	64.077	92.276
*	0.0010	0.0012	0.0008	0.010	0.010	0.010	0.10		0.000016	0.000007	0.000017	0.010	0.010	0.010
38A3	8.5831	12.9729	7.2215	90.700	115.905	87.609	722.66	26	0.129629	0.077153	0.153947	90.383	64.101	92.319
sub	0.0021	0.0027	0.0018	0.037	0.021	0.034	0.23		0.000037	0.000016	0.000040	0.030	0.021	0.027
38B3	8.5822	12.9589	7.2186	90.597	115.956	87.664	721.22	32	0.129697	0.077234	0.154078	90.473	64.046	92.307
	0.0021	0.0025	0.0017	0.028	0.023	0.026	0.23		0.000039	0.000015	0.000038	0.026	0.023	0.024
43C1	8.5855	12.9673	7.2268	90.619	115.959	87.674	722.77	72	0.129648	0.077183	0.153906	90.444	64.044	92.286
	0.0011	0.0013	0.0009	0.012	0.010	0.009	0.10		0.000016	0.000008	0.000020	0.012	0.010	0.009
46A3	8.5802	12.9612	7.2195	90.636	115.947	87.714	721.35	43	0.129712	0.077217	0.154046	90.405	64.057	92.232
sub	0.0012	0.0017	0.0009	0.016	0.010	0.016	0.12		0.000019	0.000010	0.000019	0.014	0.010	0.014
46A4	8.5829	12.9658	7.2285	90.638	115.944	87.668	722.43	75	0.129671	0.077292	0.153914	90.425	64.060	92.283
peg	0.0008	0.0011	0.0007	0.009	0.007	0.008	0.08		0.000012	0.000006	0.000013	0.009	0.007	0.008
46G1	8.5878	12.9661	7.2220	90.613	115.946	87.712	722.52	77	0.129596	0.077188	0.153992	90.432	64.057	92.246
peg	0.0008	0.0013	0.0009	0.013	0.008	0.009	0.10		0.000014	0.000008	0.000020	0.013	0.008	0.009
46I4	8.5883	12.9652	7.2190	90.587	115.924	87.676	722.32	67	0.129570	0.077195	0.154028	90.477	64.078	92.299
peg in HG	0.0014	0.0017	0.0011	0.015	0.011	0.013	0.13		0.000022	0.000010	0.000022	0.015	0.011	0.013
47A1A	8.5828	12.9671	7.2300	90.699	115.975	87.597	721.72	40	0.129712	0.077188	0.154072	90.393	64.031	92.332
pheno #	0.0025	0.0021	0.0017	0.026	0.022	0.023	0.22		0.000033	0.000012	0.000040	0.023	0.021	0.021
47A1A	8.5853	12.9684	7.2206	90.604	115.934	87.678	722.36	37	0.129625	0.077176	0.154005	90.458	64.068	92.288
matrix	0.0030	0.0030	0.0017	0.029	0.027	0.027	0.28		0.000060	0.000018	0.000038	0.029	0.028	0.026
48A1	8.5839	12.9636	7.2245	90.671	115.928	87.657	722.39	58	0.129638	0.077205	0.153913	90.393	64.077	92.279
HG#	0.0010	0.0012	0.0008	0.011	0.011	0.010	0.11		0.000020	0.000007	0.000016	0.011	0.011	0.010
48G1	8.5844	12.9707	7.2230	90.692	115.967	87.630	722.43	48	0.129675	0.077165	0.153996	90.384	64.039	92.299
	0.0017	0.0016	0.0011	0.013	0.013	0.014	0.25		0.000028	0.000010	0.000024	0.015	0.013	0.015
57C1	8.5865	12.9670	7.2234	90.620	115.962	87.644	722.46	62	0.129640	0.077187	0.153983	90.458	64.041	92.318
	0.0010	0.0011	0.0007	0.010	0.009	0.009	0.09		0.000016	0.000006	0.000014	0.010	0.009	0.009
58C1	8.5845	12.9627	7.2228	90.685	115.930	87.660	722.21	35	0.129632	0.077211	0.153953	90.409	64.074	92.283
pheno	0.0021	0.0015	0.0011	0.019	0.019	0.017	0.20		0.000040	0.000009	0.000028	0.018	0.019	0.017
58C1	8.5796	12.9654	7.2226	90.680	115.976	87.634	721.63	31	0.129759	0.077196	0.154017	90.397	64.029	92.301
matrix	0.0017	0.0022	0.0012	0.018	0.018	0.018	0.19		0.000033	0.000013	0.000033	0.019	0.018	0.019
63B3	8.5849	12.9712	7.2238	90.647	115.935	87.651	722.77	87	0.129633	0.077161	0.153939	90.429	64.069	92.300
peg	0.0008	0.0010	0.0006	0.009	0.007	0.008	0.08		0.000013	0.000006	0.000013	0.008	0.007	0.008
63C1	8.5855	12.9656	7.2226	90.600	115.912	87.662	722.54	70	0.129599	0.077194	0.153935	90.469	64.091	92.308
*	0.0008	0.0012	0.0008	0.011	0.008	0.008	0.09		0.000014	0.000007	0.000018	0.011	0.008	0.008

* Microcline without albite # Orthoclase is present @ Insufficient albite peaks to refine cell parameters

APPENDIX II (cont'd)

UNIT-CELL PARAMETERS OF Na-FELDSPAR(S) IN REPRESENTATIVE SAMPLES OF THE STRANGE LAKE COMPLEX

	a	b	c	α	β	γ	V	#	a*	b*	c*	α*	β*	γ*
34C2	8.1370	12.7876	7.1601	94.240	116.626	87.747	664.18	20	0.137478	0.078418	0.156543	86.386	63.360	90.398
peg seg	0.0022	0.0036	0.0019	0.030	0.023	0.026	0.32		0.000048	0.000031	0.000041	0.028	0.022	0.023
37A1	8.1393	12.7918	7.1611	94.222	116.585	87.670	664.93	40	0.137397	0.078391	0.156451	86.413	63.506	90.495
	0.0014	0.0018	0.0011	0.011	0.016	0.017	0.13		0.000031	0.000011	0.000026	0.016	0.017	0.013
37A4	8.1397	12.7894	7.1620	94.296	116.620	87.685	664.65	29	0.137426	0.078413	0.156498	86.353	63.470	90.439
pheno	0.0016	0.0024	0.0014	0.023	0.021	0.018	0.20		0.000044	0.000011	0.000041	0.023	0.021	0.018
37A4	8.1339	12.7903	7.1621	94.328	116.619	87.635	664.20	24	0.137524	0.078411	0.156497	86.313	63.474	90.479
matrix	0.0015	0.0029	0.0017	0.025	0.016	0.024	0.17		0.000026	0.000017	0.000041	0.023	0.017	0.023
37D1	8.1362	12.7885	7.1610	94.245	116.596	87.655	664.41	62	0.137456	0.078411	0.156475	86.375	63.496	90.499
	0.0007	0.0010	0.0007	0.010	0.008	0.007	0.08		0.000014	0.000007	0.000017	0.011	0.008	0.007
38A3	8.1347	12.7963	7.1627	94.282	116.598	87.678	664.81	32	0.137484	0.078369	0.156449	86.377	63.493	90.455
sub	0.0017	0.0020	0.0017	0.021	0.018	0.018	0.17		0.000034	0.000017	0.000041	0.018	0.018	0.014
38B3	8.1337	12.7873	7.1589	94.242	116.617	87.695	663.83	58	0.137521	0.078420	0.156553	86.409	63.477	90.455
	0.0013	0.0015	0.0010	0.014	0.014	0.013	0.13		0.000026	0.000009	0.000024	0.014	0.014	0.013
46A3	8.1349	12.7794	7.1554	94.222	116.595	87.667	663.33	35	0.137478	0.078467	0.156593	86.415	63.496	90.498
sub	0.0017	0.0020	0.0014	0.021	0.016	0.016	0.16		0.000034	0.000017	0.000033	0.021	0.016	0.016
46A4	8.1397	12.7876	7.1579	94.247	116.605	87.740	664.31	27	0.137407	0.078418	0.156563	86.381	63.481	90.403
peg	0.0011	0.0016	0.0011	0.019	0.013	0.015	0.13		0.000018	0.000010	0.000022	0.018	0.013	0.011
46A4	8.1401	12.7886	7.1627	94.275	116.620	87.669	664.72	68	0.137470	0.078415	0.156478	86.385	63.471	90.467
trans +	0.0008	0.0011	0.0007	0.011	0.008	0.008	0.08		0.000014	0.000006	0.000015	0.010	0.008	0.008
46A4	8.1354	12.7863	7.1626	94.283	116.571	87.674	664.49	32	0.137410	0.078430	0.156415	86.371	63.530	90.464
crud+	0.0012	0.0019	0.0014	0.022	0.019	0.014	0.17		0.000028	0.000011	0.000039	0.022	0.019	0.015
46G1	8.1414	12.7725	7.1592	94.446	116.582	87.630	663.71	9	0.137351	0.078543	0.156533	86.213	63.513	90.438
peg	0.0056	0.0219	0.0034	0.217	0.058	0.098	0.94		0.000106	0.000133	0.000091	0.201	0.067	0.061
46I4	8.1384	12.7884	7.1555	94.187	116.576	87.725	664.24	27	0.137395	0.078407	0.156563	86.155	63.511	90.457
peg in HG	0.0015	0.0016	0.0015	0.023	0.017	0.016	0.15		0.000032	0.000009	0.000033	0.021	0.016	0.017
47A1A	8.1369	12.7894	7.1577	94.261	116.612	87.683	664.10	45	0.137463	0.078409	0.156575	86.391	63.478	90.460
pheno	0.0013	0.0017	0.0012	0.017	0.014	0.013	0.13		0.000025	0.000011	0.000026	0.016	0.014	0.013
47A1A	8.1378	12.7903	7.1635	94.238	116.651	87.669	664.52	41	0.137501	0.078403	0.156501	86.426	63.436	90.483
matrix	0.0013	0.0017	0.0010	0.017	0.016	0.010	0.14		0.000030	0.000010	0.000033	0.017	0.016	0.010
48A1	8.1349	12.7892	7.1613	94.212	116.670	87.704	664.26	47	0.137506	0.078405	0.156499	86.438	63.469	90.460
HG	0.0014	0.0017	0.0012	0.019	0.011	0.015	0.12		0.000025	0.000011	0.000024	0.017	0.011	0.013
48G1	8.1376	12.7933	7.1628	94.274	116.635	87.663	664.69	50	0.137480	0.078387	0.156495	86.390	63.457	90.471
	0.0009	0.0011	0.0008	0.012	0.012	0.009	0.10		0.000021	0.000007	0.000021	0.013	0.012	0.009
57C1	8.1402	12.7908	7.1613	94.290	116.671	87.664	664.40	29	0.137479	0.078401	0.156581	86.371	63.430	90.467
	0.0019	0.0025	0.0016	0.030	0.021	0.022	0.21		0.000037	0.000015	0.000045	0.030	0.021	0.021
58C1	8.1418	12.7879	7.1614	94.243	116.631	87.692	664.67	56	0.137404	0.078416	0.156516	86.410	63.458	90.457
pheno	0.0009	0.0011	0.0009	0.011	0.010	0.008	0.10		0.000018	0.000007	0.000022	0.011	0.011	0.008
58C1	8.1416	12.7877	7.1614	94.286	116.595	87.681	664.81	47	0.137366	0.078422	0.156475	86.367	63.496	90.451
matrix	0.0011	0.0018	0.0010	0.014	0.011	0.012	0.12		0.000022	0.000011	0.000024	0.014	0.011	0.012
63B3	8.1419	12.7924	7.1618	94.326	116.561	87.671	665.29	12	0.137417	0.078397	0.156478	86.377	63.531	90.444
peg	0.0065	0.0072	0.0041	0.207	0.077	0.206	0.56		0.000107	0.000037	0.000122	0.186	0.081	0.052

+ Albite without microcline @ Insufficient albite peaks to refine cell parameters

APPENDIX III

Results of electron-microprobe analyses, K- and Na-feldspar

APPENDIX III

K-FELDSPAR ELECTRON-MICROPROBE SPOT ANALYSES

Sample	38B3			47A2			48A1	48A3		48A8		48B1		48G1	
unit	hyp	hyp	hyp	hyp	hyp	hyp	hyp	hyp	hyp	hyp	hyp	hyp	hyp	hyp	hyp
SiO2 wt%	64.09	64.65	64.51	65.30	65.01	65.22	65.52	65.06	65.57	65.50	65.54	64.65	64.52	65.18	64.54
Al2O3	17.37	17.77	17.16	17.38	17.69	17.01	17.73	17.77	17.76	17.73	17.27	17.86	17.99	17.49	17.65
K2O	16.57	17.30	16.35	16.31	16.37	15.76	16.56	16.63	16.95	16.87	16.27	16.97	16.94	16.76	16.73
Na2O	0.37	0.36	0.38	0.50	0.29	0.67	0.61	0.58	0.35	0.61	0.79	0.19	0.29	0.41	0.31
CaO	0.00	0.01	0.00	0.00	0.00	0.00	0.00	0.00	0.00	0.00	0.00	0.00	0.00	0.00	0.00
Fe2O3	0.49	0.35	0.43	0.39	0.06	0.63	0.60	0.72	0.40	0.96	1.00	0.10	0.18	0.91	0.71
TiO2	0.03	0.00	0.03	0.01	0.00	0.00	0.03	0.00	0.05	0.00	0.00	0.00	0.00	0.03	0.00
MgO	0.00	0.00	0.00	0.00	0.00	0.00	0.01	0.00	0.03	0.00	0.03	0.01	0.00	0.01	0.01
BaO	0.01	0.00	0.00	0.09	0.00	0.02	0.00	0.00	0.02	0.00	0.00	0.05	0.00	0.00	0.00
P2O5	0.00	0.00	0.01	0.00	0.36	0.00	0.00	0.02	0.01	0.01	0.00	0.00	0.00	0.00	0.00
SrO	0.06	0.10	0.09	0.05	0.05	0.05	0.11	0.11	0.10	0.03	0.05	0.10	0.09	0.07	0.07
PbO	0.14	0.13	0.07	0.06	0.07	0.12	0.06	0.00	0.01	0.00	0.00	0.00	0.00	0.00	0.06
Total	99.13	100.67	99.02	100.08	99.58	99.48	101.21	100.89	101.24	101.47	100.93	99.93	100.03	100.81	100.35
Structural formula based on 8 oxygens															
Si	3.007	2.996	3.022	3.024	3.020	3.033	3.006	2.997	3.009	3.000	3.015	3.005	2.997	3.006	3.001
Al	0.961	0.971	0.947	0.949	0.968	0.932	0.959	0.965	0.961	0.957	0.936	0.978	0.985	0.951	0.965
K	0.992	1.023	0.977	0.963	0.970	0.935	0.969	0.978	0.992	0.968	0.955	1.006	1.004	0.986	0.990
Na	0.034	0.032	0.035	0.045	0.027	0.061	0.054	0.052	0.031	0.054	0.071	0.017	0.026	0.037	0.028
Ca	0.000	0.001	0.000	0.000	0.000	0.000	0.000	0.000	0.000	0.000	0.000	0.000	0.000	0.000	0.000
Fe3+	0.017	0.012	0.015	0.014	0.002	0.022	0.021	0.025	0.014	0.033	0.035	0.003	0.006	0.032	0.025
Ti	0.001	0.000	0.001	0.000	0.000	0.000	0.001	0.000	0.002	0.000	0.000	0.000	0.000	0.001	0.000
Mg	0.000	0.000	0.000	0.000	0.000	0.000	0.001	0.000	0.001	0.001	0.000	0.001	0.001	0.000	0.001
Ba	0.000	0.000	0.000	0.002	0.000	0.000	0.000	0.000	0.000	0.000	0.000	0.001	0.000	0.000	0.000
P	0.000	0.000	0.000	0.000	0.001	0.000	0.000	0.001	0.000	0.000	0.000	0.000	0.000	0.000	0.000
Sr	0.002	0.003	0.003	0.001	0.001	0.001	0.003	0.003	0.003	0.001	0.001	0.003	0.003	0.003	0.003
Pb	0.002	0.002	0.001	0.001	0.001	0.002	0.001	0.000	0.000	0.000	0.000	0.000	0.000	0.000	0.001
Total	5.015	5.039	5.001	4.998	4.991	4.987	5.011	5.021	5.013	5.015	5.013	5.015	5.033	5.014	5.013
Feldspar Molecular Proportions															
OR	0.967	0.969	0.966	0.956	0.973	0.939	0.947	0.949	0.969	0.947	0.931	0.981	0.975	0.964	0.973
AB	0.033	0.031	0.034	0.044	0.027	0.061	0.053	0.051	0.031	0.053	0.069	0.017	0.025	0.036	0.027
AN	0.000	0.001	0.000	0.000	0.000	0.000	0.000	0.000	0.000	0.000	0.000	0.000	0.000	0.000	0.000

Sample	49A1				49C1		49D3		57C1			57D1			58E1	
unit	hyp	hyp	hyp	hyp	hyp	hyp	hyp	hyp	hyp	hyp	hyp	hyp	hyp	hyp	hyp	hyp
SiO2 wt%	63.61	63.62	64.50	64.29	64.27	65.29	65.02	64.70	65.65	65.49	65.74	65.05	65.43	65.93	65.46	
Al2O3	18.81	18.04	18.08	17.19	17.81	17.19	17.22	17.45	17.68	17.68	17.35	17.81	17.21	17.34	17.40	
K2O	16.54	16.19	15.36	16.47	15.50	15.14	15.73	15.95	16.97	17.18	16.71	15.61	15.63	16.49	16.05	
Na2O	0.35	0.68	1.21	0.38	0.23	0.29	0.57	0.19	0.27	0.31	0.51	0.35	0.39	0.53	0.65	
CaO	0.00	0.01	0.00	0.00	0.00	0.00	0.00	0.01	0.00	0.00	0.00	0.00	0.00	0.00	0.00	
Fe2O3	0.14	0.37	0.48	0.81	0.16	0.53	0.55	0.40	0.27	0.13	0.54	0.33	0.41	0.40	0.46	
TiO2	0.00	0.00	0.00	0.00	0.06	0.03	0.00	0.00	0.02	0.05	0.00	0.03	0.00	0.04	0.01	
MgO	0.00	0.00	0.01	0.00	0.00	0.01	0.00	0.00	0.01	0.00	0.02	0.00	0.01	0.00	0.00	
BaO	0.00	0.00	0.00	0.00	0.05	0.00	0.00	0.06	0.08	0.09	0.01	0.00	0.02	0.00	0.00	
P2O5	0.01	0.04	0.00	0.00	0.00	0.00	0.03	0.00	0.00	0.03	0.02	0.01	0.00	0.01	0.03	
SrO	0.08	0.07	0.04	0.03	0.08	0.07	0.06	0.05	0.05	0.08	0.04	0.06	0.10	0.06	0.06	
PbO	0.01	0.00	0.00	0.00	0.08	0.12	0.00	0.00	0.13	0.15	0.05	0.17	0.13	0.18	0.17	
Total	99.54	99.02	99.67	99.07	98.22	98.67	99.17	98.50	101.13	101.07	100.93	99.31	99.31	100.95	100.99	
Structural formula based on 8 oxygens																
Si	2.965	2.982	2.991	3.011	3.016	3.043	3.028	3.031	3.017	3.015	3.023	3.030	3.045	3.040	3.023	
Al	1.034	0.997	0.988	0.950	0.985	0.944	0.945	0.963	0.957	0.959	0.935	0.975	0.945	0.939	0.947	
K	0.984	0.968	0.909	0.985	0.928	0.900	0.935	0.953	0.995	1.009	0.980	0.976	0.928	0.961	0.936	
Na	0.032	0.061	0.109	0.034	0.021	0.026	0.051	0.017	0.024	0.018	0.050	0.031	0.035	0.047	0.058	
Ca	0.000	0.000	0.000	0.000	0.000	0.000	0.000	0.000	0.000	0.000	0.000	0.000	0.000	0.000	0.000	
Fe3+	0.005	0.013	0.017	0.029	0.006	0.019	0.019	0.003	0.009	0.005	0.019	0.008	0.015	0.014	0.016	
Ti	0.000	0.000	0.000	0.000	0.002	0.001	0.000	0.000	0.001	0.002	0.000	0.001	0.000	0.002	0.000	
Mg	0.000	0.000	0.001	0.000	0.000	0.001	0.000	0.000	0.001	0.000	0.002	0.000	0.001	0.000	0.000	
Ba	0.000	0.000	0.000	0.000	0.001	0.000	0.000	0.001	0.001	0.002	0.000	0.000	0.000	0.000	0.000	
P	0.000	0.002	0.000	0.000	0.000	0.000	0.001	0.000	0.000	0.001	0.001	0.000	0.000	0.000	0.001	
Sr	0.002	0.002	0.001	0.001	0.002	0.002	0.002	0.001	0.001	0.002	0.001	0.002	0.003	0.002	0.002	
Pb	0.000	0.000	0.000	0.000	0.001	0.002	0.000	0.000	0.002	0.002	0.001	0.002	0.005	0.002	0.002	
Total	5.022	5.025	5.015	5.010	4.961	4.937	4.981	4.970	5.008	5.014	5.013	4.966	4.967	4.996	4.995	
Feldspar Molecular Proportions																
OR	0.969	0.940	0.893	0.966	0.978	0.972	0.948	0.983	0.976	0.982	0.952	0.967	0.964	0.958	0.942	
AB	0.031	0.060	0.107	0.034	0.022	0.028	0.052	0.018	0.024	0.018	0.048	0.033	0.036	0.042	0.058	
AN	0.000	0.000	0.000	0.000	0.000	0.000	0.000	0.000	0.000	0.000	0.000	0.000	0.000	0.000	0.000	

APPENDIX III (cont'd)

K-FELDSPAR ELECTRON-MICROPROBE SPOT ANALYSES

Sample	58I 1	57A2			58C1		58D1A					37A1		37A3	
unit	hyp	trans	trans	trans	trans	trans	trans	trans	trans	trans	trans	fsub	fsub	fsub	fsub
SiO2 wt%	64 14	65 49	65 68	65 33	65 37	65 34	66 20	65 77	65 99	65 70	65 69	64 47	64 24	65 42	67 51
Al2O3	17 52	17 62	17 36	17 40	17 39	17 31	17 43	17 26	17 21	17 21	17 05	17 11	17 74	17 29	18 51
K2O	16 65	15 58	15 80	15 40	16 95	17 02	16 40	16 30	16 23	16 56	16 29	16 15	16 24	16 14	8 87
Na2O	0 26	0 60	0 60	0 52	0 39	0 28	0 69	0 66	0 82	0 50	0 56	0 36	0 39	0 68	5 85
CaO	0 00	0 00	0 00	0 00	0 00	0 00	0 00	0 00	0 00	0 00	0 00	0 00	0 00	0 00	0 00
Fe2O3	0 34	0 15	0 38	0 60	0 59	0 56	0 69	0 70	0 75	0 79	0 65	0 64	0 11	1 06	0 23
TiO2	0 00	0 04	0 03	0 00	0 00	0 00	0 00	0 01	0 00	0 00	0 04	0 01	0 00	0 02	0 00
MgO	0 00	0 01	0 00	0 00	0 00	0 01	0 00	0 00	0 01	0 02	0 01	0 01	0 02	0 00	0 01
BaO	0 10	0 13	0 00	0 00	0 02	0 05	0 00	0 00	0 00	0 00	0 10	0 03	0 00	0 05	0 03
P2O5	0 00	0 00	0 00	0 00	0 03	0 02	0 00	0 00	0 02	0 00	0 01	0 01	0 00	0 00	0 00
SrO	0 03	0 06	0 06	0 06	0 03	0 05	0 07	0 01	0 05	0 04	0 04	0 02	0 03	0 09	0 05
PbO	0 16	0 00	0 00	0 04	0 05	0 07	0 00	0 03	0 06	0 20	0 20	0 06	0 00	0 02	0 00
Total	99 52	99 86	99 90	99 35	100 81	100 71	101 48	100 74	101 14	101 02	100 63	98 85	98 87	100 78	101 10
Structural formula based on 8 oxygens															
Si	3 011	3 027	3 033	3 030	3 015	3 019	3 023	3 025	3 025	3 023	3 031	3 023	3 009	3 013	3 010
Al	0 965	0 960	0 945	0 951	0 946	0 943	0 938	0 936	0 930	0 933	0 927	0 945	0 979	0 939	0 973
K	0 992	0 919	0 931	0 911	0 997	1 003	0 955	0 956	0 949	0 972	0 959	0 966	0 976	0 949	0 505
Na	0 024	0 054	0 054	0 047	0 035	0 025	0 061	0 059	0 073	0 044	0 050	0 033	0 035	0 060	0 506
Ca	0 000	0 000	0 000	0 000	0 000	0 000	0 000	0 000	0 000	0 000	0 000	0 000	0 000	0 000	0 000
Fe3+	0 012	0 016	0 013	0 021	0 021	0 019	0 024	0 024	0 026	0 028	0 022	0 023	0 004	0 037	0 009
Ti	0 000	0 001	0 001	0 000	0 000	0 000	0 000	0 000	0 000	0 000	0 001	0 000	0 000	0 001	0 000
Mg	0 000	0 000	0 000	0 000	0 000	0 001	0 000	0 000	0 001	0 001	0 001	0 000	0 001	0 000	0 000
Ba	0 002	0 003	0 000	0 000	0 000	0 001	0 000	0 000	0 000	0 000	0 002	0 001	0 000	0 001	0 001
P	0 000	0 000	0 000	0 000	0 001	0 001	0 000	0 000	0 001	0 000	0 000	0 000	0 000	0 000	0 000
Sr	0 001	0 002	0 002	0 002	0 001	0 001	0 002	0 000	0 001	0 001	0 001	0 001	0 001	0 002	0 001
Pb	0 002	0 000	0 000	0 001	0 001	0 001	0 000	0 000	0 001	0 003	0 003	0 001	0 000	0 000	0 000
Total	5 008	4 975	4 979	4 962	5 016	5 013	5 004	5 002	5 007	5 005	4 997	4 991	5 005	5 002	5 004
Feldspar Molecular Proportions															
OR	0 977	0 945	0 945	0 951	0 966	0 976	0 930	0 942	0 929	0 956	0 951	0 967	0 965	0 940	0 500
AB	0 023	0 055	0 055	0 049	0 034	0 024	0 060	0 058	0 072	0 044	0 050	0 033	0 035	0 060	0 501
AN	0 000	0 000	0 000	0 000	0 000	0 000	0 000	0 000	0 000	0 000	0 000	0 000	0 000	0 000	0 000

Sample	37A4			37D1				37F4		37I6	38A1		24B1	24C1	25B1
unit	fsub	fsub	fsub	fsub	fsub	fsub	fsub	fsub	fsub	fsub	fsub	fsub	asub	asub	asub
SiO2 wt%	64 88	65 61	65 11	64 92	64 75	65 40	64 97	64 73	64 68	64 80	64 75	64 90	63 92	63 91	63 14
Al2O3	17 15	17 42	17 57	17 89	17 71	17 48	17 37	17 18	17 55	17 67	17 51	17 19	17 31	17 15	16 91
K2O	16 39	16 36	16 25	16 54	16 63	16 19	16 05	16 41	16 48	16 33	16 10	16 39	16 87	16 18	16 26
Na2O	0 52	0 64	0 55	0 28	0 23	0 52	0 50	0 49	0 32	0 38	0 56	0 57	0 40	0 41	0 41
CaO	0 00	0 00	0 00	0 00	0 00	0 00	0 00	0 00	0 00	0 00	0 00	0 00	0 00	0 01	0 00
Fe2O3	1 13	0 86	0 84	0 13	0 11	0 86	0 84	0 78	0 19	0 06	0 77	0 83	0 98	0 41	0 94
TiO2	0 01	0 01	0 01	0 00	0 10	0 01	0 00	0 00	0 00	0 00	0 00	0 00	0 01	0 00	0 08
MgO	0 00	0 00	0 00	0 00	0 03	0 00	0 01	0 01	0 00	0 00	0 01	0 00	0 00	0 00	0 00
BaO	0 01	0 00	0 01	0 00	0 01	0 04	0 01	0 03	0 03	0 03	0 00	0 00	0 00	0 00	0 00
P2O5	0 00	0 01	0 00	0 00	0 01	0 00	0 02	0 00	0 02	0 00	0 00	0 00	0 00	0 04	0 01
SrO	0 06	0 06	0 07	0 07	0 07	0 09	0 07	0 07	0 06	0 04	0 08	0 07	0 02	0 09	0 04
PbO	0 01	0 00	0 00	0 22	0 12	0 00	0 06	0 16	0 08	0 25	0 04	0 06	0 00	0 23	0 12
Total	100 16	101 07	100 61	100 03	99 18	100 59	99 89	99 85	99 38	99 55	99 81	99 14	99 50	98 43	97 91
Structural formula based on 8 oxygens															
Si	3 011	3 014	3 010	3 010	3 011	3 014	3 014	3 015	3 017	3 017	3 008	3 002	2 995	3 016	3 003
Al	0 938	0 943	0 954	0 978	0 972	0 949	0 950	0 943	0 965	0 970	0 959	0 952	0 956	0 954	0 948
K	0 971	0 959	0 958	0 978	0 970	0 952	0 950	0 975	0 980	0 970	0 954	0 988	1 008	0 974	0 986
Na	0 047	0 057	0 049	0 025	0 021	0 047	0 045	0 044	0 028	0 034	0 050	0 052	0 037	0 038	0 038
Ca	0 000	0 000	0 000	0 000	0 000	0 000	0 000	0 000	0 000	0 000	0 000	0 000	0 000	0 001	0 000
Fe3+	0 0	0 040	0 039	0 004	0 004	0 030	0 029	0 027	0 007	0 002	0 027	0 029	0 035	0 015	0 034
Ti	0 000	0 000	0 000	0 000	0 003	0 002	0 000	0 000	0 000	0 000	0 000	0 000	0 000	0 000	0 003
Mg	0 000	0 000	0 000	0 000	0 002	0 000	0 001	0 001	0 000	0 000	0 001	0 002	0 000	0 000	0 000
Ba	0 000	0 000	0 000	0 000	0 000	0 001	0 000	0 001	0 001	0 001	0 000	0 000	0 000	0 000	0 000
P	0 000	0 000	0 000	0 000	0 000	0 000	0 001	0 000	0 001	0 000	0 000	0 000	0 000	0 002	0 000
Sr	0 002	0 002	0 002	0 002	0 002	0 002	0 002	0 002	0 002	0 001	0 002	0 002	0 001	0 003	0 001
Pb	0 000	0 001	0 000	0 003	0 002	0 000	0 001	0 002	0 001	0 003	0 001	0 001	0 000	0 003	0 002
Total	5 008	5 006	5 000	5 000	4 989	4 995	4 992	5 009	5 007	4 998	5 001	5 027	5 031	5 003	5 015
Feldspar Molecular Proportions															
OR	0 954	0 944	0 951	0 975	0 979	0 954	0 955	0 957	0 972	0 966	0 950	0 950	0 965	0 962	0 963
AB	0 046	0 056	0 049	0 025	0 021	0 047	0 045	0 043	0 028	0 034	0 050	0 050	0 035	0 037	0 037
AN	0 000	0 000	0 000	0 000	0 000	0 000	0 000	0 000	0 000	0 000	0 000	0 000	0 000	0 000	0 000

APPENDIX III (cont'd)

K-FELDSPAR ELECTRON-MICROPROBE SPOT ANALYSES

Sample	25B1				25C1			25E2	25X2			27B1			33B1	
unit	asub	asub	asub	asub	asub	asub	asub	asub	asub	asub	asub	asub	asub	asub	asub	asub
SiO2 wt%	64.92	65.39	64.09	64.77	65.04	65.15	65.07	64.53	64.67	65.35	65.17	65.31	64.15	64.67	64.39	
Al2O3	17.16	17.10	17.51	17.67	17.36	16.75	17.85	17.71	17.29	17.38	17.30	17.08	17.50	17.43	17.13	
K2O	16.50	16.55	16.16	16.85	16.58	16.00	16.93	15.99	16.38	16.09	16.22	15.29	16.19	15.87	16.08	
Na2O	0.41	0.37	0.71	0.21	0.42	0.51	0.29	0.59	0.39	0.60	0.58	0.52	0.47	0.55	0.58	
CaO	0.00	0.00	0.00	0.00	0.00	0.00	0.00	0.00	0.00	0.00	0.00	0.00	0.06	0.00	0.00	
Fe2O3	1.09	1.10	0.76	0.43	1.04	0.00	0.18	0.82	1.11	0.79	1.11	0.93	0.44	0.66	0.61	
TiO2	0.04	0.00	0.00	0.05	0.00	0.00	0.00	0.01	0.03	0.01	0.00	0.03	0.06	0.02	0.00	
MgO	0.00	0.00	0.00	0.00	0.00	0.03	0.02	0.00	0.01	0.00	0.00	0.00	0.01	0.01	0.00	
BaO	0.00	0.07	0.00	0.00	0.00	0.00	0.00	0.07	0.00	0.00	0.00	0.00	0.00	0.00	0.00	
P2O5	0.01	0.07	0.00	0.00	0.00	0.01	0.00	0.00	0.00	0.00	0.00	0.01	0.00	0.00	0.03	
SrO	0.08	0.02	0.04	0.03	0.07	0.09	0.03	0.06	0.01	0.03	0.03	0.06	0.05	0.01	0.08	
PbO	0.08	0.03	0.10	0.01	0.06	0.31	0.11	0.34	0.02	0.13	0.16	0.09	0.11	0.06	0.07	
Total	100.29	100.63	99.37	100.05	100.57	99.93	100.48	99.63	99.95	100.41	100.53	99.85	99.98	99.31	98.16	
Structural formula based on 8 oxygens																
Si	3.011	3.020	2.998	3.007	3.008	3.030	3.008	3.012	3.006	3.017	3.010	3.037	3.006	3.033	3.006	
Al	0.938	0.931	0.965	0.967	0.946	0.918	0.972	0.949	0.947	0.946	0.943	0.933	0.967	0.957	0.977	
K	0.976	0.975	0.964	0.998	0.978	0.949	0.998	0.952	0.971	0.938	0.956	0.936	0.968	0.947	0.971	
Na	0.037	0.033	0.065	0.019	0.038	0.048	0.026	0.054	0.035	0.054	0.052	0.047	0.038	0.049	0.053	
Ca	0.000	0.000	0.000	0.000	0.000	0.000	0.000	0.000	0.000	0.000	0.000	0.000	0.003	0.000	0.000	
Fe3+	0.038	0.038	0.027	0.015	0.036	0.037	0.006	0.029	0.040	0.038	0.040	0.033	0.016	0.024	0.022	
Ti	0.001	0.000	0.000	0.002	0.000	0.000	0.000	0.000	0.001	0.000	0.000	0.001	0.002	0.001	0.000	
Mg	0.000	0.000	0.000	0.000	0.000	0.001	0.001	0.000	0.001	0.000	0.000	0.000	0.001	0.001	0.000	
Ba	0.000	0.001	0.000	0.000	0.000	0.000	0.000	0.001	0.000	0.000	0.000	0.000	0.000	0.000	0.000	
P	0.000	0.000	0.000	0.000	0.000	0.001	0.000	0.000	0.000	0.000	0.000	0.000	0.000	0.000	0.001	
Sr	0.002	0.001	0.001	0.001	0.002	0.003	0.001	0.002	0.001	0.002	0.001	0.003	0.002	0.001	0.002	
Pb	0.001	0.000	0.001	0.001	0.001	0.004	0.001	0.004	0.000	0.002	0.002	0.001	0.001	0.001	0.001	
Total	5.005	4.999	5.021	5.008	5.009	4.990	5.014	5.002	5.002	4.996	5.003	4.980	5.004	4.990	5.018	
Feldspar Molecular Proportions																
OR	0.963	0.967	0.937	0.982	0.963	0.952	0.975	0.947	0.965	0.946	0.949	0.953	0.959	0.950	0.948	
AB	0.037	0.033	0.063	0.018	0.037	0.049	0.025	0.053	0.035	0.054	0.051	0.048	0.038	0.050	0.052	
AN	0.000	0.000	0.000	0.000	0.000	0.000	0.000	0.000	0.000	0.000	0.000	0.000	0.003	0.000	0.000	

Sample	27B4		33A1			36A3		16A4			16J3			46G1	16H5
unit	asub	asub	asub	asub	asub	asub	asub	asub	asub	asub	asub	asub	asub	asub	asub
SiO2 wt%	63.77	62.91	64.63	65.02	64.91	64.68	64.77	64.52	63.96	63.62	64.79	65.15	64.88	65.49	65.39
Al2O3	16.90	17.36	17.82	17.09	17.70	17.09	17.38	17.71	17.60	17.56	17.63	17.54	17.51	16.96	17.57
K2O	15.94	16.21	17.12	16.57	16.46	16.70	16.56	17.05	16.18	15.97	16.17	16.21	16.51	16.37	16.35
Na2O	0.67	0.50	0.21	0.41	0.62	0.50	0.63	0.22	0.52	0.54	0.55	0.61	0.43	0.48	0.45
CaO	0.00	0.00	0.00	0.00	0.00	0.00	0.00	0.00	0.00	0.00	0.00	0.00	0.00	0.00	0.00
Fe2O3	1.03	1.04	0.13	0.89	0.48	0.86	0.60	0.23	0.30	0.40	0.61	0.50	0.15	1.11	0.17
TiO2	0.00	0.00	0.08	0.03	0.02	0.02	0.00	0.03	0.01	0.05	0.03	0.00	0.00	0.00	0.00
MgO	0.01	0.00	0.00	0.00	0.01	0.00	0.00	0.00	0.00	0.00	0.01	0.01	0.00	0.00	0.00
BaO	0.06	0.00	0.03	0.00	0.00	0.00	0.02	0.04	0.01	0.07	0.04	0.00	0.00	0.00	0.00
P2O5	0.00	0.00	0.00	0.00	0.00	0.00	0.00	0.01	0.00	0.00	0.03	0.01	0.03	0.03	0.00
SrO	0.01	0.06	0.02	0.09	0.07	0.07	0.00	0.03	0.05	0.07	0.09	0.09	0.04	0.06	0.08
PbO	0.12	0.03	0.14	0.11	0.12	0.04	0.04	0.13	0.09	0.27	0.00	0.07	0.06	0.06	0.03
Total	98.51	98.10	100.18	100.22	100.39	99.96	99.81	99.95	99.69	98.55	99.93	100.16	100.16	100.56	100.33
Structural formula based on 8 oxygens															
Si	3.010	2.986	3.002	3.018	3.004	3.017	3.016	3.004	3.017	3.000	3.006	3.014	3.012	3.041	3.039
Al	0.940	0.971	0.976	0.935	0.965	0.938	0.943	0.972	0.964	0.976	0.964	0.957	0.960	0.933	0.956
K	0.960	0.981	1.015	0.981	0.972	0.992	0.984	1.013	0.959	0.961	0.957	0.957	0.978	0.965	0.964
Na	0.062	0.046	0.019	0.037	0.056	0.045	0.057	0.020	0.046	0.049	0.049	0.055	0.038	0.043	0.040
Ca	0.000	0.000	0.000	0.000	0.000	0.000	0.000	0.000	0.000	0.000	0.000	0.000	0.000	0.000	0.000
Fe3+	0.037	0.037	0.004	0.031	0.017	0.030	0.021	0.008	0.010	0.014	0.021	0.017	0.016	0.039	0.016
Ti	0.000	0.000	0.003	0.001	0.001	0.001	0.000	0.001	0.000	0.002	0.001	0.000	0.000	0.000	0.000
Mg	0.001	0.000	0.000	0.000	0.001	0.000	0.000	0.000	0.000	0.000	0.001	0.001	0.000	0.000	0.000
Ba	0.001	0.000	0.001	0.000	0.000	0.000	0.000	0.001	0.000	0.001	0.001	0.000	0.000	0.000	0.000
P	0.000	0.000	0.000	0.000	0.000	0.000	0.000	0.001	0.000	0.000	0.001	0.001	0.001	0.001	0.000
Sr	0.000	0.002	0.001	0.003	0.002	0.002	0.000	0.001	0.001	0.002	0.002	0.002	0.001	0.002	0.002
Pb	0.002	0.000	0.002	0.001	0.002	0.001	0.001	0.002	0.001	0.003	0.000	0.001	0.001	0.001	0.000
Total	5.012	5.023	5.021	5.007	5.018	5.021	5.022	5.021	4.998	5.008	5.002	5.004	5.006	4.997	4.996
Feldspar Molecular Proportions															
OR	0.940	0.955	0.982	0.964	0.946	0.957	0.945	0.981	0.954	0.951	0.958	0.946	0.962	0.957	0.960
AB	0.060	0.045	0.018	0.037	0.054	0.043	0.055	0.019	0.046	0.049	0.049	0.054	0.038	0.043	0.040
AN	0.000	0.000	0.000	0.000	0.000	0.000	0.000	0.000	0.000	0.000	0.000	0.000	0.000	0.000	0.000

APPENDIX III (cont'd)

K-FELDSPAR ELECTRON-MICROPROBE SPOT ANALYSES

Sample	46H3	57A1		63A2			63B3				34C2				43C1	63B2
unit	asub	asub	asub	asub	asub	asub	asub	asub	asub	asub	peg	peg	peg	peg	peg	peg
SiO2 wt%	65.46	65.19	65.80	65.55	65.62	64.96	65.26	65.45	65.04	65.72	64.75	65.41	65.59	65.22	65.31	
Al2O3	17.45	17.48	17.41	17.17	16.88	16.83	17.04	17.20	16.73	16.70	17.59	17.87	17.82	17.63	17.52	
K2O	16.44	16.49	15.90	16.00	15.99	15.89	16.24	16.41	16.22	16.59	16.57	16.03	15.54	16.46	16.89	
Na2O	0.50	0.58	0.84	0.55	0.35	0.46	0.35	0.47	4.93	0.38	0.34	0.70	1.28	0.42	0.28	
CaO	0.00	0.00	0.00	0.00	0.00	0.00	0.00	0.00	0.00	0.00	0.00	0.00	0.00	0.00	0.00	
Fe2O3	0.68	0.58	0.72	0.62	1.16	1.22	0.89	0.86	0.88	0.94	0.49	0.51	0.61	0.41	0.31	
TiO2	0.00	0.00	0.01	0.00	0.06	0.00	0.03	0.01	0.01	0.00	0.02	0.01	0.00	0.00	0.03	
MnO	0.01	0.00	0.00	0.01	0.03	0.01	0.00	0.00	0.00	0.01	0.00	0.00	0.01	0.02	0.00	
BaO	0.00	0.01	0.01	0.00	0.06	0.05	0.00	0.04	0.02	0.00	0.04	0.00	0.00	0.00	0.05	
P2O5	0.00	0.00	0.01	0.00	0.02	0.00	0.00	0.00	0.02	0.00	0.00	0.00	0.00	0.00	0.02	
SrO	0.01	0.08	0.06	0.10	0.06	0.05	0.04	0.05	0.03	0.04	0.00	0.05	0.02	0.05	0.00	
PbO	0.01	0.04	0.03	0.12	0.08	0.06	0.13	0.13	0.10	0.10	0.13	0.09	0.04	0.04	0.05	
Total	100.49	100.46	100.80	100.13	100.31	99.52	99.96	100.60	99.55	100.48	99.93	100.67	100.91	100.25	100.46	
Structural formula based on 8 oxygens																
Si	3.030	3.013	3.015	3.031	3.031	3.027	3.028	3.022	3.032	3.038	3.009	3.008	3.006	3.015	3.018	
Al	0.944	0.952	0.948	0.936	0.919	0.925	0.932	0.936	0.919	0.910	0.963	0.969	0.963	0.961	0.954	
K	0.968	0.972	0.937	0.943	0.942	0.944	0.961	0.966	0.965	0.978	0.982	0.940	0.909	0.971	0.996	
Na	0.045	0.052	0.075	0.049	0.031	0.042	0.032	0.042	0.045	0.034	0.031	0.063	0.113	0.038	0.025	
Ca	0.000	0.000	0.000	0.000	0.000	0.000	0.000	0.000	0.000	0.000	0.000	0.000	0.000	0.000	0.000	
Fe3+	0.024	0.202	0.025	0.022	0.040	0.043	0.031	0.030	0.031	0.033	0.017	0.018	0.021	0.014	0.011	
Ti	0.000	0.000	0.000	0.000	0.002	0.000	0.001	0.000	0.000	0.000	0.001	0.000	0.000	0.000	0.001	
Mg	0.000	0.000	0.000	0.001	0.000	0.000	0.000	0.000	0.000	0.001	0.000	0.000	0.001	0.001	0.000	
Ba	0.000	0.000	0.000	0.000	0.001	0.001	0.000	0.001	0.000	0.000	0.001	0.000	0.000	0.000	0.001	
P	0.000	0.000	0.000	0.000	0.001	0.000	0.000	0.000	0.001	0.000	0.000	0.000	0.000	0.000	0.001	
Sr	0.000	0.002	0.002	0.003	0.002	0.001	0.001	0.001	0.001	0.001	0.000	0.001	0.001	0.001	0.000	
Pb	0.000	0.001	0.000	0.000	0.001	0.001	0.002	0.002	0.001	0.001	0.002	0.001	0.001	0.001	0.001	
Total	5.002	5.013	5.003	4.986	4.972	4.982	4.986	4.999	4.995	4.996	5.006	5.000	5.013	5.001	5.007	
Feldspar Molecular Proprtions																
OR	0.956	0.949	0.926	0.951	0.952	0.958	0.968	0.959	0.956	0.966	0.970	0.937	0.889	0.962	0.975	
AB	0.044	0.051	0.075	0.049	0.032	0.042	0.032	0.041	0.044	0.034	0.030	0.063	0.111	0.038	0.025	
AN	0.000	0.000	0.000	0.000	0.000	0.000	0.000	0.000	0.000	0.000	0.000	0.000	0.000	0.000	0.000	

Sample	63B3	63C1			SJ113						SJ120					
unit	peg	peg	peg	peg	peg	peg	peg	peg	peg	peg	peg	peg	peg	peg	peg	
SiO2 wt%	65.31	65.79	65.31	65.17	65.07	66.31	66.08	65.25	64.55	65.28	65.57	65.91	65.31	65.51		
Al2O3	17.66	17.19	17.01	17.18	17.47	17.24	17.31	17.65	17.91	17.07	17.06	16.97	16.83	17.24		
K2O	16.31	16.69	16.57	15.80	15.96	15.93	16.00	17.10	16.72	15.55	15.69	16.23	15.60	15.58		
Na2O	0.36	0.21	0.32	0.85	0.23	0.70	0.71	0.09	0.06	7.92	0.74	0.43	0.72	0.82		
CaO	0.00	0.00	0.00	0.00	0.00	0.00	0.00	0.06	0.12	0.00	0.00	0.00	0.00	0.00		
Fe2O3	0.31	0.37	0.49	0.31	0.32	0.42	0.28	0.07	0.00	0.43	0.36	0.36	0.37	0.32		
TiO2	0.00	0.02	0.00	0.00	0.00	0.00	0.03	0.01	0.01	0.00	0.00	0.03	0.00	0.00		
MnO	0.00	0.01	0.00	0.00	0.00	0.02	0.00	0.00	0.11	0.00	0.02	0.00	0.02	0.04		
BaO	0.03	0.13	0.00	0.00	0.00	0.09	0.00	0.03	0.00	0.01	0.01	0.03	0.03	0.00		
P2O5	0.00	0.01	0.00	0.00	0.00	0.00	0.00	0.01	0.02	0.00	0.03	0.02	0.01	0.01		
SrO	0.00	0.01	0.03	0.02	0.01	0.00	0.02	0.00	0.02	0.07	0.00	0.02	0.03	0.00		
PbO	0.07	0.05	0.14	0.10	0.07	0.00	0.04	0.06	0.00	0.00	0.05	0.00	0.03	0.00		
Total	100.13	100.52	99.89	99.73	100.12	100.73	100.47	100.32	99.51	99.20	99.54	100.00	98.96	99.53		
Structural formula based on 8 oxygens																
Si	3.020	3.035	3.034	3.031	3.041	3.040	3.037	3.019	3.005	3.037	3.040	3.046	3.046	3.035		
Al	0.963	0.935	0.933	0.939	0.948	0.932	0.938	0.962	0.983	0.936	0.932	0.924	0.925	0.941		
K	0.964	0.982	0.982	0.937	0.937	0.932	0.938	1.009	0.993	0.923	0.928	0.957	0.928	0.921		
Na	0.033	0.019	0.029	0.076	0.020	0.062	0.063	0.008	0.006	0.072	0.067	0.038	0.065	0.074		
Ca	0.000	0.000	0.000	0.000	0.000	0.000	0.000	0.003	0.006	0.000	0.000	0.000	0.000	0.000		
Fe3+	0.015	0.013	0.017	0.011	0.011	0.015	0.010	0.003	0.000	0.015	0.013	0.013	0.013	0.011		
Ti	0.000	0.001	0.000	0.000	0.000	0.000	0.001	0.000	0.000	0.000	0.000	0.001	0.000	0.000		
Mg	0.000	0.001	0.000	0.000	0.000	0.002	0.000	0.006	0.008	0.001	0.001	0.000	0.001	0.002		
Ba	0.001	0.002	0.000	0.000	0.000	0.002	0.000	0.001	0.000	0.000	0.000	0.001	0.001	0.000		
P	0.000	0.000	0.000	0.000	0.000	0.000	0.000	0.000	0.001	0.000	0.001	0.001	0.001	0.000		
Sr	0.000	0.000	0.001	0.001	0.000	0.000	0.001	0.000	0.000	0.002	0.000	0.001	0.001	0.000		
Pb	0.001	0.001	0.002	0.001	0.001	0.000	0.001	0.001	0.000	0.000	0.001	0.000	0.000	0.000		
Total	4.991	4.990	4.996	4.996	4.958	4.984	4.988	5.006	5.001	4.984	4.983	4.981	4.980	4.985		
Feldspar Molecular Proprtions																
OR	0.967	0.981	0.972	0.925	0.979	0.937	0.937	0.989	0.989	0.928	0.933	0.962	0.935	0.926		
AB	0.033	0.019	0.029	0.075	0.021	0.063	0.063	0.008	0.005	0.072	0.067	0.038	0.065	0.074		
AN	0.000	0.000	0.000	0.000	0.000	0.000	0.000	0.003	0.006	0.000	0.000	0.000	0.000	0.000		

APPENDIX III (cont'd)

ALBITE ELECTRON-MICROPROBE SPOT ANALYSES

Sample	38B3		46B3			46I 1		47A2	48A1	48A3	48I2		48G1		49A1
unit	hyp	hyp	hyp	hyp	hyp	hyp	hyp	hyp	hyp	hyp	hyp	hyp	hyp	hyp	hyp
SiO2 wt%	68.01	67.32	69.62	69.46	69.97	68.24	69.18	69.89	69.30	68.53	69.05	69.23	68.79	69.15	68.47
Al2O3	18.74	18.82	18.83	18.99	18.86	18.85	18.66	18.24	19.09	18.70	19.09	19.89	18.48	18.64	19.18
K2O	0.09	0.08	0.10	0.10	0.05	0.03	0.13	0.11	0.05	0.11	0.10	0.09	0.12	0.11	0.10
Na2O	11.36	11.32	11.30	11.26	11.42	11.66	11.19	11.23	11.81	11.65	11.83	11.08	11.79	11.50	11.51
CaO	0.00	0.00	0.00	0.01	0.00	0.01	0.02	0.03	0.00	0.00	0.01	0.03	0.03	0.03	0.00
Fe2O3	0.49	0.16	0.36	0.33	0.31	0.12	0.69	0.91	0.19	1.11	0.15	0.33	1.03	0.93	0.01
TiO2	0.00	0.04	0.00	0.01	0.04	0.00	0.00	0.02	0.00	0.00	0.01	0.01	0.01	0.00	0.03
MgO	0.00	0.00	0.00	0.02	0.00	0.00	0.00	0.01	0.00	0.01	0.01	0.06	0.00	0.00	0.00
BaO	0.00	0.05	0.00	0.10	0.00	0.04	0.00	0.00	0.00	0.01	0.00	0.00	0.00	0.00	0.00
P2O5	0.00	0.00	0.00	0.00	0.00	0.01	0.01	0.03	0.00	0.00	0.00	0.00	0.00	0.01	0.00
SrO	0.06	0.06	0.08	0.04	0.08	0.04	0.09	0.06	0.08	0.11	0.08	0.06	0.09	0.07	0.03
PbO	0.08	0.16	0.03	0.13	0.12	0.02	0.09	0.06	0.00	0.01	0.00	0.03	0.00	0.01	0.00
Total	98.84	98.01	100.32	100.44	100.85	99.27	100.35	100.59	100.93	100.27	100.32	100.71	100.31	100.13	99.31
Structural formula based on 8 oxygens															
Si	3.008	3.004	3.027	3.020	3.028	3.009	3.025	3.035	3.016	2.998	3.008	2.996	3.008	3.013	3.008
Al	0.977	0.990	0.965	0.973	0.962	0.981	0.957	0.934	0.973	0.964	0.980	1.014	0.954	0.956	0.991
K	0.005	0.005	0.005	0.005	0.003	0.002	0.007	0.006	0.003	0.006	0.005	0.005	0.007	0.008	0.006
Na	0.975	0.980	0.952	0.949	0.958	0.997	0.944	0.945	0.990	0.988	0.999	0.930	1.000	0.977	0.980
Ca	0.000	0.000	0.000	0.001	0.000	0.000	0.001	0.001	0.000	0.000	0.000	0.000	0.001	0.001	0.000
Fe3+	0.017	0.005	0.012	0.011	0.010	0.004	0.022	0.030	0.006	0.038	0.005	0.010	0.034	0.031	0.001
Ti	0.000	0.001	0.000	0.000	0.001	0.000	0.000	0.001	0.000	0.000	0.000	0.000	0.000	0.000	0.001
Mg	0.000	0.000	0.000	0.001	0.000	0.000	0.000	0.001	0.000	0.001	0.001	0.000	0.000	0.000	0.000
Ba	0.000	0.001	0.000	0.002	0.000	0.001	0.000	0.000	0.000	0.000	0.000	0.000	0.000	0.000	0.000
P	0.000	0.000	0.000	0.000	0.000	0.000	0.000	0.001	0.000	0.000	0.000	0.000	0.000	0.000	0.000
Sr	0.002	0.002	0.002	0.001	0.002	0.001	0.002	0.001	0.002	0.003	0.002	0.002	0.002	0.001	0.001
Pb	0.001	0.002	0.000	0.002	0.001	0.003	0.001	0.001	0.000	0.000	0.000	0.000	0.000	0.000	0.000
Total	4.984	4.989	4.963	4.965	4.965	4.997	4.966	4.956	4.991	4.998	5.001	4.959	5.033	4.983	4.988
Feldspar Molecular Proportions															
OR	0.51	0.46	0.54	0.55	0.30	0.17	0.76	0.65	0.28	0.60	0.53	0.53	0.67	0.81	0.56
AB	99.49	99.54	99.46	99.39	99.69	99.80	99.17	99.31	99.70	99.40	99.43	99.31	99.33	99.05	99.11
AN	0.00	0.00	0.00	0.06	0.01	0.03	0.08	0.04	0.02	0.00	0.04	0.16	0.00	0.14	0.00

Sample	49A1	57A2	58C1	58C1	58I1			37A1		37D1	37I1		38A1		57A1
unit	hyp	trans	trans	trans	trans	trans	trans	tsub	tsub	tsub	tsub	tsub	tsub	tsub	tsub
SiO2 wt%	67.14	69.36	69.65	69.97	70.39	70.41	69.58	68.79	68.98	69.15	68.26	68.83	68.09	68.11	68.62
Al2O3	19.40	18.51	18.14	18.12	18.59	18.65	18.67	18.12	18.63	19.18	18.41	19.22	18.41	18.38	18.38
K2O	0.05	0.13	0.13	0.10	0.10	0.14	0.18	0.06	0.15	0.07	0.13	0.18	0.16	0.15	0.17
Na2O	11.78	11.26	11.46	11.70	11.31	11.32	11.11	11.37	11.47	11.61	11.00	11.22	11.34	11.35	11.16
CaO	0.02	0.02	0.00	0.00	0.02	0.01	0.00	0.00	0.00	0.02	0.00	0.00	0.00	0.00	0.00
Fe2O3	0.11	0.50	1.27	0.97	0.63	0.61	0.31	0.70	0.25	0.13	0.75	0.29	1.10	1.05	0.85
TiO2	0.00	0.00	0.00	0.00	0.01	0.02	0.00	0.02	0.00	0.00	0.01	0.05	0.00	0.00	0.03
MgO	0.00	0.00	0.00	0.01	0.01	0.01	0.00	0.00	0.01	0.00	0.00	0.03	0.00	0.00	0.00
BaO	0.32	0.00	0.00	0.03	0.02	0.03	0.01	0.06	0.00	0.00	0.03	0.00	0.06	0.07	0.01
P2O5	0.02	0.00	0.02	0.01	0.00	0.00	0.02	0.00	0.00	0.00	0.00	0.00	0.00	0.00	0.00
SrO	0.08	0.07	0.07	0.02	0.05	0.03	0.00	0.11	0.09	0.09	0.05	0.07	0.07	0.10	0.07
PbO	0.00	0.01	0.16	0.09	0.14	0.10	0.18	0.00	0.00	0.06	0.11	0.09	0.03	0.01	0.02
Total	98.63	99.86	100.89	101.01	101.40	101.33	100.36	99.24	99.57	100.53	98.74	99.98	99.35	99.16	99.40
Structural formula based on 8 oxygens															
Si	2.979	3.031	3.026	3.033	3.036	3.034	3.029	3.031	3.024	3.007	3.021	3.006	3.007	3.013	3.020
Al	1.015	0.953	0.929	0.926	0.944	0.947	0.958	0.941	0.963	0.983	0.960	0.989	0.958	0.957	0.954
K	0.003	0.007	0.007	0.006	0.006	0.008	0.010	0.003	0.008	0.004	0.007	0.010	0.009	0.008	0.015
Na	1.014	0.954	0.965	0.926	0.947	0.946	0.963	0.971	0.975	0.981	0.944	0.950	0.971	0.972	0.953
Ca	0.001	0.001	0.000	0.000	0.001	0.000	0.000	0.000	0.000	0.001	0.000	0.000	0.000	0.000	0.000
Fe3+	0.004	0.017	0.042	0.032	0.021	0.020	0.010	0.023	0.008	0.010	0.025	0.009	0.034	0.035	0.028
Ti	0.000	0.000	0.000	0.000	0.000	0.001	0.000	0.001	0.000	0.000	0.000	0.002	0.000	0.000	0.001
Mg	0.000	0.000	0.000	0.001	0.000	0.000	0.000	0.000	0.001	0.000	0.000	0.002	0.000	0.000	0.000
Ba	0.001	0.000	0.000	0.000	0.000	0.000	0.000	0.001	0.000	0.000	0.001	0.000	0.001	0.001	0.000
P	0.001	0.000	0.001	0.001	0.000	0.000	0.001	0.000	0.000	0.000	0.000	0.000	0.000	0.000	0.000
Sr	0.002	0.002	0.002	0.001	0.001	0.001	0.000	0.003	0.002	0.002	0.001	0.002	0.002	0.003	0.002
Pb	0.000	0.000	0.002	0.001	0.002	0.001	0.002	0.000	0.000	0.001	0.001	0.001	0.000	0.000	0.000
Total	5.018	4.979	4.973	4.982	4.957	4.958	4.972	4.974	4.982	4.989	4.961	4.972	4.985	4.984	4.972
Feldspar Molecular Proportions															
OR	0.27	0.76	0.74	0.57	0.60	0.79	1.00	0.33	0.83	0.41	0.73	1.06	0.90	0.83	1.57
AB	99.64	99.16	99.26	99.41	99.32	99.17	99.00	99.67	99.17	99.52	99.27	98.93	99.09	99.17	98.43
AN	0.09	0.07	0.00	0.01	0.08	0.04	0.00	0.00	0.00	0.07	0.00	0.01	0.01	0.00	0.00

APPENDIX III (cont'd)

ALBITE ELECTRON-MICROPROBE SPOT ANALYSES

Sample	57A1	24B1	24C1	25C1	36A1	36A3	46A3	46G3	
unit	lsub	asub	asub	asub	asub	asub	asub	asub	asub
SiO2 wt%	68.89	69.08	67.56	69.23	69.10	68.68	69.51	70.06	69.83
Al2O3	18.64	18.47	19.17	18.81	18.79	19.16	18.54	18.54	18.41
K2O	0.11	0.29	0.16	0.14	0.18	0.11	0.16	0.18	0.22
Na2O	11.65	11.43	11.49	11.50	11.17	11.40	11.38	11.46	11.47
CaO	0.00	0.00	0.00	0.01	0.01	0.00	0.01	0.01	0.01
Fe2O3	1.08	0.57	0.74	0.15	0.59	0.21	0.55	0.70	0.74
TiO2	0.00	0.02	0.02	0.04	0.00	0.01	0.00	0.02	0.02
MgO	0.00	0.01	0.00	0.00	0.00	0.01	0.00	0.01	0.00
BaO	0.02	0.00	0.00	0.00	0.00	0.00	0.00	0.00	0.00
P2O5	0.00	0.03	0.01	0.00	0.00	0.00	0.01	0.00	0.01
SrO	0.06	0.05	0.10	0.08	0.05	0.06	0.07	0.05	0.10
PbO	0.00	0.07	0.00	0.16	0.08	0.03	0.08	0.06	0.16
Total	100.45	100.00	99.21	100.12	99.97	99.68	100.31	101.10	100.97
Structural formula based on 8 oxygens									
Si	3.006	3.022	2.984	3.022	3.019	3.008	3.028	3.029	3.028
Al	0.958	0.952	0.995	0.967	0.968	0.989	0.952	0.945	0.941
K	0.006	0.016	0.009	0.008	0.010	0.006	0.009	0.010	0.012
Na	0.985	0.969	0.984	0.973	0.946	0.968	0.961	0.961	0.965
Ca	0.000	0.000	0.000	0.001	0.001	0.000	0.001	0.001	0.001
Fe3+	0.035	0.019	0.025	0.005	0.020	0.007	0.018	0.023	0.024
Ti	0.000	0.001	0.001	0.001	0.000	0.000	0.000	0.001	0.001
Mg	0.000	0.001	0.000	0.000	0.000	0.001	0.000	0.001	0.000
Ba	0.000	0.000	0.000	0.000	0.000	0.000	0.000	0.000	0.000
P	0.000	0.001	0.000	0.000	0.000	0.000	0.001	0.000	0.000
Sr	0.002	0.001	0.003	0.002	0.001	0.001	0.002	0.001	0.003
Pb	0.000	0.001	0.000	0.002	0.001	0.000	0.001	0.001	0.002
Total	4.993	4.983	5.001	4.981	4.965	4.981	4.971	4.972	4.976
Feldspar Molecular Proportions									
OR	0.62	1.63	0.92	0.82	1.07	0.64	0.90	1.03	1.25
AB	99.38	98.37	99.08	99.11	98.93	99.36	99.06	98.91	98.69
AN	0.00	0.00	0.00	0.07	0.05	0.00	0.05	0.06	0.06

Sample	36G3	13C1	63A3		63B2		63C1	SI120
unit	lsub	peg	peg	peg	peg	peg	peg	peg
SiO2 wt%	69.80	69.59	70.24	70.50	69.27	69.47	70.19	69.56
Al2O3	18.35	18.23	18.54	18.31	18.31	18.66	18.08	18.51
K2O	0.13	0.27	0.15	0.27	0.23	0.25	0.21	0.22
Na2O	11.64	11.68	11.37	10.97	11.46	11.40	11.09	11.58
CaO	0.00	0.01	0.00	0.00	0.02	0.02	0.02	0.01
Fe2O3	0.75	1.04	0.50	0.84	0.39	0.45	0.37	0.44
TiO2	0.00	0.03	0.02	0.00	0.00	0.00	0.00	0.02
MgO	0.00	0.01	0.01	0.02	0.00	0.01	0.01	0.00
BaO	0.01	0.12	0.00	0.02	0.03	0.00	0.04	0.04
P2O5	0.02	0.01	0.01	0.00	0.02	0.03	0.00	0.03
SrO	0.12	0.06	0.08	0.05	0.06	0.04	0.02	0.02
PbO	0.16	0.10	0.07	0.08	0.06	0.04	0.07	0.00
Total	100.97	101.12	100.99	101.03	99.84	100.36	100.10	100.08
Structural formula based on 8 oxygens								
Si	3.028	3.022	3.036	3.045	3.033	3.024	3.056	3.037
Al	0.938	0.933	0.944	0.932	0.945	0.957	0.928	0.934
K	0.007	0.015	0.009	0.015	0.013	0.014	0.012	0.012
Na	0.979	0.984	0.953	0.919	0.973	0.962	0.936	0.980
Ca	0.000	0.001	0.000	0.000	0.001	0.001	0.001	0.001
Fe3+	0.035	0.034	0.016	0.027	0.013	0.015	0.012	0.014
Ti	0.000	0.000	0.001	0.000	0.000	0.000	0.000	0.001
Mg	0.000	0.001	0.001	0.001	0.000	0.001	0.000	0.000
Ba	0.000	0.002	0.000	0.000	0.001	0.000	0.001	0.001
P	0.001	0.000	0.000	0.000	0.001	0.001	0.000	0.001
Sr	0.003	0.001	0.002	0.001	0.001	0.001	0.001	0.001
Pb	0.002	0.001	0.001	0.001	0.001	0.000	0.001	0.000
Total	4.982	4.993	4.963	4.942	4.980	4.976	4.947	4.982
Feldspar Molecular Proportions								
OR	0.74	1.48	0.88	1.61	1.30	1.40	1.25	1.24
AB	99.24	98.47	99.12	98.39	98.62	98.50	98.66	98.71
AN	0.02	0.05	0.00	0.00	0.08	0.11	0.10	0.05

APPENDIX IV

Mol. % Or and trace-element concentrations in bulk feldspar separates

APPENDIX IV

MOL % OR and TRACE ELEMENT CONCENTRATIONS OF BULK FELDSPAR SEPARATES

Sample	37A1	38B3	38A1	45G1	37A4	47A1A	56C1	35A3	27A4	46A3	34C2	36B3	37E6	43C1	46A4	46G1	46I4	63B3	63C1	SL120	SL113
unit	hyp	hyp	hyp	hyp	trans	trans	trans	fsub	asub	asub	peg	peg	peg	peg	peg	peg	peg	peg	peg	peg	peg
mol % Or	41.2	43.8	46.5	48.4	45.0	53.9	49.5	63.1	63.3	59.3	75.4	94.6	98.0	82.0	83.6	87.0	80.1	89.2	95.6	87.0	91.3
Li ppm	5.4	2.0	20.6	0.8	1.3	0.9	1.2	2.2	2.7	5.5	1.8	1.0	11.1	16.7	0.7	8.7	5.9	1.2	1.1	30.7	24.9
Be	19.8	7.8	80.1	119.0	26.4	26.7	26.7	28.0	31.9	19.5	29.9	24.0	13.5	18.3	27.5	147.9	46.8	42.3	38.0	141.4	244.5
Sc	1.5	0.0	1.5	0.0	3.4	0.0	0.0	2.3	2.7	3.6	0.1	0.1	2.1	1.5	2.4	2.2	1.6	0.0	2.1	0.0	0.8
V	3.0	1.4	0.0	0.0	0.0	0.0	0.0	0.0	0.5	5.3	2.0	3.9	0.0	0.0	0.0	0.0	0.1	0.0	0.0	0.0	1.9
Rb	5613	8157	8400	12819	16097	9059	6905	18024	18548	13275	27329	30473	21163	25099	19427	36522	23518	44839	45945	39437	47060
Sr	5.4	10.3	6.6	1.7	7.9	2.0	1.9	4.8	8.3	4.0	0.0	0.0	0.5	2.5	1.2	0.0	0.1	0.4	0.0	2.9	12.3
Y	21.4	16.8	122.1	97.1	180.2	34.2	22.6	62.5	64.6	121.3	7.2	1.8	6.3	14.3	25.5	2.1	2.8	2.0	11.1	10.9	139.8
Zr	66.8	29.7	440.5	499.3	4381.2	102.0	109.2	345.2	448.3	171.5	22.2	14.1	8.3	22.0	11.6	8.2	16.2	2.4	148.3	4.7	19.1
Nb	11.8	14.9	208.6	66.1	54.8	15.7	38.9	30.2	18.0	57.3	6.4	22.3	22.1	6.3	12.0	3.3	14.9	3.9	41.7	13.2	38.5
Mo	7.1	1.4	1.6	0.6	1.0	4.3	5.1	0.3	0.3	3.4	0.3	1.4	0.6	0.4	1.0	1.2	0.1	0.1	1.4	0.6	0.5
Cs	0.9	1.4	6.5	2.6	1.6	1.9	1.9	1.6	0.9	1.9	1.9	1.7	1.0	1.2	1.7	3.1	3.1	2.7	2.6	3.5	6.6
Ba	360	316	263	986	530	312	750	235	551	603	177	253	235	287	578	642	398	183	341	582	1090
La	8.4	5.5	43.3	25.6	254.2	12.1	16.1	31.6	87.6	18.8	1.9	9.5	3.4	3.4	5.3	1.1	1.0	1.6	8.1	13.2	71.9
Ce	17.9	12.1	114.1	76.3	471.0	28.2	36.5	69.5	197.1	43.3	5.1	20.5	7.8	8.1	12.4	2.3	5.4	3.1	13.8	9.8	31.4
Pr	2.2	1.4	13.1	7.9	55.8	4.0	4.3	7.6	20.9	4.9	0.5	1.9	0.9	1.1	1.5	0.3	0.4	0.4	1.7	1.8	13.9
Nd	7.5	5.4	43.7	27.0	193.0	18.6	13.9	26.1	66.6	19.9	2.0	5.9	3.1	5.7	5.4	0.9	1.3	1.5	5.9	5.1	45.3
Sm	2.1	1.1	12.7	8.1	38.9	5.4	3.2	6.9	14.0	8.9	0.6	1.0	0.7	1.9	1.8	0.4	0.4	0.3	1.2	0.9	13.1
Eu	0.2	0.3	0.7	0.5	2.2	0.4	0.2	0.5	0.6	0.8	0.1	0.0	0.0	0.1	0.2	0.0	0.0	0.0	0.1	0.0	0.7
Gd	2.5	1.2	13.1	9.6	35.6	5.6	2.5	7.9	14.0	14.8	0.7	0.6	0.7	2.1	2.7	0.3	0.4	0.3	1.1	0.9	14.0
Tb	0.6	0.3	2.9	2.6	5.0	0.9	0.6	1.6	2.2	2.9	0.2	0.1	0.1	0.4	0.6	0.1	0.1	0.1	0.2	0.2	3.4
Dy	3.6	2.0	23.3	22.2	29.4	6.0	4.3	11.8	13.0	19.4	1.2	0.4	1.1	2.8	3.9	0.6	0.4	0.3	1.5	1.6	24.5
Ho	0.8	0.5	5.7	5.4	5.9	1.3	1.0	2.4	2.6	4.1	0.3	0.1	0.3	0.5	0.8	0.1	0.1	0.1	0.4	0.4	5.5
Er	2.8	1.6	21.7	19.8	16.5	3.9	3.5	7.9	7.7	11.1	0.9	0.4	1.0	1.5	2.1	0.4	0.3	0.2	1.2	1.3	16.6
Tm	0.4	0.3	4.1	3.4	2.4	0.6	0.6	1.2	1.1	1.5	0.1	0.1	0.1	0.2	0.2	0.1	0.1	0.0	0.2	0.2	2.2
Yb	2.5	1.9	30.3	22.3	13.8	3.8	3.5	8.0	6.6	9.1	0.8	0.5	0.9	1.1	1.0	0.5	0.3	0.1	1.6	0.9	10.8
Lu	0.3	0.2	4.3	2.6	1.7	0.4	0.4	1.1	0.9	1.1	0.1	0.1	0.1	0.1	0.1	0.1	0.0	0.0	0.3	0.1	1.2
Hf	1.9	1.0	14.1	15.3	147.0	3.3	3.9	10.5	13.9	4.9	0.7	0.3	0.4	0.6	0.3	0.3	0.4	0.0	4.1	0.0	0.5
Ta	0.4	0.7	1.8	0.7	2.1	0.7	1.0	1.1	0.9	2.0	0.3	1.2	1.3	0.3	0.4	0.3	0.5	0.1	0.6	1.6	1.7
Tl	2.8	2.6	4.5	6.0	7.2	4.7	7.6	8.6	4.1	5.5	7.0	8.1	4.7	6.1	6.3	9.8	7.4	6.3	9.2	11.2	14.8
Pb	5.7	11.5	65.4	84.3	112.4	23.3	52.6	30.6	108.1	32.9	24.6	8.0	16.8	10.3	17.0	18.9	16.8	19.3	7.6	17.7	79.3
Bi	0.0	0.1	0.1	0.5	0.7	0.0	0.3	0.4	0.2	0.1	0.0	0.0	0.0	1.6	0.1	0.1	0.0	0.0	0.0	0.1	0.0
Th	6.3	2.4	10.2	47.2	10.3	6.4	23.2	9.3	5.7	22.3	2.8	1.4	6.2	1.3	2.2	2.0	0.4	0.3	0.5	0.2	1.7
U	0.7	0.4	5.8	6.2	8.2	0.7	2.2	2.7	1.8	2.4	0.5	0.4	0.8	0.5	0.5	0.9	0.9	0.2	1.4	0.6	32.7

APPENDIX V

Location of chemically analyzed samples

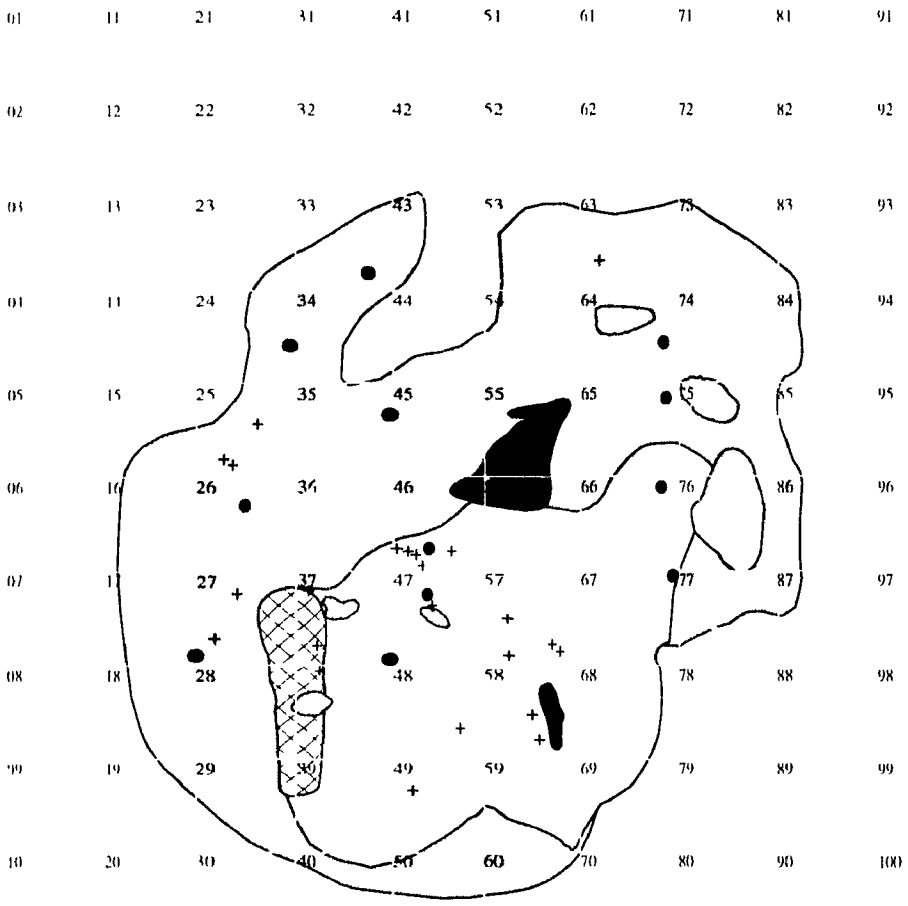

APPENDIX V

LOCATION OF CHEMICALLY ANALYZED SAMPLES

Sample	Grid no	x	y	Sample	Grid no	x	y	Sample	Grid no	x	y
38A1	38	2	9	57F1	57	3	1	LB13D8	24	9	3
46A1	46	1	2	58C4	58	4	4	LB15D16	33	8	2
46B3	46	2	2	58D1	58	5	2	LB54D29	26	5	7
46C1	46	2	3	37A4	37	3	2	LB54D44	26	5	7
46F1	46	1	3	38A1	38	3	9	LB7D14	45	0	7
47A1	47	4	7	57D1	57	7	2	SL16D2	67	9	9
48A2	48	8	3	25B1	25	6	6	SL183D1	55	2	1
48A3	48	8	3	25C1	25	4	1	SL38D3	65	9	8
48A8	48	8	3	25E1	25	3	2	SL5D36	64	9	4
49A1	49	2	7	27A4	27	2	3	SL5D9	64	9	4
57C1C	57	8	2	27B1	27	4	8	SL8D13	46	4	2
LB10D18	47	0	0	27B5	27	4	8	37F6	37	2	8
LB10D33	47	0	0	46G3	46	7	2	63C1	63	2	3
LB9D13	47	3	8	LB11D17	27	0	0	LB13D12	24	9	3
SL13D12	66	3	8	LB13D46	24	9	3	LB13D43	24	9	3
57A2	57	8	9	SL8D3	46	4	2				

Samples from outcrops are marked with "+" (numbered samples) and those from drill core are marked with "●" (LB and SL samples). For each sample, x (horizontal) and y (vertical) coordinates (between 0 and 10) give the location within the cell.